THE SCATTERING OF A FEW PARTICLES WITH SHORT-RANGE INTERACTIONS AT LOW ENERGIES

A Dissertation
Presented to
The Academic Faculty

By

Shangguo Zhu

In Partial Fulfillment
of the Requirements for the Degree
Doctor of Philosophy in the
School of Physics

Georgia Institute of Technology

December 2018

THE SCATTERING OF A FEW PARTICLES WITH SHORT-RANGE INTERACTIONS AT LOW ENERGIES

Approved by:

Dr. Shina Tan, Advisor
School of Physics
Georgia Institute of Technology

Dr. Michael Chapman
School of Physics
Georgia Institute of Technology

Dr. Carlos Sa de Melo
School of Physics
Georgia Institute of Technology

Dr. Colin Parker
School of Physics
Georgia Institute of Technology

Dr. Yingjie Liu
School of Mathematics
Georgia Institute of Technology

Date Approved: July 30, 2018

To my beloved family.

ACKNOWLEDGEMENTS

I would like to express my deepest gratitude to my adviser, Dr. Shina Tan, for his continuous guidance, nurturing, and support in this life-changing journey. Shina offered me the opportunity of working with him, when I was on the waiting list of the PhD program years ago. I have been constantly benefiting from his vast knowledge and excellent skills of research, his philosophies about research and life, and his encouragement and inspiration through many ups and downs. Most importantly, his innovative thinking towards research led me the way to be a physicist of independent and open mind. Also, I am deeply grateful to my thesis committee members, Dr. Michael Chapman, Dr. Carlos Sa de Melo, Dr. Colin Parker, and Dr. Yingjie Liu for their time and support.

I would like to thank Kevin Driscoll and Dr. Ran Qi for many fruitful discussions and sharing their valuable knowledge. I heartily thank Dr. Predrag Cvitanović, Dr. Turgay Uzer, and Dr. David Ballantyne for their huge support and valuable advice on my career. I would like to thank my colleagues and friends, Dr. Wenchao Jiang, Dr. Wenlong Yu, Dr. Xiaofeng Meng, Dr. Lede Xian, Dr. Yuntao Li, Shengnan Huang, Dr. Zhe Guang, Dr. Yuxuan Jiang, Di Chen, Dr. Qi Ge, Dr. Yun Long, and Chao Li for their kindness and help. I thank all my friends in China, the US, and other countries for their support over the years.

Special thanks to my beloved family, my parents Tinggang Zhu and Yunping Wang, and my wife Xueli Xiao, who always support and believe in me. I thank Xueli for pleasant company and all the good efforts that we made together towards a wonderful life.

I would like to acknowledge support by National Science Foundation under Grant No. PHY-1068511 and No. PHY-1352208, and by the Alfred P. Sloan Foundation. I acknowledge the high-performance computing resources and services provided by PACE at Georgia Tech. I also thank the hospitality and support of the Kavli Institute for Theoretical Physics at Santa Barbara during the program Universality in Few-Body Systems.

TABLE OF CONTENTS

LIST OF TABLES

LIST OF FIGURES

SUMMARY

The low-energy scattering of three bosons or distinguishable particles with short-range interactions is characterized by a fundamental parameter, the three-body scattering hypervolume, which is responsible for the nonuniversal effects in dilute Bose-Einstein condensates. We derive an analytical formula of the three-body scattering hypervolumes for weak interactions. When the interaction supports two-body bound states, the three-body scattering hypervolume gains a negative imaginary part, which is directly related to the rate constant for three-body recombinations. We develop a numerical method to calculate the three-body scattering hypervolumes for some model potentials with variable strengths. For real atoms with van der Waals potential, the three-body scattering hypervolumes are much harder to compute, because the three-body wave function is highly oscillatory at smaller inter-atomic distances. However, they may be extractable from precision data such as the collective-mode frequencies of trapped Bose-Einstein condensates.

In many numerical simulations, the system being simulated is put into a large but finite volume, such as a large periodic box of size L. To extract the low-energy scattering properties of two particles in infinite space from such simulations, Lüscher's formula must be used. In the second part of this thesis, we generalize Lüscher's formula to d spatial dimensions. We obtain its s-wave and p-wave approximations and the systematic expansions of the energies of the low-lying states. At a s-wave resonance in $d \geq 4$ dimensions, we identify two low-lying states close to the threshold with nearly opposite energies, $E \sim \pm 1/L^{d/2}$ when $d \geq 5$, or $E \sim \pm 1/L^2\sqrt{\ln L}$ when $d = 4$. These calculations provide important insights to the physics of three particles at a three-body resonance in finite volumes in two or three dimensions. Three-body resonances are important phenomena not yet completely explored in the experiments on cold atoms.

CHAPTER 1

INTRODUCTION

1.1 Introducing the three-body scattering hypervolume

When the de Broglie wavelength of the cold atoms is much greater than the range of interaction, many cold atom systems demonstrate remarkable *universal* properties which are determined by one or only a few two-body parameters such as the scattering length a [1, 2, 3]. One of the most prominent examples is the ground state energy per particle of a dilute Bose-Einstein condensate (BEC) [4]:

$$\frac{E}{N} \approx \frac{2\pi\hbar^2 na}{M}, \tag{1.1}$$

where the $\hbar$, M, N, and n are the Planck constant over 2π, the mass of one boson, the number of bosons, and the number density, respectively.

A more accurate version of this formula can be expressed as as a series expansion in powers of the small parameter $\sqrt{na^3}$:

$$\frac{E}{N} = \frac{2\pi\hbar^2 na}{M}\Big[1 + \frac{128}{25\sqrt{\pi}}(na^3)^{1/2} + 8wna^3\ln(na^3) + \mathcal{E}_3' na^3\Big] + o(n^2), \tag{1.2}$$

where

$$w \equiv 4\pi/3 - \sqrt{3} \approx 2.4567393972 \tag{1.3}$$

and $\mathcal{E}_3'$ is an undetermined coefficient. Inside the square brackets, the order $(na^3)^{1/2}$ and $na^3\ln(na^3)$ terms are obtained in 1957 [5, 6, 7, 8] and 1959 [9, 10, 11], respectively. Those correction terms are both universal. However, the order na^3 term was found to be sensitive to the three-body physics and cannot be solely determined by the two-body scattering parameters [9, 12]. The fact that different Bose gases with the same two-body scattering

length differ slightly in their equations of state is known as the *nonuniversal effect*, and the three-body physics is the main cause of it [12, 13, 14, 2]. It was first calculated by Braaten and Nieto in 1999 [12]. For bosons with large scattering lengths, the coefficient $\mathcal{E}_3'$ was obtained using the effective field theory [14]. For some other model interactions, people tried to extract it from the quantum Monte Carlo calculations [15], however, the statistical error is too large to identify any clear signal of the order na^3 term [13].

In 2008, Shina Tan determined the coefficient $\mathcal{E}_3'$ to be

$$\mathcal{E}_3' = \frac{D}{12\pi a^4} + \frac{\pi r_s}{a} + C^E, \tag{1.4}$$

where r_s is the two-body s-wave effective range defined in Eq. (2.3), and $C^E \approx 118.49892$ is a universal number for all Bose gases [16]. The parameter D, having dimension $[\text{length}]^4$, is called the *three-body scattering hypervolume*. It is a fundamental parameter characterizing the effective three-body interaction at low energies, in analogy to the two-body scattering length a characterizing the two-body interaction [1]. It is important in the systems of three or more bosons or distinguishable particles, such as ultracold atomic gases [16], multi-meson systems [17, 18], halo nuclei consisting of three loosely bound subsystems [19], *etc*. Not only the zero-temperature properties, the three-body scattering hypervolume D also affects the properties at finite temperatures (even above the critical temperature), such as the critical temperature itself, the equation of state, and other thermodynamic properties and dynamical properties of dilute Bose gases [16]. In fact, the three-body scattering hypervolume D influences three-body physics, four-body physics, ..., many-body physics ubiquitously and is conceptually nearly as important as the two-body scattering length.

Then, the nonuniversal effect is captured by the three-body scattering hypervolume D in a somewhat universal way. Remarkably, we see that when $a = 0$, the ground state energy

per particle of a dilute BEC becomes

$$\frac{E}{N} = \frac{\hbar^2}{6M} D n^2 + o(n^2). \tag{1.5}$$

This means when the two-body terms containing a are negligible, the leading order term is solely determined by D. Experimentally, it is possible to tune the scattering length of cold atoms to a zero crossing [20, 21, 22, 23, 24, 25, 26, 27] to eliminate the dominant two-body interaction effect such that the three-body scattering effect becomes prominent. Another avenue to make the three-body effect more prominent is to tune the interaction near a three-body resonance and away from any two-body resonances.

The three-body scattering hypervolume D is defined in a similar way to the two-body scattering length a, which can be defined such that the two-body wave function outside the range of interaction at *zero* energy, *zero* total momentum, and *zero* orbital angular momentum is

$$\phi(r) = 1 - \frac{a}{r}, \tag{1.6}$$

where r is the relative distance between the two particles. The three-body scattering hypervolume D appears in the $1/\rho^4$ term of three-body wave function with *zero* total energy, *zero* total momentum and *zero* total orbital angular momentum at large interparticle distances [16]:

$$\begin{aligned} \psi \;=\; & 1 + \Big(\sum_{i=1}^{3} -\frac{a}{x_i} + \frac{8a^2\theta_i}{\sqrt{3}\pi x_i y_i} - \frac{2wa^3}{\pi x_i \rho^2} + \frac{8\sqrt{3}wa^4(t - 1 - \theta_i \cot 2\theta_i)}{\pi^2 \rho^4} \Big) \\ & - \frac{\sqrt{3}D}{8\pi^3\rho^4} + o\Big(\frac{1}{\rho^4}\Big). \end{aligned} \tag{1.7}$$

Here the hyperradius $\rho \equiv \sqrt{(x_1^2 + x_2^2 + x_3^2)/2}$, and x_i and y_i are the lengths of the Jacobi vectors $\mathbf{x}_i$ and $\mathbf{y}_i$ defined in Eq. (2.6). $t \equiv \ln(\mathrm{e}^{\gamma}\rho/|a|)$, $\theta_i \equiv \arctan(y_i/x_i)$, and $\gamma \approx 0.5772157$ is the the Euler-Mascheroni constant. Remarkably, when the two-body

scattering length a vanishes, the three-body wave function becomes

$$\psi \;=\; 1-\frac{\sqrt{3}D}{8\pi^3\rho^4}+O\Big(\frac{1}{\rho^8}\Big). \tag{1.8}$$

For the hard-sphere bosons (later defined in Eq. (2.95)), the three-body scattering hypervolume D was found to be $D_{\rm HS}=(1761.5430\pm 0.0024)a^4$ [16]. For bosons with large scattering lengths, D can be inferred from the three to three scattering coupling constant g_3 calculated using the effective field theory by Braaten, Hammer, and Mehen [14, 16]. For almost all bosonic systems, the knowledge of this fundamental parameter are lacking and therefore their nonuniversal effects are not yet revealed.

When the interaction supports two-body bound states, after three particles collide, two of them may form a dimer (a two-body bound state). The dimer and the third particle kinetically gain the released binding energy. This process is known as the three-body recombination, which causes atom loss in dilute ultracold gases [28, 29, 30]. The measurement of the three-body recombination rate constant L_3 serves as a probe of few-body phenomena, such as the Efimov effect [31, 32, 33]. L_3 for atoms with large $|a|$ has been calculated [34, 35, 13, 3]. Meanwhile, the three-body recombination contributes a negative imaginary part to the energy, and this suggests a complex D according to Eq. (1.2). Then, the imaginary part of D can be experimentally obtained through the measurement of L_3.

Experimentally, the real part of the three-body scattering hypervolume D can be obtained through the measurement of collective mode frequencies of cold Bose gases [36, 37]. For noninteracting Bose gases in the isotropic harmonic trap, the frequency of the breathing or quadrupole mode is $2\omega_{ho}$ with ω_{ho} the trapping angular frequency [36]. Only considering the two-body weak interaction and neglecting the effect of D, the relative correction to the frequency of the breathing or quadrupole mode is of order $nal_{\rm ho}^2$, where $l_{\rm ho}\equiv\sqrt{\hbar/M\omega_{ho}}$ is the oscillator length. As D contributes a density squared term to the Gross-Pitaevskii equation, at $a=0$, the relative correction due to the effect of D is of order

$n^2\mathrm{Re}(D)l_{\mathrm{ho}}^2$ [38]. This means that the relative sensitivity is of order $n\mathrm{Re}(D)/a$. This effect is prominent near a zero crossing of the scattering length or a three-body resonance.

1.2 Scattering of particles in a finite volume

The relation between the scattering properties and the energy spectrum of the two-body states in a finite volume (a periodic box) is described by Lüscher's formula [39, 40, 41]. Lüscher's formula is widely used to extract two-body scattering parameters from lattice quantum chromodynamics (QCD) simulations [42], lattice Monte Carlo calculations for cold atoms [43, 44, 45, 46]. The systems people have studied include unitary fermions in a finite box [44], few two-component ferimions [47, 48, 49], and cold dilute neutron matter on the lattice [50, 51].

Lüscher's formula has been studied in many other scenarios: asymmetric boxes [52, 53], moving frames [54, 55], multi-channel scattering [56, 57], *etc*. Although many attempts have been made [58, 59, 60, 61, 62, 63, 64, 65], it is challenging to truly extend Lüscher's formula to the system of three particles in a finite volume. Kreuzer et al. studied the modification of the Efimov spectrum due to the finite volume [63, 64]. Meißner, Ríos, and Rusetsky investigated the three-body bound states in the unitary limit in a finite volume [66]. Recently, Guo and Gasparian studied a solvable three-body model in a finite volume and suggested that the multiple-body problem can be mapped into a higher dimensional two-body problem [67]. Then, the two-body Lüscher's formula in higher dimensions provides important insights to the three-body systems in a two- or three- dimensional finite volume. It may also be useful when studying high dimensional objects, like the strings in the string theory [68].

Originally, Lüscher's formula is derived for two particles in a finite volume in three spatial dimensions [39, 40, 41]. In one dimension, Lüscher and Wolff obtained the result for the symmetric wave function [69]. In two dimensions, Fiebig et al. derived the similar formula with all the partial waves included [70]. In 2010, Beane derived the s-wave ap-

proximation of the Lüscher's formula in d spatial dimensions [71], however, it is divergent when $d \geq 4$. The complete form of Lüscher's formula with all the partial waves included in arbitrary d dimensions has not been addressed.

1.3 Thesis outline

In Chapter 2, we study the three-body scattering hypervolume D analytically and numerically. First, in the limit of weak two-body interactions, we analytically derive the approximate formula for D, and find that D depends on the interaction strength quadratically. Second, when the interaction supports two-body bound states, we extend the definition of D to the complex plane. The imaginary part of D is directly related to L_3 and is expressed as a sum of the contributions from different dimer product states. This provides an novel *ab initio* method to evaluate L_3. Third, we perform the first numerical calculations of D for bosons with nonzero-range interactions with variable strengths. Our results are consistent with the previous result for hard-sphere bosons in the strong-repulsion limit and the analytical formula in the weak interaction limit. Then, for the first time, we determine the leading nonuniversal corrections to the ground state energies of dilute BECs having nonzero-range interactions of variable strengths.

In Section 2.1, we first introduce the two-body scattering theory, the two-body scattering parameters, and the two-body special functions. Second, we give the definition of the Jacobi vectors. Third, we show the asymptotic expansions of the three-body wave function of three bosons colliding at zero energy and then introduce the definition of the three-body scattering hypervolume D.

In Section 2.2, we derive the three-body wave function for three bosons with weak interactions and analytically obtain the leading and subleading order terms of D.

In Section 2.3, we generalize the definition of D to the complex plane when the two-body interaction supports bound states. We establish a relation between the imaginary part of D and the three-body recombination rate L_3.

In Section 2.4, we develop the numerical method to calculate D for nonzero-range interactions with variable strengths.

In Section 2.5, we present our numerical results and discuss the significant findings.

In Section 2.6, we discuss the possible experimental methods to measure the three-body scattering hypervolume D.

In Section 2.7, we summarize our findings of Chapter 2, and discuss possible extensions.

In Chapter 3, we generalize Lüscher's formula to arbitrary d dimensions. We work in the momentum space, in which the form of the wave function remains the same in different spatial dimensions and derive Lüscher's formula with a natural way of regularization. Then, we obtain its s-wave and p-wave approximation and the systematic expansions of the energies of the low-lying states at large box size L.

In Section 3.1, we introduce the two-body scattering theory and the effective range expansion in d dimensions. Then, we discuss the pseudo wave function in the real and momentum space and the Helmholtz equation which the pseudo wave function satisfies.

In Section 3.2, we obtain the right periodic pseudo wave function in the d-dimensional finite volume.

In Section 3.3, we obtain the quantization condition, namely, the generalized Lüscher's formula in d dimensions.

In Section 3.4 and 3.5, we study the s-wave and p-wave approximation, respectilvey. We obtain the systematic expansion of the energy eigenvalues at large L.

In Section 3.6, we summarize our findings of Chapter 3.

CHAPTER 2

THE THREE-BODY SCATTERING HYPERVOLUMES AND THE NONUNIVERSAL EFFECTS IN DILUTE BOSE-EINSTEIN CONDENSATES

2.1 Preliminaries

2.1.1 Two-body scattering parameters and two-body special functions

In this section, we introduce the two-body scattering theory at low energies. For simplicity, we use the units such that $\hbar = M = 1$ in the following discussions.

Consider the scattering of two particles with short-range interactions. We write the Schrödinger equation of the relative motion

$$\Big[-\nabla^2 + V(\mathbf{r}) \Big] \psi(\mathbf{r}) = E\psi(\mathbf{r}), \tag{2.1}$$

where E and $\mathbf{r}$ are the colliding energy and the relative position vector, respectively. Note that for the relative motion, the reduced mass is $1/2$. The short-range potential $V(\mathbf{r})$ vanishes when $r > r_e$ with r_e the range of interaction. Then, we can write down the wave function of the partial wave channel with orbital angular momentum l and magnetic quantum number m outside the range of interaction

$$\psi_{lm}(\mathbf{r}) = A_{lm} \Big[j_l(pr) \cot\delta_l - n_l(pr) \Big] Y_{lm}(\hat{\mathbf{r}}), \tag{2.2}$$

where j_l and n_l are the spherical Bessel function of the first and second kind, respectively, Y_{lm} are the spherical harmonics, δ_l is the phase shift, A_{lm} is a coefficient determined by the choice of normalization, and the energy $E = p^2$. At low energies, we have the following

effective range expansion for the phase shift [72, 73]

$$p^{2l+1}\cot\delta_l = -\frac{1}{a_l} + \frac{1}{2}r_l p^2 + \frac{1}{4!}r_l' p^4 + O(p^6). \tag{2.3}$$

Here we have defined the scattering parameters, the scattering length a_l, the effective range r_l and a higher order parameter r_l', with dimension $[\text{length}]^{2l+1}$, $[\text{length}]^{-2l+1}$, and $[\text{length}]^{-2l+3}$, respectively. For bosons, l is even and we use symbols $s, d, g, i, \cdots$ for $l = 0, 2, 4, 6, \cdots$.

Alternatively, we can also obtain the scattering parameters by defining the following special functions [16]. We define the special functions $\phi^{(l)}_{\hat{\mathbf{n}}}(\mathbf{r}), f^{(l)}_{\hat{\mathbf{n}}}(\mathbf{r}), g^{(l)}_{\hat{\mathbf{n}}}(\mathbf{r}), \cdots$, in the l-wave channel with zero magnetic quantum number along the direction $\hat{\mathbf{n}}$, satisfying

$$H_{2\text{b}}\phi^{(l)}_{\hat{\mathbf{n}}}(\mathbf{r}) = 0, \;\; H_{2\text{b}}f^{(l)}_{\hat{\mathbf{n}}}(\mathbf{r}) = \phi^{(l)}_{\hat{\mathbf{n}}}(\mathbf{r}), \;\; H_{2\text{b}}g^{(l)}_{\hat{\mathbf{n}}}(\mathbf{r}) = f^{(l)}_{\hat{\mathbf{n}}}(\mathbf{r}), \;\; \cdots, \tag{2.4}$$

where the two-body Hamiltonian $H_{2\text{b}} = -\nabla^2 + V(\mathbf{r})$. When $l = 0$, we suppress the superscript and write the special functions as $\phi, f, g, \cdots$. When $l > 0$, we use symbols $d, g, i, \cdots$. Outside the range of interaction $r > r_e$, the special functions are defined to have the following forms [16]

$$\phi(\mathbf{r}) = 1 - \frac{a}{r}, \tag{2.5a}$$

$$f(\mathbf{r}) = -\frac{r^2}{6} + \frac{ar}{2} - \frac{ar_s}{2}, \tag{2.5b}$$

$$g(\mathbf{r}) = \frac{r^4}{120} - \frac{ar^3}{24} + \frac{ar_s r^2}{12} - \frac{ar_s'}{24}, \tag{2.5c}$$

$$\phi^{(d)}_{\hat{\mathbf{n}}}(\mathbf{r}) = \Big(\frac{r^2}{15} - \frac{3a_d}{r^3}\Big)P_2(\hat{\mathbf{n}}\cdot\hat{\mathbf{r}}), \tag{2.5d}$$

$$f^{(d)}_{\hat{\mathbf{n}}}(\mathbf{r}) = \Big(-\frac{r^4}{210} - \frac{a_d r_d r^2}{30} - \frac{a_d}{2r}\Big)P_2(\hat{\mathbf{n}}\cdot\hat{\mathbf{r}}), \tag{2.5e}$$

$$\phi^{(g)}_{\hat{\mathbf{n}}}(\mathbf{r}) = \Big(\frac{r^4}{945} - \frac{105a_g}{r^5}\Big)P_4(\hat{\mathbf{n}}\cdot\hat{\mathbf{r}}), \tag{2.5f}$$

$$\phi^{(i)}_{\hat{\mathbf{n}}}(\mathbf{r}) = \Big(\frac{r^6}{135135} - \frac{10395a_i}{r^7}\Big)P_6(\hat{\mathbf{n}}\cdot\hat{\mathbf{r}}), \tag{2.5g}$$

where P_l is the Legendre polynomial [$P_l(1) = 1$].

2.1.2 Jacobi vectors

To describe the three-body configuration space, it is convenient to introduce the Jacobi vectors and the center-of-mass position vector

$$\mathbf{r}_c = \frac{1}{3}\Big(\mathbf{r}_1 + \mathbf{r}_2 + \mathbf{r}_3\Big), \tag{2.6a}$$

$$\mathbf{x}_1 = \mathbf{r}_2 - \mathbf{r}_3, \quad \mathbf{y}_1 = \frac{2}{\sqrt{3}}\Big(\mathbf{r}_1 - \frac{\mathbf{r}_2 + \mathbf{r}_3}{2}\Big), \tag{2.6b}$$

$$\mathbf{x}_2 = \mathbf{r}_3 - \mathbf{r}_1, \quad \mathbf{y}_2 = \frac{2}{\sqrt{3}}\Big(\mathbf{r}_2 - \frac{\mathbf{r}_3 + \mathbf{r}_1}{2}\Big), \tag{2.6c}$$

$$\mathbf{x}_3 = \mathbf{r}_1 - \mathbf{r}_2, \quad \mathbf{y}_3 = \frac{2}{\sqrt{3}}\Big(\mathbf{r}_3 - \frac{\mathbf{r}_1 + \mathbf{r}_2}{2}\Big), \tag{2.6d}$$

where $\mathbf{r}_1$, $\mathbf{r}_2$, and $\mathbf{r}_3$ are the position vectors of the three bosons. The cartoon of the Jacobi vectors are shown in Figure 2.1. The positions of the three bosons are uniquely determined given the center-of-mass position vector $\mathbf{r}_c$ and one pair of the Jacobi vectors, $\mathbf{x}_i$ and $\mathbf{y}_i$ with $i = 1$, 2 or 3. The Jacobi vectors are related by the following transform

$$\mathbf{x}_i = \mathbf{x}_j \cos\frac{2\pi(i-j)}{3} - \mathbf{y}_j \sin\frac{2\pi(i-j)}{3}, \tag{2.7a}$$

$$\mathbf{y}_i = \mathbf{x}_j \sin\frac{2\pi(i-j)}{3} + \mathbf{y}_j \cos\frac{2\pi(i-j)}{3}. \tag{2.7b}$$

We also define the hyperradius

$$\rho = \sqrt{\frac{x_1^2 + x_2^2 + x_3^2}{2}} = \frac{\sqrt{3}}{2}\sqrt{x_i^2 + y_i^2}, \tag{2.8}$$

which characterizes the size of the triangle formed by the three particles.

In most cases, we can simply suppress the subscription due to the particle exchange

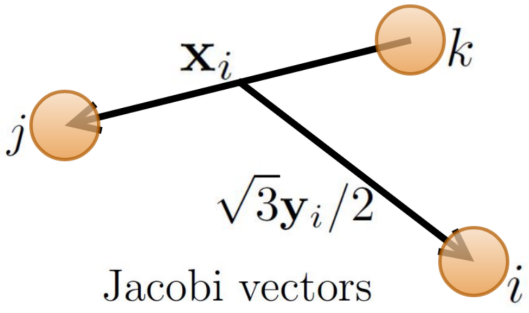

Figure 2.1: The cartoon of the Jacobi vectors defined in Eq. (2.6). Here (ijk) is an even permutation of (123), namely $(ijk) = (123)$, (231), or (312).

symmetry and let $\mathbf{x}$ and $\mathbf{y}$ represent *any* pair of the Jacobi vectors

$$\mathbf{x} \equiv \mathbf{x}_i, \quad \mathbf{y} \equiv \mathbf{y}_i. \tag{2.9a}$$

The other two sets of Jacobi vectors can be expressed as

$$\mathbf{x}_+ = -\frac{1}{2}\mathbf{x} - \frac{\sqrt{3}}{2}\mathbf{y}, \quad \mathbf{y}_+ = \frac{\sqrt{3}}{2}\mathbf{x} - \frac{1}{2}\mathbf{y} \tag{2.9b}$$

$$\mathbf{x}_- = -\frac{1}{2}\mathbf{x} + \frac{\sqrt{3}}{2}\mathbf{y}, \quad \mathbf{y}_- = -\frac{\sqrt{3}}{2}\mathbf{x} - \frac{1}{2}\mathbf{y}, \tag{2.9c}$$

where the $\pm$ sign in the subscript represents Jacobi vectors related by two types of transforms defined in Eq. (2.7).

The Jacobi vectors enable us to neatly express the Laplace operator with respect to $\mathbf{r}_1$, $\mathbf{r}_2$, and $\mathbf{r}_3$ as

$$\frac{1}{2}(\nabla_1^2 + \nabla_2^2 + \nabla_3^2) = \frac{1}{6}\nabla_{\mathbf{r}_c}^2 + \nabla_{\mathbf{x}}^2 + \nabla_{\mathbf{y}}^2. \tag{2.10}$$

If we assume that the wave function does not dependent on the center-of-mass position, the $\nabla_{\mathbf{r}_c}^2$ term acting on the wave function vanishes. Then, we solve the Schrödinger equation essentially in the six-dimensional space $(\mathbf{x}, \mathbf{y})$, where we can conveniently utilize the six-

dimensional Green's function

$$g(\mathbf{x},\mathbf{y};\mathbf{x}',\mathbf{y}') = -\frac{1}{4\pi^3}\Big[(\mathbf{x}-\mathbf{x}')^2+(\mathbf{y}-\mathbf{y}')^2\Big]^{-2}, \tag{2.11}$$

satisfying the Poisson equation with a delta function source

$$(\nabla^2_{\mathbf{x}}+\nabla^2_{\mathbf{y}})g(\mathbf{x},\mathbf{y};\mathbf{x}',\mathbf{y}') = \delta(\mathbf{x}-\mathbf{x}')\delta(\mathbf{y}-\mathbf{y}'). \tag{2.12}$$

2.1.3 Three-body scattering hypervolume and nonuniversal effect

Here we introduce the definition of the three-body scattering hypervolume. As we know, the two-body scattering length can be defined in the zero-energy two-body wave function at large distances where the two particles are outside the range of interaction. Similarly, the three-body scattering hypervolume can be defined in the zero-energy three-body wave function at large inter-particle distances. For simplicity, we consider three identical bosons colliding at *zero energy*, *zero total momentum* and *zero total orbital angular momentum*. Then, the wave function is invariant under rotations, translations, and particle exchanges.

In this problem, we solve the following Schrödinger equation,

$$\Big[-\frac{1}{2}(\nabla_1^2+\nabla_2^2+\nabla_3^2)+V(\mathbf{x}_1)+V(\mathbf{x}_2)+V(\mathbf{x}_3)\Big]\psi = 0, \tag{2.13}$$

where the two-body interaction is isotropic and short-range, *i.e.*, $V(\mathbf{x}) = V(x)$ and $V(\mathbf{x}) = 0$ if $x > r_e$.

At large hyperradii ρ, there exist two asymptotic expansions of the three-body wave function [16]. One expansion, called the 111-expansion, is obtained when the three pair-wise distances go to infinity simultaneously (with the ratio $x_1 : x_2 : x_3$ fixed); the other, called the 21-expansion, is obtained when the distance between two particles stays fixed and the distance between the third particle and the pair goes to infinity. The leading order of the 111-expansion is assumed to be 1, which corresponds to the most important incom-

ing three-body channel and fixes the wave function uniquely. Both expansions have been obtained up to the $1/\rho^7$ order [16]. Here we list the 111- and 21- expansions [1],

$$\begin{aligned}
\phi^{(111)} &= 1+\Big(\sum_{i=1}^{3}-\frac{a}{x_i}+\frac{8a^2\theta_i}{\sqrt{3}\pi x_i y_i}-\frac{2wa^3}{\pi x_i\rho^2}+\frac{8\sqrt{3}wa^4(t-1-\theta_i\cot 2\theta_i)}{\pi^2\rho^4}\Big)-\frac{\sqrt{3}D}{8\pi^3\rho^4}\\
&+\sum_{i=1}^{3}\Big\{\frac{36a^5w[(2t-3)\sin 3\theta_i-2\theta_i\cos 3\theta_i]-\sqrt{3}a\xi_1\sin 3\theta_i}{\pi^2\rho^5\sin 2\theta_i}\\
&-\frac{96a^6w[3\theta_i^2\sin 4\theta_i+(6t-11)\theta_i\cos 4\theta_i]}{\pi^3\rho^6\sin 2\theta_i}+\frac{3\sqrt{3}a\xi_2\theta_i\cos 4\theta_i}{\pi^2\rho^6\sin 2\theta_i}\\
&+\frac{45\sqrt{3}aa_d(24\theta_i-8\sin 4\theta_i+\sin 8\theta_i)}{8\pi\rho^6\sin^3 2\theta_i}P_2(\hat{\mathbf{x}}_i\cdot\hat{\mathbf{y}}_i)\\
&+\frac{\sqrt{3}a\zeta_3[12\theta_i\cos 5\theta_i+(25-12t)\sin 5\theta_i]}{\pi^2\rho^7\sin 2\theta_i}-\frac{12\sqrt{3}a\xi_3\sin 5\theta_i}{\pi^2\rho^7\sin 2\theta_i}\\
&-\frac{45(\sqrt{3}-9/2\pi)a^2a_d(4-3\cos 4\theta_i-\cos 6\theta_i)}{\rho^7\cos^3\theta_i}P_2(\hat{\mathbf{x}}_i\cdot\hat{\mathbf{y}}_i)\Big\}+O(\frac{1}{\rho^8}), \qquad (2.14)
\end{aligned}$$

and

$$\begin{aligned}
\phi^{(21)} &= \Big[1-\frac{4a}{\sqrt{3}y}+\frac{8a^2w}{3\pi y^2}-\frac{32a^3w}{3\sqrt{3}\pi y^3}+\frac{16(24\sqrt{3}wa^4(\tau-3/2)-\xi_1)}{9\pi^2y^4}\\
&+\frac{16(32\sqrt{3}wa^5(6\tau-11)-3\pi\xi_2)}{9\sqrt{3}\pi^2y^5}+\frac{64(\zeta_3(12\tau-25)+12\xi_3)}{27\pi^2y^6}\\
&+\frac{128(\zeta_4(60\tau-137)+30\xi_4)}{27\sqrt{3}\pi y^7}\Big]\phi(x)+\Big[\frac{16a^2w}{3\pi y^4}-\frac{64a^3w}{\sqrt{3}\pi y^5}\\
&+\frac{64(18\sqrt{3}wa^4(12\tau-25)-9\xi_1)}{27\pi^2y^6}+\frac{64(48\sqrt{3}wa^5(60\tau-137)-45\pi\xi_2)}{27\sqrt{3}\pi^2y^7}\Big]f(x)\\
&+\Big[\frac{64a^2w}{\pi y^6}-\frac{1280a^3w}{\sqrt{3}\pi y^7}\Big]g(x)+\Big[-\frac{20a}{\sqrt{3}y^3}+\frac{640(2\pi-3\sqrt{3})a^2}{9\pi y^4}-\frac{160a^3w}{3\sqrt{3}\pi y^5}\\
&+\frac{512\xi_3^{(d)}}{9\pi^2y^6}+\frac{2240\xi_4^{(d)}}{9\sqrt{3}\pi y^7}-\frac{512a^5w(210\tau-457)}{63\pi^2y^7}\Big]\phi^{(d)}_{\hat{\mathbf{y}}}(\mathbf{x})+\Big[\frac{1280a^2(2\pi-3\sqrt{3})}{3\pi y^6}\\
&-\frac{2240a^3w}{3\sqrt{3}\pi y^7}\Big]f^{(d)}_{\hat{\mathbf{y}}}(\mathbf{x})+\Big[-\frac{140\sqrt{3}a}{y^5}+\frac{1024a^2(76\pi-135\sqrt{3})}{3\pi y^6}\\
&-\frac{1120a^3w}{\sqrt{3}\pi y^7}\Big]\phi^{(g)}_{\hat{\mathbf{y}}}(\mathbf{x})-\frac{20020a}{\sqrt{3}y^7}\phi^{(i)}_{\hat{\mathbf{y}}}(\mathbf{x})+O(\frac{1}{y^8}), \qquad (2.15)
\end{aligned}$$

[1] Note that we have used notations that are different from those of Ref. [16]. Compared to Ref. [16], here $\rho\equiv B$, $\mathbf{x}_i\equiv\mathbf{s}_i$, and $\mathbf{y}_i\equiv\frac{2}{\sqrt{3}}\mathbf{R}_i$.

where $t \equiv \ln \frac{e^\gamma \rho}{|a|}$, $\tau \equiv \ln \frac{\sqrt{3}e^\gamma y}{2|a|}$, $\theta_i \equiv \arctan(y_i/x_i)$, $w \equiv 4\pi/3 - \sqrt{3}$, $\gamma \approx 0.5772157$ is the Euler's constant, and we have defined the following parameters

$$\xi_1 = \frac{\sqrt{3}D}{8\pi} - 8\Big(\sqrt{3} - \frac{\pi}{3}\Big)wa^4 - \frac{3\pi w}{2}a^3 r_s, \tag{2.16a}$$

$$\xi_2 = \frac{aD}{\sqrt{3}\pi^2} - \Big(\frac{260}{9} + \frac{128}{\sqrt{3}\pi}\Big)wa^5 + 2wa^4 r_s, \tag{2.16b}$$

$$\begin{aligned}\xi_3 = &-\Big[\Big(\frac{1}{8\pi^2} + \frac{1}{12\sqrt{3}\pi}\Big)a + \frac{3\sqrt{3}}{64\pi}r_s\Big]aD + \Big(\frac{17\sqrt{3}}{2} + \frac{22}{\pi} + \frac{353\pi}{27}\Big)wa^6 \\ &+\Big(\frac{11\sqrt{3}}{4} - \frac{7\pi}{6}\Big)wa^5 r_s + \frac{9}{16}\pi w a^4 r_s^2 + \frac{3}{32}\pi w a^3 r_s' \\ &+\Big(10\pi^2 - \frac{45}{4}\sqrt{3}\pi\Big)aa_d,\end{aligned} \tag{2.16c}$$

$$\begin{aligned}\xi_4 = &\Big[\Big(\frac{1}{10\pi^3} + \frac{1}{15\sqrt{3}\pi^2}\Big)a - \frac{7\sqrt{3}}{80\pi^2}r_s\Big]a^2 D - \Big(\frac{536}{25\pi^2} + \frac{124}{27} - \frac{86}{25\sqrt{3}\pi}\Big)wa^7 \\ &+\Big(\frac{65}{3} + \frac{309\sqrt{3}}{25\pi}\Big)wa^6 r_s - \frac{6}{5}wa^5 r_s^2 - (60\pi - 87\sqrt{3})a^2 a_d \\ &-\frac{9}{20}wa^4 r_s',\end{aligned} \tag{2.16d}$$

$$\xi_3^{(d)} = \frac{5}{3}\Big(9\sqrt{3} - 4\pi\Big)wa^4 + \frac{15}{4}\pi\Big(2\pi - 3\sqrt{3}\Big)a^2 a_d r_d, \tag{2.16e}$$

$$\xi_4^{(d)} = \frac{\sqrt{3}}{28\pi^2}aD - \Big(\frac{416}{21} - \frac{8384\sqrt{3}}{245\pi}\Big)wa^5 - \frac{3}{7}wa^4 r_s - \frac{3}{2}wa^3 a_d r_d, \tag{2.16f}$$

$$\zeta_3 = \Big(\frac{24}{\pi} + \frac{16}{\sqrt{3}}\Big)wa^6 + 9\sqrt{3}wa^5 r_s, \tag{2.16g}$$

$$\zeta_4 = \frac{42\sqrt{3}}{5\pi}wa^6 r_s - \Big(\frac{48}{5\pi^2} + \frac{32}{5\sqrt{3}\pi}\Big)wa^7, \tag{2.16h}$$

We see that the three-body scattering hypervolume D appears in the $1/\rho^4$ and $1/y^4$ order term in the two expansions. Then, either expansion can serve as the definition of the three-body scattering hypervolume D. With this defintion, we can obtain D by calculating the zero-energy wave function of three bosons up to the $1/\rho^4$ or $1/y^4$ order term. Note that the two expansions match in the common region $r_e \ll x \ll y$. Also, we have not considered the case of two-body interactions supporting two-body bound states. The 21-expansion here is valid only when there is no two-body bound state. In the presence of two-body bound states, the system may experience three-body recombination. The 21-expansion

will be modified and D will be complex. Further discussion is given in Section 2.3.

2.2 Three-body scattering hypervolume for weak interactions

In this section, we analytically derive an approximate formula of D for bosons with weak interactions. In order to calculate the three-body scattering hypervolume, one needs to get the asymptotic wave function by solving the three-body Schrödinger equation. When the interaction is weak, this is possible by expressing the wave function analytically in Born series

$$\psi = \psi_0 + G\mathcal{V}\psi_0 + (G\mathcal{V})^2\psi_0 + (G\mathcal{V})^3\psi_0 + \cdots, \tag{2.17}$$

where ψ_0 is the solution to the free Schrödinger equation. Here $\mathcal{V}$ is the intearction, $G \equiv (-\widehat{T})^{-1}$ is Green's operator, and $\widehat{T}$ is the kinetic operator. In the coordinate repersentation, $\widehat{T} = -\frac{1}{2}(\nabla_1^2 + \nabla_2^2 + \nabla_3^2)$, and $\mathcal{V} = V(x_1) + V(x_2) + V(x_3)$ if the interaction only contains the two-body interaction. As we have assumed that the wave function approaches 1 at large inter-particle distances, we can uniquely determine $\psi_0 = 1$. We define $\psi_n = (G\mathcal{V})^n\psi_0$, with $n = 0, 1, 2, \cdots$.

2.2.1 First order

First, calculate the first order term ψ_1. Using the Green's function in Eq. (2.11), we have the expression

$$\psi_1 = \int \mathrm{d}^3x'\mathrm{d}^3y'\; g(\mathbf{x}, \mathbf{y}; \mathbf{x}', \mathbf{y}')\Big[V(x') + V(x'_+) + V(x'_-)\Big]\psi_0, \tag{2.18}$$

where $x'_\pm = |-\mathbf{x}'/2 \mp \sqrt{3}\mathbf{y}'/2|$ defined in (2.9). Then, we can rewrite it as $\psi_1 = \sum_{i=1}^3 \phi_1(\mathbf{x}_i, \mathbf{y}_i)$, where

$$\phi_1(\mathbf{x}, \mathbf{y}) = \int \mathrm{d}^3x'\mathrm{d}^3y'\; g(\mathbf{x}, \mathbf{y}; \mathbf{x}', \mathbf{y}')V(x')\psi_0 = -\frac{u(x)}{x}, \tag{2.19}$$

and

$$u(x) = \int_0^\infty \mathrm{d}x'\, x' \min(x, x') V(x'). \tag{2.20}$$

Here $\min(x, x')$ takes the minimum between x and x'.

As $V(x')$ is a short-range interaction, $u(x) = \alpha_1$ when $x > r_e$. Here we have defined the parameter,

$$\alpha_n = \int_0^\infty \mathrm{d}x\, x^{n+1} V(x), \tag{2.21}$$

which has dimension $[\mathrm{length}]^n$. We define an localized function

$$\widehat{u}(x) \equiv \alpha_1 - u(x), \tag{2.22}$$

which vanishes when $x > r_e$.

We see that the first order does not contributes to $1/\rho^4$ term of the 111-expansion. Then, D is at least quadratic in the interaction, namely, $D = O(V^2)$. However, compared to the 111-expansion, we see that the scattering length a is linear in the interaction strength, and $a = \alpha_1 + O(V^2)$.

2.2.2 Second order

Here we calculate the second order Born approximation. Similarly, we write down the expression $\psi_2 = \sum_{i=1}^3 \phi_2(\mathbf{x}_i, \mathbf{y}_i)$, where

$$\phi_2(\mathbf{x}, \mathbf{y}) = \int \mathrm{d}^3x' \mathrm{d}^3y'\; g(\mathbf{x}, \mathbf{y}; \mathbf{x}', \mathbf{y}') V(x') \Big[\phi_1(\mathbf{x}', \mathbf{y}') + \phi_1(\mathbf{x}'_+, \mathbf{y}'_+) + \phi_1(\mathbf{x}'_-, \mathbf{y}'_-)\Big], \tag{2.23}$$

where $\mathbf{x}'_\pm = -\mathbf{x}'/2 \mp \sqrt{3}\mathbf{y}'/2$ and $\mathbf{y}'_\pm = \pm\sqrt{3}\mathbf{x}'/2 - \mathbf{y}'/2$ defined in Eq. (2.9). We can split the integral into two parts and calculate them separately.

The first part is

$$I_1(\mathbf{x}, \mathbf{y}) = \int \mathrm{d}^3x' \mathrm{d}^3y'\; g(\mathbf{x}, \mathbf{y}; \mathbf{x}', \mathbf{y}') V(x') \phi_1(\mathbf{x}', \mathbf{y}'). \tag{2.24}$$

As $\phi_1(\mathbf{x}', \mathbf{y}')$ only depends on $\mathbf{x}'$, we can easily integrate out $\mathbf{y}'$ and the angular part of $\mathbf{x}'$,

$$I_1 = \frac{\omega(x)}{x}, \tag{2.25}$$

where

$$\begin{aligned} \omega(x) &= \int_0^\infty \mathrm{d}x' \ \min(x, x') V(x') u(x') \\ &= \int_0^\infty \mathrm{d}x' \int_0^\infty \mathrm{d}x'' \ \min(x, x') \min(x', x'') V(x') V(x'') x''. \end{aligned} \tag{2.26}$$

When $x > r_e$, $\omega(x) = \beta_1$. Here we define the parameter

$$\beta_n = \int_0^\infty \mathrm{d}x \ x^n V(x) u(x). \tag{2.27}$$

and a localized function

$$\widehat{\omega}(x) \equiv \beta_1 - \omega(x). \tag{2.28}$$

The second part is

$$\begin{aligned} I_2 &= \int \mathrm{d}^3x' \mathrm{d}^3y' \ g(\mathbf{x}, \mathbf{y}; \mathbf{x}', \mathbf{y}') V(x') \Big[\phi_1(\mathbf{x}'_+, \mathbf{y}'_+) + \phi_1(\mathbf{x}'_-, \mathbf{y}'_-) \Big] \\ &= \Big(\frac{2}{\sqrt{3}} \Big)^3 \int \mathrm{d}^3x' \mathrm{d}^3x'' \ V(x') \Big(\frac{\alpha_1 - \widehat{u}(x'')}{-x''} \Big) \\ &\quad \times \Big\{ g\Big(\mathbf{x}, -\mathbf{y}; \mathbf{x}', \frac{2}{\sqrt{3}} (\mathbf{x}'' + \frac{\mathbf{x}'}{2}) \Big) + g\Big(\mathbf{x}, \mathbf{y}; \mathbf{x}', \frac{2}{\sqrt{3}} (\mathbf{x}'' + \frac{\mathbf{x}'}{2}) \Big) \Big\}, \end{aligned} \tag{2.29}$$

where we have used the transform $\mathbf{y}' \to \mp \frac{2}{\sqrt{3}} (\mathbf{x}'_\pm + \mathbf{x}'/\mathbf{2})$. Notice that $V(x')$ and $\widehat{u}(x'')$ are localized functions. We can further split the integral into two parts $I_2 = I_2^{(1)} + I_2^{(2)}$, with

$$\begin{aligned} I_2^{(1)}(\mathbf{x}, \mathbf{y}) &= \Big(\frac{2}{\sqrt{3}} \Big)^3 \int \mathrm{d}^3x' \mathrm{d}^3x'' \ \Big(\frac{V(x') \alpha_1}{-x''} \Big) \\ &\quad \times \Big\{ g\Big(\mathbf{x}, -\mathbf{y}; \mathbf{x}', \frac{2}{\sqrt{3}} (\mathbf{x}'' + \frac{\mathbf{x}'}{2}) \Big) + g\Big(\mathbf{x}, \mathbf{y}; \mathbf{x}', \frac{2}{\sqrt{3}} (\mathbf{x}'' + \frac{\mathbf{x}'}{2}) \Big) \Big\}, \end{aligned} \tag{2.30}$$

and

$$I_2^{(2)}(\mathbf{x},\mathbf{y}) = \Big(\frac{2}{\sqrt{3}}\Big)^3 \int \mathrm{d}^3x'\mathrm{d}^3x'' \Big(\frac{V(x')\widehat{u}(x'')}{x''}\Big) \times\Big\{g\Big(\mathbf{x},-\mathbf{y};\mathbf{x}',\frac{2}{\sqrt{3}}(\mathbf{x}''+\frac{\mathbf{x}'}{2})\Big)+g\Big(\mathbf{x},\mathbf{y};\mathbf{x}',\frac{2}{\sqrt{3}}(\mathbf{x}''+\frac{\mathbf{x}'}{2})\Big)\Big\}. \tag{2.31}$$

In the part $I_2^{(1)}$, x' is a localized variable of the integrand. We can first integrate over x''. Using the expression of the Green's function in Eq. (2.11), we find

$$I_2^{(1)} = \frac{\alpha_1}{\sqrt{3}\pi^2}\int \mathrm{d}^3x'\, V(x') \times\Big\{\frac{\arctan\Big(|\mathbf{y}+\frac{\mathbf{x}'}{\sqrt{3}}|/|\mathbf{x}-\mathbf{x}'|\Big)}{|\mathbf{y}+\frac{\mathbf{x}'}{\sqrt{3}}||\mathbf{x}-\mathbf{x}'|}+(\mathbf{y}\to-\mathbf{y})\Big\}, \tag{2.32}$$

where $(\mathbf{y}\to-\mathbf{y})$ means the term with $\mathbf{y}$ replaced by $-\mathbf{y}$. We can directly do large ρ expansion of the integrand and find that

$$I_2^{(1)} = \frac{8\alpha_1^2\theta}{\sqrt{3}\pi xy}+\frac{\alpha_1\alpha_3}{\sqrt{3}\pi\rho^4}+O\Big(\frac{1}{\rho^6}\Big), \tag{2.33}$$

where $\theta\equiv\arctan(y/x)$ and $\rho\equiv\frac{\sqrt{3}}{2}\sqrt{x^2+y^2}$. In the part $I_2^{(2)}$, both x' and x'' are localized variables of the integrand. Then, we can directly do large ρ expansion of the integrand and find that

$$I_2^{(2)} = -\frac{2\alpha_1\alpha_3}{\sqrt{3}\pi\rho^4}+O\Big(\frac{1}{\rho^6}\Big), \tag{2.34}$$

where we used the identity $\alpha_n = n(n-1)\int_0^\infty \mathrm{d}x\; x^{n-2}\widehat{u}(x)$ with $n\geq 3$.

In summary, we have obtained the second order of the wave function at large ρ,

$$\psi_2 = \Big\{\sum_{i=1}^{3}\frac{\beta_1}{x_i}+\frac{8\alpha_1^2\theta_i}{\sqrt{3}\pi x_i y_i}\Big\}-\frac{\sqrt{3}\alpha_1\alpha_3}{\pi\rho^4}+O\Big(\frac{1}{\rho^6}\Big). \tag{2.35}$$

Compared to the 111-expansion in Eq. (2.14), we find the scattering length $a = \alpha_1 - \beta_1 + O(V^3)$, which is consistent with the two-body Born approximation. From the $1/\rho^4$ term, we obtain the leading order formula for the three-body scattering hypervolume

$$D = 8\pi^2 \alpha_1 \alpha_3 + O(V^3). \tag{2.36}$$

2.2.3 Third order

One can further calculate the wave function of the third-order Born approximation $\psi_3 = (G\mathcal{V})\psi_2 = \sum_{i=1}^{3} \phi_3(\mathbf{x}_i, \mathbf{y}_i)$, where

$$\phi_3(\mathbf{x}, \mathbf{y}) = \int \mathrm{d}^3x' \mathrm{d}^3y' \; g(\mathbf{x}, \mathbf{y}; \mathbf{x}', \mathbf{y}') V(x') \Big[\phi_2(\mathbf{x}', \mathbf{y}') + \phi_2(\mathbf{x}'_+, \mathbf{y}'_+) + \phi_2(\mathbf{x}'_-, \mathbf{y}'_-) \Big]. \tag{2.37}$$

As $\phi_2 = I_1 + I_2^{(1)} + I_2^{(2)}$, we can write ϕ_3 as a summation of three terms $\phi_3 = J_1 + J_2^{(1)} + J_2^{(2)}$ with

$$\begin{aligned}
J_1(\mathbf{x}, \mathbf{y}) &= \int \mathrm{d}^3x' \mathrm{d}^3y' \; g(\mathbf{x}, \mathbf{y}; \mathbf{x}', \mathbf{y}') V(x') \Big[I_1(\mathbf{x}', \mathbf{y}') + I_1(\mathbf{x}'_+, \mathbf{y}'_+) + I_1(\mathbf{x}'_-, \mathbf{y}'_-) \Big], \\
J_2^{(1)}(\mathbf{x}, \mathbf{y}) &= \int \mathrm{d}^3x' \mathrm{d}^3y' \; g(\mathbf{x}, \mathbf{y}; \mathbf{x}', \mathbf{y}') V(x') \Big[I_2^{(1)}(\mathbf{x}', \mathbf{y}') + I_2^{(1)}(\mathbf{x}'_+, \mathbf{y}'_+) + I_2^{(1)}(\mathbf{x}'_-, \mathbf{y}'_-) \Big], \\
J_2^{(2)}(\mathbf{x}, \mathbf{y}) &= \int \mathrm{d}^3x' \mathrm{d}^3y' \; g(\mathbf{x}, \mathbf{y}; \mathbf{x}', \mathbf{y}') V(x') \Big[I_2^{(2)}(\mathbf{x}', \mathbf{y}') + I_2^{(2)}(\mathbf{x}'_+, \mathbf{y}'_+) + I_2^{(2)}(\mathbf{x}'_-, \mathbf{y}'_-) \Big].
\end{aligned} \tag{2.38}$$

We calculate J_1, $J_2^{(1)}$, and $J_2^{(2)}$ term by term.

As $I_1(\mathbf{x}, \mathbf{y})$ only depends on x, the calculation of J_1 is similar to that of ϕ_2 in Eq. (2.23). We can directly write down the expression of J_1 at large x and y:

$$J_1(\mathbf{x}, \mathbf{y}) = -\frac{\sigma_1}{x} - \frac{8\alpha_1\beta_1\theta}{\sqrt{3}\pi xy} - \frac{\alpha_3\beta_1 - 2\alpha_1\beta_3}{\sqrt{3}\pi\rho^4} + O\Big(\frac{1}{\rho^6}\Big), \tag{2.39}$$

where $\sigma_n \equiv \int_0^\infty \mathrm{d}x \, x^n V(x)\omega(x)$, and we have used the fact $\beta_n = n(n-1)\int_0^\infty \mathrm{d}x \, x^{n-2}\widehat{\omega}(x)$

with $n \geq 3$.

Using Eq. (2.32), $J_2^{(1)}$ can expressed as

$$\begin{aligned} J_2^{(1)}(\mathbf{x},\mathbf{y}) &= \frac{\alpha_1}{\sqrt{3}\pi^2}\int \mathrm{d}^3x'\mathrm{d}^3y'\; g(\mathbf{x},\mathbf{y};\mathbf{x}',\mathbf{y}')V(x')\int \mathrm{d}^3x''V(x'') \\ &\times\Big\{\frac{\arctan\Big(|\mathbf{y}'+\frac{\mathbf{x}''}{\sqrt{3}}|/|\mathbf{x}'-\mathbf{x}''|\Big)}{|\mathbf{y}'+\frac{\mathbf{x}''}{\sqrt{3}}||\mathbf{x}'-\mathbf{x}''|}+\Big(\mathbf{y}'\to-\mathbf{y}'\Big) \\ &+\Big(\mathbf{x}'\to\mathbf{x}'_+,\mathbf{y}'\to\mathbf{y}'_+\Big)+\Big(\mathbf{x}'\to\mathbf{x}'_+,\mathbf{y}'\to-\mathbf{y}'_+\Big) \\ &+\Big(\mathbf{x}'\to\mathbf{x}'_-,\mathbf{y}'\to\mathbf{y}'_-\Big)+\Big(\mathbf{x}'\to\mathbf{x}'_-,\mathbf{y}'\to-\mathbf{y}'_-\Big)\Big\}. \end{aligned} \tag{2.40}$$

We see that in the integral, x' and x'' are both localized variables. Notice that

$$\int \mathrm{d}^3y'\; g(\mathbf{x},\mathbf{y};\mathbf{x}',\mathbf{y}')\frac{Z}{y'^4} = O\Big(\frac{1}{\rho^5}\Big) \tag{2.41}$$

at large x and y. The Z symbol represents the Z functions defined in Ref. [16]. To obtain the $1/\rho^4$ term, we only need the Z-δ expansion [16] of the term in the curly brackets up to the y'^{-3} order at large y'. Here we have the following Z-δ expansions

$$\begin{aligned} \Big\{\frac{\arctan\Big(|\mathbf{y}'+\frac{\mathbf{x}''}{\sqrt{3}}|/d\Big)}{|\mathbf{y}'+\frac{\mathbf{x}''}{\sqrt{3}}|d}+\Big(\mathbf{y}'\to-\mathbf{y}'\Big)\Big\} &= \frac{\pi}{dy'}-\frac{2}{y'^2}+\frac{\pi x''^2}{3dy'^3}P_2(\hat{\mathbf{x}}''\cdot\hat{\mathbf{y}}') \\ &+2\pi^2 d\delta(\mathbf{y}')+O\Big(\frac{1}{y'^4}\Big), \end{aligned} \tag{2.42}$$

and

$$\begin{aligned} &\Big\{\frac{\arctan\Big(|\mathbf{y}'_+ +\frac{\mathbf{x}''}{\sqrt{3}}|/|\mathbf{x}'_+ -\mathbf{x}''|\Big)}{|\mathbf{y}'_+ +\frac{\mathbf{x}''}{\sqrt{3}}||\mathbf{x}'_+ -\mathbf{x}''|}+\Big(\mathbf{y}'_+\to-\mathbf{y}'_+\Big)+\Big(\mathbf{x}'_+\to\mathbf{x}'_-,\mathbf{y}'_+\to\mathbf{y}'_-\Big) \\ &+\Big(\mathbf{x}'_+\to\mathbf{x}'_-,\mathbf{y}'_+\to-\mathbf{y}'_-\Big)\Big\} \\ &=\frac{8\pi}{3\sqrt{3}y'^2}-\frac{8\pi^2}{3}(x'+|\mathbf{x}'+\mathbf{x}''|)\delta(\mathbf{y}')+O\Big(\frac{1}{y'^4}\Big), \end{aligned} \tag{2.43}$$

where $\mathbf{d} \equiv \mathbf{x}' - \mathbf{x}''$, and we have used the identities

$$\int \mathrm{d}^3y \Big[\frac{\arctan(y/d)}{yd} - \Big(\frac{\pi}{2yd} - \frac{1}{y^2}\Big)\Big] = \pi^2 d, \tag{2.44a}$$

$$\int \mathrm{d}^3y \Big[\frac{\arctan(\frac{|\mathbf{y}+\mathbf{u}|}{\sqrt{3}|\mathbf{y}+\mathbf{v}|})}{|\mathbf{y}+\mathbf{u}||\mathbf{y}+\mathbf{v}|} - \frac{\pi}{6y^2}\Big] = -\frac{\pi^2}{4}|\mathbf{u}-\mathbf{v}|, \tag{2.44b}$$

with $\mathbf{u}$ and $\mathbf{v}$ constant vectors. Then, we obtain

$$\begin{aligned} J_2^{(1)}(\mathbf{x},\mathbf{y}) = \Big\{ & \frac{\alpha_1}{\sqrt{3}\pi^2} \int \mathrm{d}^3x' \mathrm{d}^3x'' V(x')V(x'') \int \mathrm{d}^3y'\, g(\mathbf{x},\mathbf{y};\mathbf{x}',\mathbf{y}') \\ & \times \Big[\frac{\pi}{|\mathbf{x}'-\mathbf{x}''|y'} + \frac{2w}{\sqrt{3}y'^2} + \frac{2\pi^2}{3}(3|\mathbf{x}'-\mathbf{x}''| - 4x' - 4|\mathbf{x}'+\mathbf{x}''|)\delta(\mathbf{y}')\Big]\Big\} \\ & + O\Big(\frac{1}{\rho^5}\Big), \end{aligned} \tag{2.45}$$

where the term contains $P_2(\hat{\mathbf{x}}'' \cdot \hat{\mathbf{y}}')$ vanishes after integration. Evaluate the integral term by term, and we find at large x and y,

$$J_2^{(1)}(\mathbf{x},\mathbf{y}) = -\frac{8\alpha_1\beta_1\theta}{\sqrt{3}\pi xy} - \frac{2\alpha_1^3 w}{\pi x\rho^2} + \frac{\alpha_1}{\sqrt{3}\pi\rho^4}\Big(8\alpha_1\alpha_2 - \frac{1}{2}\beta_3 - \widetilde{\beta}_3\Big) + O\Big(\frac{1}{\rho^5}\Big), \tag{2.46}$$

where

$$\widetilde{\beta}_3 = \int_0^\infty \mathrm{d}x \int_0^\infty \mathrm{d}x'\ \min(x,x')x^2x'^2V(x)V(x'). \tag{2.47}$$

Now we calculate $J_2^{(1)}(\mathbf{x},\mathbf{y})$. According to Eq. (2.31), we see that the only non-localized variable of the integrand is $\mathbf{y}'$ in Eq. (2.38). First, we do the Z-δ expansion

$$\begin{aligned} & I_2^{(2)}(\mathbf{x},\mathbf{y}) + I_2^{(2)}(\mathbf{x}_+,\mathbf{y}_+) + I_2^{(2)}(\mathbf{x}_-,\mathbf{y}_-) = \\ & \quad -\frac{4\delta(\mathbf{y})}{3\sqrt{3}\pi} \int \mathrm{d}^3x' \mathrm{d}^3x''\, \frac{V(x')\widehat{u}(x'')}{x''}\Big(\frac{1}{|\mathbf{x}-\mathbf{x}'|} + \frac{1}{|\mathbf{x}-\mathbf{x}''|} + \frac{1}{|\mathbf{x}+\mathbf{x}'+\mathbf{x}''|}\Big) \\ & \quad + O\Big(\frac{1}{y^4}\Big). \end{aligned} \tag{2.48}$$

Straightforwardly, we obtain

$$J_2^{(2)}(\mathbf{x},\mathbf{y}) = \frac{2}{3\sqrt{3}\pi\rho^4}\Big(\frac{3\eta_4}{64\pi^3} + 5\alpha_1^2\alpha_2 + 3\alpha_3\beta_1 + 4\alpha_1\beta_3 - 4\alpha_1\widetilde{\beta}_3\Big) + O\Big(\frac{1}{\rho^5}\Big), \quad (2.49)$$

where

$$\eta_4 = \int \mathrm{d}^3x\mathrm{d}^3x'\mathrm{d}^3x'' \frac{(x-|\mathbf{x}'-\mathbf{x}''|)^2}{x|\mathbf{x}'-\mathbf{x}''|}\min(x,|\mathbf{x}'-\mathbf{x}''|)V(x)V(x')V(x''). \quad (2.50)$$

In summary, we have obtained the third order of the wave function

$$\begin{aligned}\psi_3 &= \Big\{\sum_{i=1}^{3} -\frac{\sigma_1}{x_i} - \frac{16\alpha_1\beta_1\theta_i}{\sqrt{3}\pi x_i y_i} - \frac{2\alpha_1^3 w}{\pi x_i \rho^2}\Big\} \\ &\quad + \frac{1}{2\sqrt{3}\pi\rho^4}\Big(\frac{3\eta_4}{16\pi^3} + 68\alpha_1^2\alpha_2 + 6\alpha_3\beta_1 + 25\alpha_1\beta_3 - 22\alpha_1\widetilde{\beta}_3\Big) + O\Big(\frac{1}{\rho^5}\Big) \quad (2.51)\end{aligned}$$

Compared to the 111-expansion in Eq. (2.14), we find the scattering length

$$a = \alpha_1 - \beta_1 + \sigma_1 + O(V^4), \quad (2.52)$$

and the leading and sub-leading order terms of the three-body scattering hypervolume

$$D = 8\pi^2\alpha_1\alpha_3 - \frac{4\pi^2}{3}\Big(\frac{3\eta_4}{16\pi^3} + 68\alpha_1^2\alpha_2 + 6\alpha_3\beta_1 + 25\alpha_1\beta_3 - 22\alpha_1\widetilde{\beta}_3\Big) + O(V^4), \quad (2.53)$$

where the parameters α_n, β_n, $\widetilde{\beta}_3$, and η_4 are defined in Eq. (2.21), (2.27), (2.47), and (2.50), respectively. Note that the integer subscript gives the dimension of the parameter. For example, η_4 has dimension $[\mathrm{length}]^4$.

2.3 Complex three-body scattering hypervolume and the three-body recombination

The original 21-expansion in Eq. (2.15) is applicable when the interaction does not support any two-body bound state [16]. In this case, the collision of three bosons is elastic and

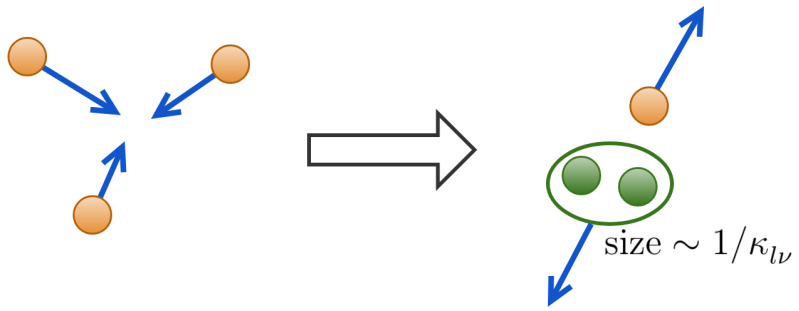

Figure 2.2: The cartoon of the three-body recombination of three atoms. The brown and green disks represent the atoms. After recombination, the two atoms in green form a two-body bound state (a dimer) of size $\sim 1/\kappa_{l\nu}$. The released bind energy $\kappa_{l\nu}^2$ transfer to the kinetic energy of the dimer and the third atom.

the three-body scattering hypervolume D is real. When the two-body pairwise interaction is attractive and strong enough to support two-body bound states, the collision may be inelastic. Three colliding bosons may recombine into a two-body bound state (a dimer) and a free boson (see Figure 2.2). The dimer and the free boson kinetically gain the released binding energy. This process is known as the three-body recombination, which causes heating and atom loss in dilute ultracold gases [28, 29, 30].

The dimer and the free boson form an outgoing wave. At large hyperradii, the wave function of three bosons colliding at zero energy can be expressed as

$$\psi = \phi_0 + \sum_{l=0}^{l_{\max}} \sum_{\nu=0}^{\nu_l} C_{l\nu} \Big[\phi_{l\nu}(\mathbf{x}, \mathbf{y}) + \phi_{l\nu}(\mathbf{x}_+, \mathbf{y}_+) + \phi_{l\nu}(\mathbf{x}_-, \mathbf{y}_-) \Big], \tag{2.54}$$

where ϕ_0 is the incoming wave plus the elastically scattered wave. ϕ_0 obeys the original 111- and 21-expansions in Eq. (2.14) and (2.15). $\phi_{l\nu}(\mathbf{x}, \mathbf{y})$ is the outgoing wave in the $l\nu$-channel, where l and ν are the orbital angular momentum quantum number and the vibrational quantum number of the dimer, respectively. ν_l is the maximum ν at a particular l, and $l_{\max}$ is the maximum l for the dimer states. At large y, such that the free boson is outside the range of interaction with the other two bosons, $\phi_{l\nu}$ can be expressed as

$$\phi_{l\nu}(\mathbf{x}, \mathbf{y}) = X_{l\nu}(x) \mathrm{i}^{l+1} h_l^{(1)}(\kappa_{l\nu} y) P_l(\hat{\mathbf{x}} \cdot \hat{\mathbf{y}}), \tag{2.55}$$

where P_l is the Legendre polynomial, $h_l^{(1)}$ is the spherical Hankel function of the first kind, and $\kappa_{l\nu} > 0$ is the binding wave number defined such that the binding energy of the dimer is $\kappa_{l\nu}^2$. $X_{l\nu}(x)$ is the radial part of the dimer wave function, satisfying the two-body Shrödinger equation and the normalization condition

$$[-\nabla_x^2 + V(x) + \kappa_{l\nu}^2] X_{l\nu}(x) P_l(\hat{\mathbf{x}} \cdot \hat{\mathbf{y}}) = 0, \tag{2.56}$$

$$\int_0^\infty \mathrm{d}x\, x^2 X_{l\nu}^*(x) X_{l\nu'}(x) = \delta_{\nu\nu'}(2l+1)/4\pi\kappa_{l\nu}^3. \tag{2.57}$$

At large x, $X_{l\nu}(x) \propto \exp(-\kappa_{l\nu} x)$ is exponentially decaying.

The outgoing wave contributes to a positive probability flux towards the outside of a large hyperspherical surface with hyperradius ρ_c. To make the net flux vanish and conserve the probability, D gains a negative imaginary. We can see this by computing the flux through the hyperspherical surface

$$\Phi = \int \mathrm{d}^5\Omega_\rho \hat{\mathbf{n}} \cdot \mathbf{j}, \tag{2.58}$$

where $\hat{\mathbf{n}} = (\frac{\mathbf{x}}{\sqrt{x^2+y^2}}, \frac{\mathbf{y}}{\sqrt{x^2+y^2}})$ is the normal unit vector in six-dimensional space $(\mathbf{x}, \mathbf{y})$, and Ω_ρ denotes the 5-dimensional hyperspherical surface area element. Here

$$\mathbf{j} = \mathrm{Im}(\psi^* \nabla_6 \psi), \tag{2.59}$$

where Im takes the imaginary part, and $\nabla_6 \equiv (\nabla_{\mathbf{x}}, \nabla_{\mathbf{y}})$ the six-dimensional gradient. We see that a part of the flux due to the outgoing wave formed by the recombination product is

$$\mathrm{Im} \int \mathrm{d}^5\Omega_\rho\, \phi_{l\nu}^* \hat{\mathbf{n}} \cdot \nabla_6 \phi_{l\nu} = \frac{4\pi}{\kappa_{l\nu}^4} + O\Big(\frac{1}{\rho_c}\Big). \tag{2.60}$$

Notice that from Eq. (2.14),

$$\mathrm{Im}\int \mathrm{d}^5\Omega_\rho\, \phi_0^*\hat{\mathbf{n}}\cdot\nabla\phi_0 = \frac{8}{3\sqrt{3}}\mathrm{Im}(D) + O\Big(\frac{1}{\rho_c}\Big). \tag{2.61}$$

Also, all the mixed terms containing both ϕ_0 and $\phi_{l\nu}$ have contribution $O(1/\rho_c)$. Because the net flux in Eq. (2.58) vanishes, we establish the following relation

$$\mathrm{Im}(D) = -\frac{9\pi\sqrt{3}}{2}\sum_{l\nu}\frac{|C_{l\nu}|^2}{\kappa_{l\nu}^4}, \tag{2.62}$$

where the summation is over all the dimer states. This relation shows that the imaginary part of the three-body scattering hypervolume characterizes the overall inelastic collision of three bosons.

When D becomes complex, the ground state energy in Eq. (1.2) gains a negative imaginary part, indicating the decaying of the BEC. At a short time t, the probability that no recombination occurs is $\exp(-2|\mathrm{Im}(E)|t) \approx 1 - 2|\mathrm{Im}(E)|t$. Then, the probability for one recombination is $2|\mathrm{Im}(E)|t$. After each recombination, three atoms escape from the trap. Therefore, the expectation of the atom number after a short time t is

$$N(t) \approx N(0)\Big[1 - 2|\mathrm{Im}(E)|t\Big] + \Big[N(0) - 3\Big]\Big(2|\mathrm{Im}(E)|t\Big). \tag{2.63}$$

Then, we can obtain the derivative $N'(t) = -6|\mathrm{Im}(E)|t$. Together with Eq. (1.2), we find the formula of the three-body recombination rate constant (with SI units recovered)

$$L_3 = -\frac{\hbar}{m}\mathrm{Im}(D), \tag{2.64}$$

where L_3 is defined as $\mathrm{d}n/\mathrm{d}t = -L_3 n^3$. Notice that $\mathrm{Im}(D)$ is always negative and L_3 is positive. According to the relation between D and the three to three scattering coupling constant g_3, Eq. (2.64) is consistent with the effective field theory formulation [16, 14].

More importantly, from Eq. (2.62), the number of the produced dimers in each channel can be predicted given the coefficient $C_{l\nu}$ and the binding wave number $\kappa_{l\nu}$.

2.4 Numerical calculation of D

For a general pairwise short-range interaction, we need to solve the Shrödinger equation numerically to extract D and the coefficients $C_{l\nu}$. At a large hyperadious ρ, the wave function ψ can be approximated by the outgoing wave function and the asymptotic 111- and 21-expansions according to Eq. (2.54). We can treat it as the Dirichlet boundary condition on a large hyperspherical surface with $\rho = \rho_c$. Then, the wave function inside the hypersphere is uniquely determined. The unknown D and $C_{l\nu}$ can be fixed by making the hyperradial derivative of the wave function continuous along the hyperradial direction.

2.4.1 The improved expansions

To have the Dirichlet boundary condition, we need an accurate wave function on the hyperspherical surface. However, the 111- and 21-expansions do not have the same error $O(1/\rho_c^8)$ uniformly on the whole hyperspherical surface [16]. The 111-expansion has been obtained up to the $1/\rho^7$ order (with the ratio $x_1 : x_2 : x_3$ fixed), and the 21-expansion up to the $1/y^7$ order (with x fixed) [16]. This means that the 111-expansion has error $O(1/x_{\min}^8)$ with $x_{\min}$ the minimum of the three distances x_1, x_2, and x_3, and the 21-expansion $O(1/y^8)$. On a large hyperspherical surface with hyperradius ρ_c in the six dimensional space $(\mathbf{x}, \mathbf{y})$, both expansions may have larger errors than $O(1/\rho_c^8)$ in the intermediate region $r_e \ll x \ll y$. For example, when $x \sim \rho_c^{1/3}$, and $y \sim \rho_c$, the error of both expansions are $O(1/\rho_c^6)$. We can see this by expressing both expansions in the following form,

$$\phi^{(111)} = \sum_{s=0}^{\infty} \sum_{n} t^{(s-n,n)}(\mathbf{x}, \mathbf{y}), \quad \phi^{(21)} = \sum_{s=0}^{\infty} \sum_{m} t^{(m,s)}(\mathbf{x}, \mathbf{y}). \tag{2.65}$$

Here $t^{(m,n)}(\mathbf{x},\mathbf{y})$ scales like $\frac{1}{x^m y^n}$. More exactly, by scaling $\mathbf{x} \to \lambda_1 \mathbf{x}$, and $\mathbf{y} \to \lambda_2 \mathbf{y}$, we have

$$t^{(m,n)}(\lambda_1 \mathbf{x}, \lambda_2 \mathbf{y}) = \frac{1}{\lambda_1^m \lambda_2^n} t^{(m,n)}(\mathbf{x},\mathbf{y}). \tag{2.66}$$

In Figure 2.3, we label all the non-zero terms in the 111- and 21-expansions. We see that the two set of terms have an overlap at locations of (m,n) with both red disk and blue circle. The 111-expansion (21-expansion) misses the terms at locations with blue circle (red disk) only. The largest term with blue circle only, or red disk only is $t^{(3,5)}(\mathbf{x},\mathbf{y})$, or $t^{(-6,8)}(\mathbf{x},\mathbf{y})$, which serves as the error of 111- or 21-expansion, respectively. We can simply equate the two terms

$$t^{(3,5)}(\mathbf{x},\mathbf{y}) \sim t^{(-6,8)}(\mathbf{x},\mathbf{y}), \text{ or } \frac{1}{x^3 y^5} \sim \frac{x^6}{y^8}, \tag{2.67}$$

then we get $x \sim y^{1/3}$. Thus, the error is $O(1/\rho_c^6)$ when $x \sim \rho_c^{1/3}$, and $y \sim \rho_c$. Then, on a large hyperspherical suface with hyperradius ρ_c, the two expansions do not have error $O(1/\rho_c^8)$ uniformly everywhere. Note that the three-body scattering hypervolume D appears in the $1/\rho_c^4$ order. In the numerical evaluation, the error of D is $O(1/\rho_c^2)$, as the wave function has error $O(1/\rho_c^6)$ in the intermediate region $r_e \ll x \ll y$. Thus, the error may not be sufficiently small for accurate numerical evaluations of D, as it is difficult to calculate the three-body wave function at large ρ_c.

There are two possible ways to reduce the overall error of the two expansions on the hyperspherical surface: 1) directly obtaining more high order terms in both expansions, or 2) improving the two expansions in the intermediate regions $r_e \ll x \ll y$.

To obtain the $1/\rho^8$ $(1/y^8)$ term in the 111-expansion (21-expansion), we need to introduce another three-body scattering parameter in addition to D. We can see this by simply considering three bosons with short-range three-body interaction only. The wave function satisfies the following Schrödinger equation

$$-(\nabla_{\mathbf{x}}^2 + \nabla_{\mathbf{y}}^2)\psi + V_3(\mathbf{x}_1,\mathbf{x}_2,\mathbf{x}_3)\psi = 0, \tag{2.68}$$

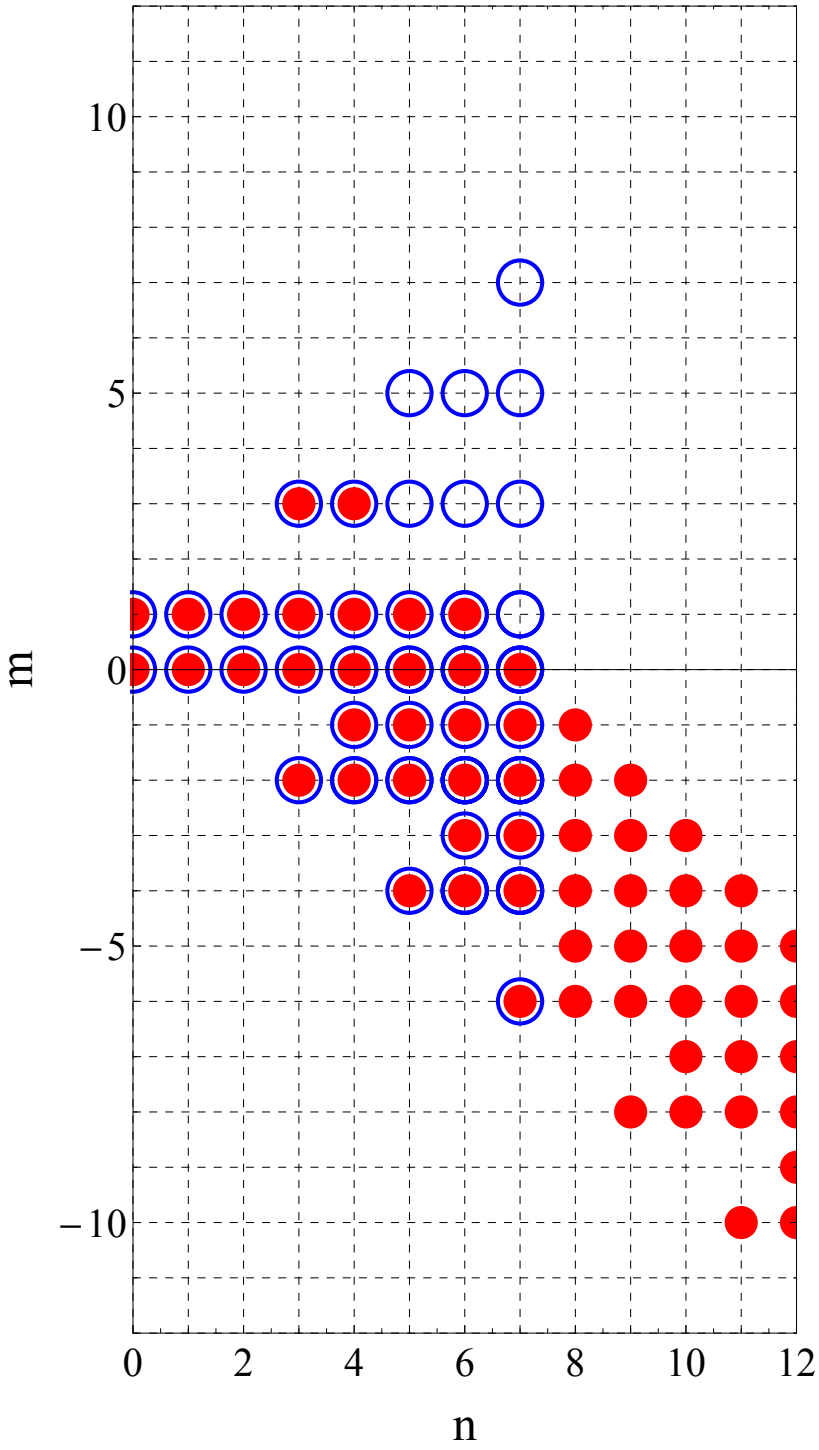

Figure 2.3: The plot of nonzero term $t^{(m,n)}(\mathbf{x},\mathbf{y})$ in the 111- and 21-expansions up to $s=7$ in Eq. (2.65). Each of the red disks (blue circles) represents a nonzero term $t^{(m,n)}(\mathbf{x},\mathbf{y})$ in the 111-expansion (21-expansion).

where $V_3(\mathbf{x}_1, \mathbf{x}_2, \mathbf{x}_3)$ vanishes when the hyperradius ρ exceeds a certain range ρ_e. If we approximate V_3 by a pseudo potential such that

$$V_3\psi = \frac{8D}{3\sqrt{3}}\delta(\mathbf{x})\delta(\mathbf{y}), \tag{2.69}$$

we can easily recover the first two terms of the 111-expansion

$$\psi = 1 - \frac{\sqrt{3}D}{8\pi^3\rho^4}. \tag{2.70}$$

More accurately, we can include one more high order term in the pseudo potential

$$V_3\psi = \frac{8D}{3\sqrt{3}}\delta(\mathbf{x})\delta(\mathbf{y}) + D'p_n(\nabla_\mathbf{x}, \nabla_\mathbf{y})[\delta(\mathbf{x})\delta(\mathbf{y})] + \cdots, \tag{2.71}$$

where D' is another three-body scattering parameter and $p_n(\mathbf{x}, \mathbf{y})$ is a n-degree harmonic polynomial of $\mathbf{x}$ and $\mathbf{y}$, or equivalently $\mathbf{x}_1$, $\mathbf{x}_2$, and $\mathbf{x}_3$.[2] Due to the exchange symmetry of the bosonic system, $p_n(\mathbf{x}, \mathbf{y})$ is invariant under any exchange of three bosons, equivalently, the inversion $\mathbf{x}_i \to -\mathbf{x}_i$ ($i = 1$, 2, or 3), and any permutation of $(\mathbf{x}_1, \mathbf{x}_2, \mathbf{x}_3)$. The smallest nonzero n is 4, and we find

$$p_4(\mathbf{x}, \mathbf{y}) = x_1^4 + x_2^4 + x_3^4 - 3(x_1^2x_2^2 + x_2^2x_3^2 + x_3^2x_1^2). \tag{2.72}$$

Then, the corresponding solution to the source $p_4(\nabla_\mathbf{x}, \nabla_\mathbf{y})[\delta(\mathbf{x})\delta(\mathbf{y})]$ will be D' times a term of order $1/\rho^8$. Similarly, D' also appears in the $1/y^8$ term in the 21-expansion. The appearance of the parameter D' may complicate the numerical calculation of the three-body scattering hypervolume D.

Instead of directly obtaining more higher order terms in the 111- and 21-expansions, we consider improving the two expansions in the intermediate region without introducing another three-body parameter. On the hyperspherical surface with hyperradius ρ_c, when

[2] See the Z-δ expansions in Ref. [16].

$x \sim r_e$ and $y \sim \rho_c$, the 21-expansion error $O(1/\rho_c^8)$, but the 111-expansion has a much larger error $O(1/x^8)$. The reason is that the 111-expansion does not have the terms labeled by the blue circles only in Figure 2.3. If we obtain the corresponding terms in the 111-expansion such that all the blue circles contains red disks inside, the 111-expansion will always have error $O(1/\rho_c^8)$ when $x > r_e$. As a result, we have an accurate three-body wave function, which described by the 21-expansion when $x < r_e$ and the 111-expansion when $x > r_e$.

Now we calculate the extra terms by considering the following Poisson equation in six dimensions,

$$(\nabla_{\mathbf{x}}^2 + \nabla_{\mathbf{y}}^2)\psi(\mathbf{x}, \mathbf{y}) = S(\mathbf{x}_1, \mathbf{y}_1) + S(\mathbf{x}_2, \mathbf{y}_2) + S(\mathbf{x}_3, \mathbf{y}_3), \tag{2.73}$$

where the source term

$$S(\mathbf{x}, \mathbf{y}) = V(x)\psi(\mathbf{x}, \mathbf{y}). \tag{2.74}$$

Here we have assumed that the interaction only contains the pairwise two-body interactions. We can approximate the source term by using the pseudo potential, or equivalently do the Z-δ expansion at large y,

$$\begin{aligned} S(\mathbf{x}, \mathbf{y}) &= u^{(s)}(\mathbf{y})\delta(\mathbf{x}) + u^{(d)}(\mathbf{y})Q^{(d)}_{\hat{\mathbf{y}}}(\nabla_{\mathbf{x}})\delta(\mathbf{x}) + u^{(g)}(\mathbf{y})Q^{(g)}_{\hat{\mathbf{y}}}(\nabla_{\mathbf{x}})\delta(\mathbf{x}) \\ &\quad + u^{(i)}(\mathbf{y})Q^{(i)}_{\hat{\mathbf{y}}}(\nabla_{\mathbf{x}})\delta(\mathbf{x}) + \cdots, \end{aligned} \tag{2.75}$$

where $Q^{(l)}_{\hat{\mathbf{n}}}(\mathbf{x}) \equiv x^l P_l(\hat{\mathbf{n}} \cdot \hat{\mathbf{x}})$ is the harmonic polynomial of degree l, and $u^{(l)}(\mathbf{y})$ is the series of $1/y$ represented by the Z functions [16]. We can obtain $u^{(l)}$ by applying the Laplace operator $(\nabla_{\mathbf{x}}^2 + \nabla_{\mathbf{y}}^2)$ on the 21-expanison $\phi^{(21)}$. First, we treat the two-body special function $\phi^{(l)}_{\hat{\mathbf{n}}}(\mathbf{r})$ in Eq. (2.5) and its continuation inside the range of interaction as the pseudo

two-body wave function, satisfying

$$\nabla^2_{\mathbf{r}}\phi^{(l)}_{\hat{\mathbf{n}}}(\mathbf{r}) = (-1)^l 4\pi a_l Q^{(l)}_{\hat{\mathbf{n}}}(\nabla_{\mathbf{r}})\delta(\mathbf{r}). \tag{2.76}$$

Then, we find the leading orders: $u^{(s)}(\mathbf{y}) \sim 1$, $u^{(d)}(\mathbf{y}) \sim 1/y^3$, $u^{(g)}(\mathbf{y}) \sim 1/y^5$, and $u^{(i)}(\mathbf{y}) \sim 1/y^7$. The terms in the 21-expansion with blue circles only in Figure 2.3 corresponds to the following terms in the source:

- the $1/y^7$ order term of $u^{(s)}(\mathbf{y})$,
- $1/y^5$, $1/y^6$, and $1/y^7$ of $u^{(d)}(\mathbf{y})$,
- $1/y^5$, $1/y^6$, and $1/y^7$ of $u^{(g)}(\mathbf{y})$,
- $1/y^7$ of $u^{(i)}(\mathbf{y})$.

The solution of Eq. (2.73) due to these sources has not been included in the 111-expansion in Eq. (2.14) and are exactly the extra terms that let the 111-expansion have error $O(1/\rho_c^8)$ whenever $x > r_e$. By solving the Eq. (2.73) with above sources (see Appendix A for details), we found the improved 111-expansion

$$\begin{aligned}
\widetilde{\phi}^{(111)} &= \phi^{(111)} + \sum_{i=1}^{3}\Big\{\frac{U_8^{(0)}(t,\theta_i)}{\rho^8} + \frac{U_8^{(2)}(t,\theta_i)}{\rho^8}P_2(\hat{\mathbf{x}}_i\cdot\hat{\mathbf{y}}_i) + \frac{U_9^{(2)}(t,\theta_i)}{\rho^9}P_2(\hat{\mathbf{x}}_i\cdot\hat{\mathbf{y}}_i) \\
&\quad + \frac{U_{10}^{(2)}(t,\theta_i)}{\rho^{10}}P_2(\hat{\mathbf{x}}_i\cdot\hat{\mathbf{y}}_i) + \frac{U_{10}^{(4)}(t,\theta_i)}{\rho^{10}}P_4(\hat{\mathbf{x}}_i\cdot\hat{\mathbf{y}}_i) + \frac{U_{11}^{(4)}(t,\theta_i)}{\rho^{11}}P_4(\hat{\mathbf{x}}_i\cdot\hat{\mathbf{y}}_i) \\
&\quad + \frac{U_{12}^{(4)}(t,\theta_i)}{\rho^{12}}P_4(\hat{\mathbf{x}}_i\cdot\hat{\mathbf{y}}_i) + \frac{U_{14}^{(6)}(t,\theta_i)}{\rho^{14}}P_6(\hat{\mathbf{x}}_i\cdot\hat{\mathbf{y}}_i)\Big\},
\end{aligned} \tag{2.77}$$

where the term $U_n^{(l)}(t,\theta_i)$ depends on t and θ_i, not the directions of $\mathbf{x}_i$ and $\mathbf{y}_i$:

$$\begin{aligned}
U_8^{(0)}(t,\theta_i) &= \frac{\sqrt{3}a}{\pi^2\sin 2\theta_i}\Big[\zeta_4(-5\pi^2+274t-60t^2+60\theta_i^2)\sin 6\theta_i \\
&\quad + 2\zeta_4(60t-137)\theta_i\cos 6\theta_i + 60\xi_4(\theta_i\cos 6\theta_i - t\sin 6\theta_i)\Big],
\end{aligned} \tag{2.78a}$$

$$\begin{aligned}
U_8^{(2)}(t,\theta_i) &= \frac{45\sqrt{3}wa^3a_d}{2\pi^2\sin^2 2\theta_i}\Big[32t\sin^4 2\theta_i + 9\cos 4\theta_i - 3\cos 8\theta_i
\end{aligned}$$

$$+2\theta_i\Big(-3\cot\theta_i-8\sin 4\theta_i+2\sin 8\theta_i+3\tan\theta_i\Big)\Big], \tag{2.78b}$$

$$U_9^{(2)}(t,\theta_i) = \frac{27\sqrt{3}a_d\xi_3^{(d)}\tan^2\theta_i}{\pi^2\cos\theta_i}\Big[65+106\cos 2\theta_i+50\cos 4\theta_i+10\cos 6\theta_i\Big], \tag{2.78c}$$

$$\begin{aligned}U_{10}^{(2)}(t,\theta_i) = {}& \frac{-9a_d(10968a^5w+245\sqrt{3}\pi\xi_4^{(d)})}{56\pi^3\sin^3 2\theta_i}\Big[12\theta_i\Big(5\cos 4\theta_i-4\cos 8\theta_i+\cos 12\theta_i\Big)\\ &+2\Big(8-16\cos 4\theta_i+5\cos 8\theta_i-96t\sin^4 2\theta_i\Big)\sin 4\theta_i\Big]\\ &+\frac{-405wa^5a_d}{\pi^3\sin^3 2\theta_i}\Big[-4\sin^2 2\theta_i\Big(-6\theta_i-12\theta_i\cos 4\theta_i+10\theta_i\cos 8\theta_i\\ &-8(\pi^2-12\theta_i^2)\cos 2\theta_i\sin^3 2\theta_i+\sin 8\theta_i\Big)\\ &-24t\theta_i\Big(5\cos 4\theta_i-4\cos 8\theta_i+\cos 12\theta_i\Big)\\ &-2t\Big(11\sin 4\theta_i-16\sin 8\theta_i+5\sin 12\theta_i\Big)\\ &+384t^2\cos 2\theta_i\sin^5 2\theta_i\Big],\end{aligned} \tag{2.78d}$$

$$\begin{aligned}U_{10}^{(4)}(t,\theta_i) = {}& \frac{8505\sqrt{3}aa_g}{64\pi\sin^5 2\theta_i}\Big[1680\theta_i-672\sin 4\theta_i+168\sin 8\theta_i-32\sin 12\theta_i\\ &+3\sin 16\theta_i\Big],\end{aligned} \tag{2.78e}$$

$$\begin{aligned}U_{11}^{(4)}(t,\theta_i) = {}& \frac{1215(405-76\sqrt{3}\pi)a^2a_g\tan^4\theta_i}{2\pi\cos\theta_i}\Big[711+1086\cos 2\theta_i\\ &+494\cos 4\theta_i+126\cos 6\theta_i+14\cos 8\theta_i\Big],\end{aligned} \tag{2.78f}$$

$$\begin{aligned}U_{12}^{(4)}(t,\theta_i) = {}& -\frac{8505\sqrt{3}wa^3a_g}{32\pi^2\sin^5 2\theta_i}\Big[-6144t\sin^9 2\theta_i\\ &+24\theta_i\Big(126\cos 2\theta_i-84\cos 6\theta_i+36\cos 10\theta_i-9\cos 14\theta_i+\cos 18\theta_i\Big)\\ &+5\Big(165\sin 2\theta_i-278\sin 6\theta_i+150\sin 10\theta_i-42\sin 14\theta_i\\ &+5\sin 18\theta_i\Big)\Big],\end{aligned} \tag{2.78g}$$

$$\begin{aligned}U_{14}^{(6)}(t,\theta_i) = {}& -\frac{10945935\sqrt{3}aa_i}{256\pi\sin^7 2\theta_i}\Big[55440\theta_i-23760\sin 4\theta_i+7425\sin 8\theta_i\\ &-2200\sin 12\theta_i+495\sin 16\theta_i-72\sin 20\theta_i+5\sin 24\theta_i\Big].\end{aligned} \tag{2.78h}$$

The improved 111-expansion plus the 21-expansion provided us an accurate Dirichlet boundary condition such that the wave function inside the hypersphere is uniquely determined.

2.4.2 Cone, Zernike polynomials, and hyperradial equations

Now we solve the Schrödinger equation Eq. (2.13). We assume that the three bosons collide at zero energy, zero total momentum and zero total orbital angular momentum. Then, the wave function is invariant under any translation or rotation in the three-dimensional space. Instead of 9 degrees of freedom, the motion of the three bosons is determined by three variables, which conveniently can be chosen to be the three interparticle distances x_1, x_2, and x_3. In the space of (x_1, x_2, x_3), the allowed region is confined by the triangular inequalities $|x_2 - x_3| \leq x_1 \leq x_2 + x_3$. As the wave function only depends on (x_1, x_2, x_3), the Laplace operator in Eq. (2.13) becomes

$$\begin{aligned}\frac{1}{2}(\nabla_1^2 + \nabla_2^2 + \nabla_3^2)\psi(x_1, x_2, x_3) = \Big[\Big(\frac{2}{x_1}\frac{\partial}{\partial x_1} + \frac{\partial^2}{\partial x_1^2}\Big) + \frac{x_2^2 + x_3^2 - x_1^2}{2x_2x_3}\frac{\partial^2}{\partial x_2 \partial x_3} \\ + \Big(\frac{2}{x_2}\frac{\partial}{\partial x_2} + \frac{\partial^2}{\partial x_2^2}\Big) + \frac{x_3^2 + x_1^2 - x_2^2}{2x_3x_1}\frac{\partial^2}{\partial x_3 \partial x_1} \\ + \Big(\frac{2}{x_3}\frac{\partial}{\partial x_3} + \frac{\partial^2}{\partial x_3^2}\Big) + \frac{x_1^2 + x_2^2 - x_3^2}{2x_1x_2}\frac{\partial^2}{\partial x_1 \partial x_2}\Big]\psi(x_1, x_2, x_3). \qquad (2.79)\end{aligned}$$

To simplify the expression and better parametrize the allowed region, we can use another set of variables

$$\eta_1 \equiv x_1^2, \quad \eta_2 \equiv x_2^2, \quad \eta_3 \equiv x_3^2, \qquad (2.80)$$

and the triangular inequalities lead to $\eta_1^2 + \eta_1^2 + \eta_1^2 - 2\eta_1\eta_2 - 2\eta_2\eta_3 - 2\eta_3\eta_1 \leq 0$. The allowed region in the space of (η_1, η_2, η_3) is inside a cone with its vertex located at the origin and its lateral surface tangent to the three axial planes ($\eta_1 = 0, \eta_2 = 0, \eta_3 = 0$) in the first octant (see Figure 2.4). The hyperspherical surface with $\rho = \rho_c$ corresponds to the base of the cone with $\eta_1 + \eta_2 + \eta_3 = 2\rho_c^2$. Now we can use the dimensionless variables (λ, r, Θ) to parametrize the region inside the cone with $0 \leq \lambda \leq 1$, $0 \leq r \leq 1$, $-\pi \leq \Theta < \pi$, and

$$\eta_1 = \frac{2}{3}\rho_c^2\lambda^2\Big[1 - r\cos\Theta\Big]$$

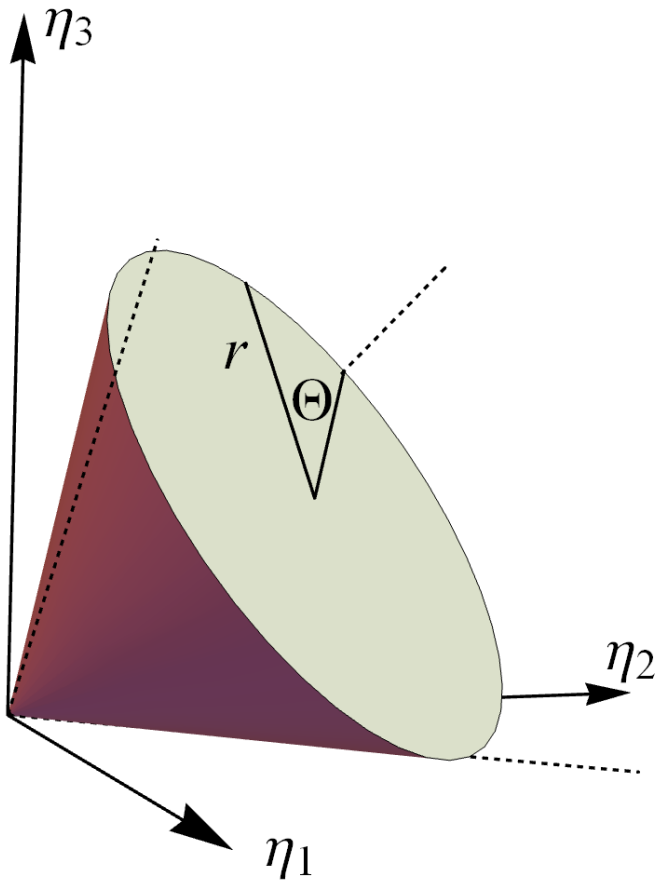

Figure 2.4: The allowed region displayed as a cone in the space of (η_1, η_2, η_3). The base of the cone is of constant hyperradius $\rho = \rho_c$ with $\eta_1 + \eta_2 + \eta_3 = 2\rho_c^2$. The lateral surface is tangent to the three axial planes ($\eta_1 = 0, \eta_2 = 0, \eta_3 = 0$) in the first octant. The dashed lines represent their intersections. The bottom disk is parameterized by the normalized radius r and the angle Θ, where $0 \leq r \leq 1$ and $-\pi \leq \Theta < \pi$. At $\Theta = 0, 2\pi/3$, or $-2\pi/3$, $\eta_1 = 0$, $\eta_2 = 0$, or $\eta_3 = 0$, respectively.

$$\begin{aligned} \eta_2 &= \frac{2}{3}\rho_c^2\lambda^2\Big[1 - r\cos\Big(\Theta - \frac{2\pi}{3}\Big)\Big] \\ \eta_3 &= \frac{2}{3}\rho_c^2\lambda^2\Big[1 - r\cos\Big(\Theta + \frac{2\pi}{3}\Big)\Big]. \end{aligned} \tag{2.81}$$

We see that $\lambda = \rho/\rho_c$. From Eq. (2.55), we see that the outgoing wave has a factor $\exp(\mathrm{i}\kappa_{l\nu}y) \sim \exp(\mathrm{i}\kappa_{l\nu}\rho)$ at large ρ. Then, during the numerical calculation, it is better to discretized ρ with equal spacing in the hyperradial direction. This is the reason to make the parameter λ linear instead of quadratic in ρ.

Then, the Laplace operator further becomes

$$\frac{1}{2}(\nabla_1^2+\nabla_2^2+\nabla_3^2)\psi(x_1,x_2,x_3)=\frac{3}{\rho_c^2}\Big(\frac{1}{4}\frac{\partial^2}{\partial\lambda^2}+\frac{5}{4\lambda}\frac{\partial}{\partial\lambda}-\frac{\widehat{T}_{r\Theta}}{\lambda^2}\Big)\psi(\lambda,r,\Theta). \tag{2.82}$$

Here $\widehat{T}_{r\Theta}$ is an operator on the unit disk

$$\widehat{T}_{r\Theta}=-\Big[(1-r^2)\frac{\partial^2}{\partial r^2}+\frac{1-3r^2}{r}\frac{\partial}{\partial r}+\frac{1}{r^2}\frac{\partial^2}{\partial\Theta^2}\Big]. \tag{2.83}$$

We find the normalized eigenfunction of this operator

$$\widehat{T}_{r\Theta}\varphi_{nm}(r,\Theta)=n(n+2)\varphi_{nm}(r,\Theta), \tag{2.84}$$

$$\varphi_{nm}(r,\Theta)=\sqrt{\frac{2n+2}{\epsilon_m\pi}}R_n^m(r)\cos m\Theta, \tag{2.85}$$

satisfying the normalization condition $\int_0^1 \mathrm{d}r\int_{-\pi}^{\pi}\mathrm{d}\Theta\ r\varphi^*_{nm}(r,\Theta)\varphi_{n'm'}(r,\Theta)=\delta_{nn'}\delta_{mm'}$. Here $\epsilon_m=2$ if $m=0$, or $\epsilon_m=1$ if $m\neq 0$. We see that $\varphi_{nm}(r,\Theta)$ is the normalized even Zernike polynomials with degree n on a unit disk, and $R_n^m(r)$ is the radial Zernike polynomials ($R_n^n(r)\equiv r^n$). We have the following constraints:

- n and m are nonnegative integers,
- $n\geq m$ and $n-m$ is even,
- m is a multiple of 3.

We can verify that under this definition $\varphi_{nm}(r,\Theta)$ is invariant under arbitrary combinations of operations $\Theta\rightarrow-\Theta$ and $\Theta\rightarrow\Theta+2\pi/3$, which are equivalently any the possible permutations of the three particles. This is required by the bosonic nature of the system. Then, we can use the set of the basis functions $\varphi_{nm}(r,\Theta)$ to expand the three-boson wave function on a hyperspherical surface.

Notice that previously people have used the symmetrized hyperspherical harmonics on the five-dimensional hyperspherical surface to expand the three-boson wave function [74].

We do the same thing by mapping the five-dimensional hyperspherical surface to a unit disk and using the Zernike polynomials. Then, we have revealed the unique correspondence between the symmetrized hyperspherical harmonics and the Zernike polynomials. The latter is much conceptually simpler and easier to implement.

Using the Zernike polynomials, we can expand the three-body wave function

$$\psi(\lambda, r, \Theta) = \sum_{nm} \psi_{nm}(\lambda)\varphi_{nm}(r, \Theta). \tag{2.86}$$

Then, the Schrödinger equation becomes a set of ordinary differential equations

$$\frac{3}{\rho_c^2}\Big(-\frac{1}{4}\frac{\mathrm{d}^2}{\mathrm{d}\lambda^2} - \frac{5}{4\lambda}\frac{\mathrm{d}}{\mathrm{d}\lambda} + \frac{n(n+2)}{\lambda^2}\Big)\psi_{nm}(\lambda) + \sum_{n'm'} V_{nm,n'm'}(\lambda)\psi_{n'm'}(\lambda) = 0, \tag{2.87}$$

where the hyperradial part of the wave function

$$\psi_{nm}(\lambda) = \int_0^1 \mathrm{d}r \int_{-\pi}^{\pi} \mathrm{d}\Theta \; r\varphi^*_{nm}(r, \Theta)\psi(\lambda, r, \Theta), \tag{2.88}$$

and the potential matrix element

$$V_{nm,n'm'}(\lambda) = \int_0^1 \mathrm{d}r \int_{-\pi}^{\pi} \mathrm{d}\Theta \; r\varphi^*_{nm}(r, \Theta)\varphi_{n'm'}(r, \Theta)\Big[V(x_1) + V(x_2) + V(x_3)\Big], \tag{2.89}$$

with the three distances x_1, x_2, and x_3 related to (λ, r, Θ) through Eq. (2.81).

We can numerically solve Eq. (2.87) with the Dirichlet boundary conditions. At $\lambda = 0$, we have $\psi_{nm}(0) = 0$ if $n = 0$, or $\psi'_{nm}(0) = 0$ if $n \neq 0$. At $\lambda = 1$ ($\rho = \rho_c$) and large ρ_c, we use the three-body wave function in Eq. (2.54) as the Dirichlet boundary condition. Then, at $\lambda = 1$, we obtain the values of $\psi_{nm}(1)$ with error $O(1/\rho_c^8)$. Notice that the three-body wave function is linear in the unknown parameters D and $C_{l\nu}$. The values of $\psi_{nm}(1)$ are linear in D and $C_{l\nu}$. So are the numerical solution of Eq. (2.87). To evaluate D and $C_{l\nu}$, we need to impose the condition that the hyperradial derivative of the wave function at $\rho = \rho_c$

is continuous. On one hand, we can get the hyperradial derivative from the numerical solution

$$\frac{\partial}{\partial\lambda}\psi^{(\text{numerical})}(\lambda,r,\Theta)|_{\lambda=1}=\sum_{nm}\left[c_{nm}^{(0)}+c_{nm}^{(1)}D+\sum_{l\nu}c_{nm}^{(l\nu)}C_{l\nu}\right]\varphi_{nm}(r,\Theta), \tag{2.90}$$

where $c_{nm}^{(0)}$, $c_{nm}^{(1)}$, and $c_{nm}^{(l\nu)}$ are constants. On the other hand, the hyperradial derivative can be calculated theoretically through Eq. (2.54), and we get

$$\frac{\partial}{\partial\lambda}\psi^{(\text{theory})}(\lambda,r,\Theta)|_{\lambda=1}=\sum_{nm}\left[d_{nm}^{(0)}+d_{nm}^{(1)}D+\sum_{l\nu}d_{nm}^{(l\nu)}C_{l\nu}\right]\varphi_{nm}(r,\Theta). \tag{2.91}$$

where $d_{nm}^{(0)}$, $d_{nm}^{(1)}$, and $d_{nm}^{(l\nu)}$ are constants. Then, we determine the values of D and $C_{l\nu}$ by minimizing the integral of the norm square of the difference on the disk

$$\begin{aligned}&\int_0^1 \mathrm{d}r\int_{-\pi}^{\pi}\mathrm{d}\Theta\, r\left|\frac{\partial}{\partial\lambda}\psi^{(\text{numerical})}(\lambda,r,\Theta)|_{\lambda=1}-\frac{\partial}{\partial\lambda}\psi^{(\text{theory})}(\lambda,r,\Theta)|_{\lambda=1}\right|^2\\&\quad=\sum_{nm}\left|\left(c_{nm}^{(0)}-d_{nm}^{(0)}\right)+\left(c_{nm}^{(1)}-d_{nm}^{(1)}\right)D+\sum_{l\nu}\left(c_{nm}^{(l\nu)}-d_{nm}^{(l\nu)}\right)C_{l\nu}\right|^2.\end{aligned} \tag{2.92}$$

We see that this quantity is a quadratic form. Then, the values of D and $C_{l\nu}$ is the minimizer of this quadratic form.

2.4.3 Numerical method and the model interaction potentials

Here we discuss the numerical method to solve Eq. (2.87). From the modified 111- and 21-expansions, the Dirichlet boundary condition has error $O(1/\rho_c^8)$, or more precisely $\sim a^8/\rho_c^8$. Also, the outgoing wave of the dimer and the boson in Eq. (2.55) is accurate when y is much greater than the size of the dimer, namely, $\rho_c \gg 1/\kappa_{l\nu}$. Therefore, we need to chose as large ρ_c as possible to have an accurate Dirichlet boundary condition. On the other hand, the area of the region where two bosons are within the range of interaction is about r_e^3/ρ_c^3 times the total area of the unit disk in Figure 2.4. Then, the two-body potential are

highly localized on the hyperspherical surface. For larger ρ_c, we need more basis functions to resolve the localized two-body potential and the two-body part of the wave function. However, the maximum number of basis functions is limited by the numerical computation power (CPU time and memory). Then, we choose a reasonable ρ_c, which leads to relatively small error and requires feasible numerical computation cost. For bosons near a two-body resonance, the two-body scattering length a can be enormously large. This requires an even larger ρ_c and therefore larger number of basis functions. This may exceed the maximum available computation power. Thus, we are not able to calculate the system with very large a due to the limit of available computation power. The maximum a that we have considered is of order $10r_e$. A more efficient way of expanding the wave function on the hyperspehrical surface, such as the adiabatic hyperspherical representation [75], may allow doing calculations for larger a. When $a \gg r_e$, the system is well-decribed by Efimov physics [32, 31, 3] as it enters the universal region.

With a chosen ρ_c, we first discretize the interval from $\rho = 0$ to $\rho = \rho_c$ in the hyperradial direction. The parameter λ takes the discrete values $\lambda_i = i/i_{\max}$ with $i = 0, 1, 2, \cdots, i_{\max}$. Here $i_{\max}$ is set to be large enough such that $\rho_c/i_{\max} \ll 1/\kappa_{l\nu}$. Multiple values of $i_{\max}$ are chosen to make the final result converge. Second, the potential matrix $V_{nm,n'm'}(\lambda_i)$ at each grid point and the Dirichlet boundary condition at $\lambda = 1$ are calculated. We use higher order Gaussian quadrature to numerically evaluate the double integral in Eqs. (2.89) and (2.88). A typical number of quadrature points is 200×200, and the maximum is 360×360. The number of quadrature points is chosen to be large enough to reach a good convergence. We use a finite number of basis functions $\varphi_{nm}(r, \Theta)$ with a maximum degree $n_{\max}$. At large $n_{\max}$, the total number of basis functions is approximately $n_{\max}^2/12$. The convergence about the parameter $n_{\max}$ is also checked. Third, we use a P_{FDM}-point finite difference method to approximate the first order and the second order differential operators.

Thus, after the discretization, the set of differential equations in Eq. (2.87) becomes a linear system. The total number of the nonzero elements of the matrix associated with the

Table 2.1: The values of χ and v_0 of the FD potential in Eq. (2.97), such that the scattering length $a = R/5$ (FD-5) or $a = R/10$ (FD-10).

χ	v_0	
	FD-5 ($a = R/5$)	FD-10 ($a = R/10$)
6	0.7483455036348871	0.3267196389819383
8	0.7651873920145196	0.3327616932142853
10	0.7733313289564459	0.3356198270575988
12	0.7778664686366843	0.3371916222897568
14	0.7806452862366277	0.3381471930271405
16	0.7824690236264082	0.3387710175805677
18	0.7837295278790037	0.3392005444905166

linear system is roughly $i_{\max} P_{\rm FDM} (n_{\max}^2/12)^2$. For a typical set of parameters ($P_{\rm FDM} = 9, n_{\max} = 110, i_{\max} = 200$), the total number of nonzero elements can be about 2×10^9. At large a, more basis functions are used. For example, when $a = 10 r_e$, we use $\rho_c = 50$, $n_{\max} = 300$, $i_{\max} = 250$. Then, the number of nonzero elements is about 10^{11}. To solve this large linear system, we utilize the PETSc package [76, 77, 78] and a distributed parallel method, the generalized minimal residual method (GMRES) [79].

As the three-body wave function is expanded in the basis functions on the large hyperspherical surface, we use smooth potentials to have optimal convergence. Here we consider bosons with several model interaction potentials, listed as follows.

1) The Gaussian potential:

$$V^{(\rm G)}(r) = \frac{v_0}{R^2} \exp(-\frac{r^2}{R^2}). \tag{2.93}$$

2) The FD potential:

$$V^{(\rm FD)}(r) = \frac{v_0}{R^2} \frac{1}{\exp[\chi(r^2/R^2 - 1)] + 1}. \tag{2.94}$$

The parameter χ controls the steepness at $r = R$. The FD potential resembles the Fermi-Dirac ("FD") distribution. For a large and positive v_0, both the Gaussian potential and the FD potential approach the hard-sphere (HS) potential

$$V^{(\mathrm{HS})}(r) = \begin{cases} \infty, & \text{at } r < a, \\ 0, & \text{at } r > a. \end{cases} \tag{2.95}$$

For a large and positive χ, the FD potential approaches the soft-sphere (SS) potential

$$V^{(\mathrm{SS})}(r) = \begin{cases} v_0/R^2, & \text{at } r < R, \\ 0, & \text{at } r > R, \end{cases} \tag{2.96}$$

In Ref.[13], two soft-sphere potentials with $a = R/5$ (SS-5) and $a = R/10$ (SS-10) are considered. In Table 2.1, we list the values of χ and v_0 for the FD potentials with $a = R/5$ (FD-5) and $a = R/10$ (FD-10).

3) The core-well (CW) potential:

$$V^{(\mathrm{CW})}(r) = \frac{1}{R^2}\Big\{\frac{v_1 + v_2}{\exp[\chi_1(r^2/R_c^2 - 1)] + 1} - \frac{v_2}{\exp[\chi_2(r^2/R^2 - 1)] + 1}\Big\}, \tag{2.97}$$

where $R_c = R/5$, $\chi_1 = 2$, $\chi_2 = 10$, $v_1 > 0$ and $v_2 > 0$. Qualitatively, we see that $V^{(\mathrm{CW})}(r)$ has a repulsive core at $r \lesssim R_c$, forms a attractive well at $R_c \lesssim r \lesssim R$, and vanishes at $r \gtrsim R$. We can choose a large positive v_1 so that the potential approximately has a hard core at $r \lesssim R_c$. We also adjust v_2 to control the depth of the attractive well, such that the scattering length a equals a relative large positive value and the potential supports one s-wave bound state. We can use the core-well (CW) potential to approach the hard-core

Table 2.2: For different scattering lengths a, the values of v_1 and v_2 of the SW potential in Eq. (2.94) and the corresponding binding wave number κ of the s-wave bound state. Here the binding energy of the s-wave bound state is $E = \kappa^2$.

a/R	v_1	v_2	κR
5	10	3.1888419134470640	0.22397834724607211
8	10	2.9743812467673436	0.13389854588233910
10	10	2.9092132905255266	0.10560196751174359
5	20	3.3246907923436906	0.22449380335517765
8	20	3.1054208696672423	0.13408598084724888
10	20	3.0388239071640920	0.10571921790000408

square-well (HCSW) potential defined in Ref. [13]

$$V^{(\mathrm{HCSW})}(r) = \begin{cases} \infty, & \text{at } r < R_c, \\ -v_0/R^2, & \text{at } R_c < r < R, \\ 0, & \text{at } r > R. \end{cases} \tag{2.98}$$

By adjusting $v_0 \approx 4.128152056922045$, the scattering length $a = 10R$ and the HCSW potential supports a single s-wave bound state [13]. In Table 2.2, we list the values of v_2 and the corresponding binding wave number κ for the CW potentials with scattering lengths $a/R = 5, 8, 10$ and a single s-wave bound state.

2.5 Results and Discussions

2.5.1 Strong repulsive interactions

In the strong repulsive limit where v_0 is large and positive, the Gaussian and FD potentials approach the hard-sphere potential. In Ref. [16], the three-body scattering hypervolume D for the hard-sphere bosons was found to be $D_{\mathrm{HS}} \approx 1761.5a^4$, which may serve as a benchmark. So, we first calculate v_0 for bosons with the Gaussian and FD potentials at

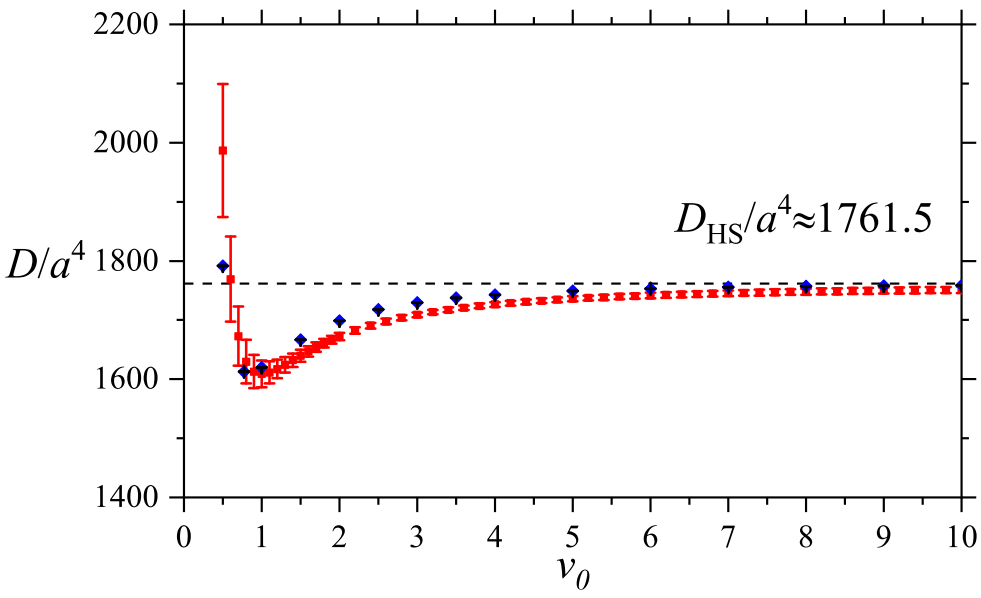

Figure 2.5: Three-body scattering hypervolume D in units of a^4 for repulsive interaction potentials as a function of v_0. The red squares (blue diamonds) represent the Gaussian (FD with $\chi = 10$) potential. The horizontal dashed line represents the value for hard-sphere bosons $D_{\rm HS}/a^4 \approx 1761.5$ [16].

large and positive v_0. The results are plotted in Figure 2.5. The error bars are due to a finite number of basis functions that we used to expand the wave function on the hyperspherical surface with a finite hyperradius ρ_c. We see that the three-body scattering hypervolume D for both the Gaussian and FD potentials approaches $D_{\rm HS} \approx 1761.5a^4$ when $v_0 \gtrsim 5$. This verifies the calculation of D for the hard-sphere bosons in Ref. [16] and also demonstrates the validity of our numerical method.

Moreover, from Figure 2.5, we see that D/a^4 diverges at small v_0. Note that from Eq. (2.52) and (2.53), a is linear in v_0 and D quadratic in v_0 for weak interactions. Therefore, D/a^4 naturally diverges like $1/v_0^2$ at small v_0.

Table 2.3: The list of the coefficients $c_2^{(\mathrm{D})}$, $c_3^{(\mathrm{D})}$, $c_4^{(\mathrm{D})}$, and $c_5^{(\mathrm{D})}$ in Eq. (2.99) for the Gaussian and FD potential with $\chi = 10$. The "Theory" columns list the values of $c_2^{(\mathrm{D})}$ and $c_3^{(\mathrm{D})}$ theoretically calculated from Eq. (2.53). The "Fitting" columns list the values from the fitting results of the model in Eq. (2.99). The "Difference" columns list the relative differences between the "Theory" and "Fitting" values.

	Gaussian			FD		
	Theory	Fitting	Difference	Theory	Fitting	Difference
$c_2^{(\mathrm{D})}$	23.255	23.271(6)	0.07%	5.6571	5.700(6)	0.8%
$c_3^{(\mathrm{D})}$	−108.65	−111.0(2)	2.2%	−31.404	−32.5(1)	3.5%
$c_4^{(\mathrm{D})}$		374(2)			116(1)	
$c_5^{(\mathrm{D})}$		−594(35)			−149(19)	

2.5.2 Weak interactions

We further verify Eq. (2.53) by calculating D at small v_0. For weak interactions, D can be expressed as a power series in v_0:

$$D/R^4 = c_2^{(\mathrm{D})} v_0^2 + c_3^{(\mathrm{D})} v_0^3 + c_4^{(\mathrm{D})} v_0^4 + c_5^{(\mathrm{D})} v_0^5 + \cdots . \tag{2.99}$$

The first two coefficients $c_2^{(\mathrm{D})}$ and $c_3^{(\mathrm{D})}$ can be theoretically calculated through Eq. (2.53). Their values for the Gaussian and FD potential are listed in the "Theory" columns of Table 2.3. In Figure 2.6, we plot the numerical values of D at small $|v_0|$. The solid lines represents the theoretical prediction of Eq. (2.99) including only the leading and subleading order terms with $c_2^{(\mathrm{D})}$ and $c_3^{(\mathrm{D})}$ given by the theoretical values. We see that the data points agree well with the theoretical lines. Quantitatively, using the numerical data with $|v_0| \leq 0.1$, we do a polynomial fitting according to the model in Eq. (2.99). From the fitting results, the coefficients are listed in the "Fitting" columns of Table 2.3. We see that, the fitted values of $c_2^{(\mathrm{D})}$ and $c_3^{(\mathrm{D})}$ are very close to the theoretical values. This demonstrates that our numerical calculations agrees with the theoretical formula Eq. (2.53).

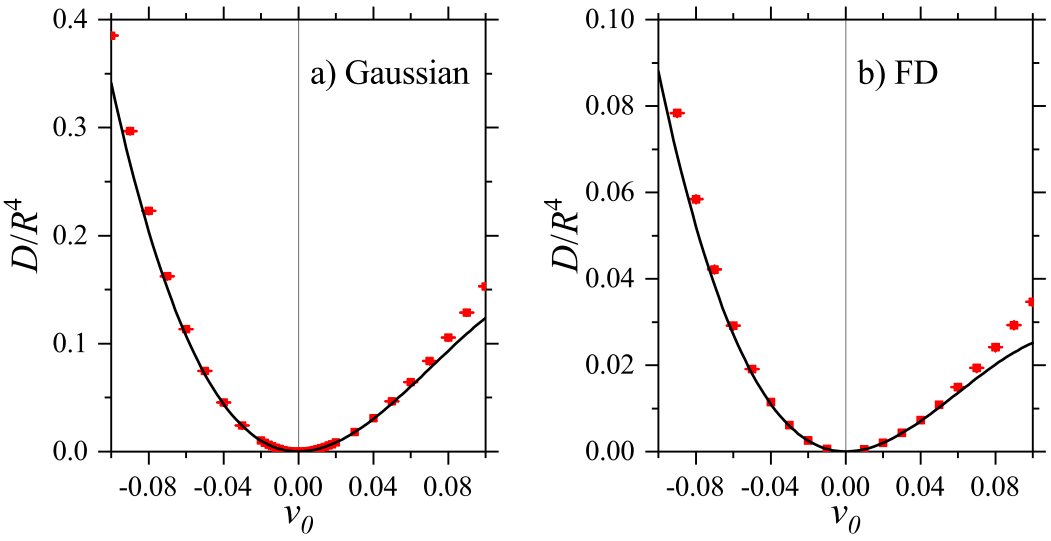

Figure 2.6: Three-body scattering hypervolume D in units of R^4 at small $|v_0|$. a), or b) corresponds to the Gaussian or FD potential with $\chi = 10$, respectively. The red squares represent the numerical results. The black solid lines represent the theoretical prediction in Eq. (2.99) including only the leading and subleading order terms. The coefficients $c_2^{(\mathrm{D})}$ and $c_3^{(\mathrm{D})}$ are given by the "Theory" values in Table 2.3.

2.5.3 Overall picture

Besides the strong repulsive or weak interaction limit, we calculate the three-body scattering hypervolume D for the Gaussian potential with a vast range of v_0. As we tune the parameter v_0 from a large positive value to a large negative value, the two-body scattering length a changes accordingly. Whenever there emerges a s-wave bound state as v_0 decreases, the scattering length a forms a pole structure, and goes from a large negative value to a large positive value. The picture is the same for the d-wave bound states and the d-wave scattering length a_d. Right at the poles where a or a_d diverges. We say the system is at a two-body s-wave or d-wave resonance. Experimentally, this can be realized by Feshbach resonances [80].

In a) of Figure 2.7, we plot a and a_d as a function of v_0. We see that the scattering length a has simple poles at $v_0 \approx -2.6840, -17.796$, and -45.574. Right at the poles, a diverges

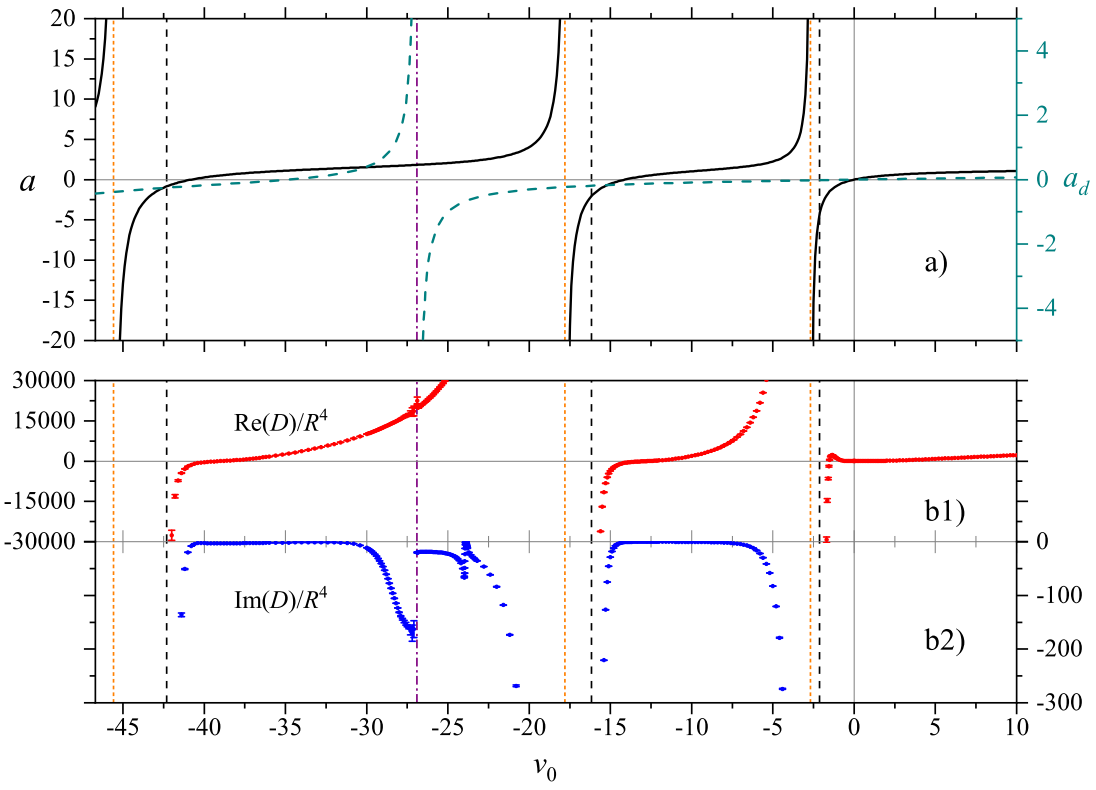

Figure 2.7: The two-body s-wave and d-wave scattering length a in units of R and a_d in units of R^5 (the upper part), and the three-body scattering hypervolume D (the lower part) as a function of v_0 for the Gaussian potentials. The upper part a) and the lower part b1) and b2) share the same horizontal v_0 axis. In a), the black solid lines (the dark cyan dashed line) represents a (a_d). In b1) and b2), the red (blue) dots with error bars represents the real (imaginary) part of D. The vertical orange dotted (purple dotdashed) lines at $v_0 \approx -2.6840, -17.796$, and -45.574 ($v_0 \approx -26.901$) indicate the simple poles of a (a_d), where the interaction reaches two-body s-wave (d-wave) resonances. The vertical black dashed lines at $v_0 \approx -2.1308, -16.163$, and -42.32 indicate the identified three-body resonances.

and the system is at a s-wave resonance. For the system of three bosons, there exist a infinite number of three body bound states, the Efimov states [32, 31], whose binding energies and sizes form a geometric sequence. When v_0 is slightly below these values and a is large and positive, a new shallow s-wave bound state emerges with binding energy $E = 1/a^2$. Also, we see that the d-wave scattering length a_d has a simple pole at $v_0 \approx -26.901$. Similarly, slightly to the left of the pole, a_d is large and positive. A shallow d-wave bound states

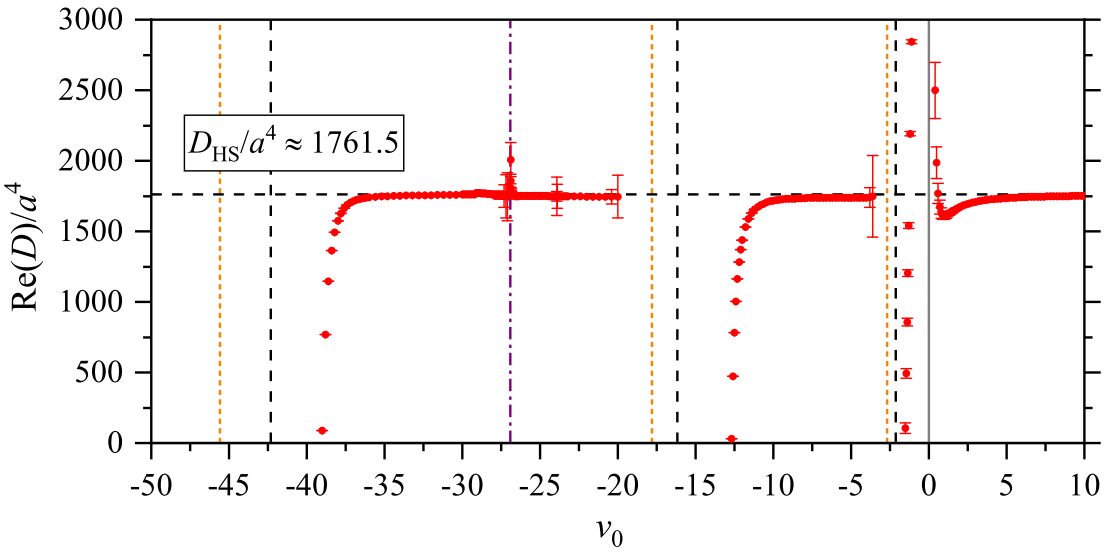

Figure 2.8: The real part of D in units of a^4 as a function of v_0 for the Gaussian potentials. The horizontal black dashed line represents the values for the hard-sphere bosons $D_{\rm HS}/a^4 \approx 1761.5$. The format of the other reference lines are the same as Figure 2.7.

emerges with binding energy $E \propto 1/a_d$.

In the lower part of Figure 2.7, b1) and b2), we plot the numerical results of the real and imaginary part of D for the Gaussian potential, respectively. This is the first numerical calculation of the three-body scattering parameter D for bosons with a nonzero-range strength-variable interaction. As mentioned previously, the error bars are due to a finite number of basis functions and a finite hyperradius ρ_c. The errors become larger when the size of the dimer or the two-body parameters like a and a_d increases. As the computation power limits the maximum number of the basis functions and the maximum ρ_c, the calculation has large errors when the system is too close to the two-body resonances.

In Figure 2.8, we plot the real part of D in units of a^4. We see that when the system is away from the two-body resonances and the zeros of the scattering length a, the real part of D is approximated by the value for the hard-sphere bosons $D_{\rm HS} \approx 1761.5$. This suggests that the hard-sphere bosons may serve as a good model when considering three-body effective interactions for bosons away from the two-body resonances and the zeros of

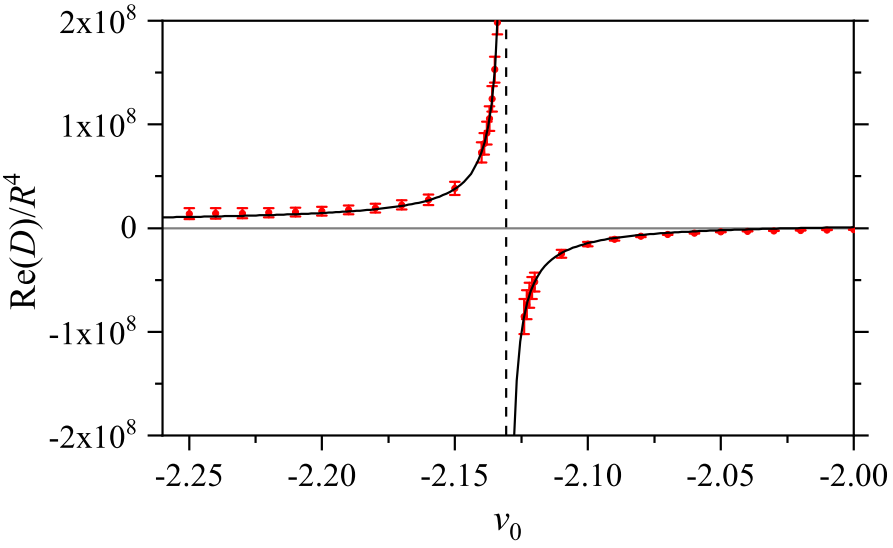

Figure 2.9: The three body scattering hypervolume D as a function of v_0 near the three-body resonance at $v_0 \approx -2.1308$ (indicated by the vertical black dashed line). The red dots represents the numerical results of the real part. Here the imaginary part vanishes. The solid line represents the fitted approximate formula $D/R^4 \approx [-6.2/(v_0 + 2.1308) + 56] \times 10^5$.

the scattering length.

We find several three-body resonances at $v_0 < 0$. In Figure 2.9, we show that D has a simple pole at $v_0 \approx -2.1308$. As there is no two-body bound state, the imaginary part of D is zero here. We find an approximate formula near the pole: $D/r_0^4 \approx (\frac{-6.2}{v_0+2.1308} + 56) \times 10^5$. As D characterizes the effective three-body interaction, the pole indicates a three-body resonance. When v_0 is slightly less than -2.1308, D becomes large and positive and a shallow three-body bound state emerges. This can be verified by a numerical solution of the Schrödinger equation at nonzero energy. Such a shallow three-body bound state is a Borromean state [19] because any two of the particles are not bound, and it is qualitatively similar to some nuclear halo states [19]. At the pole, $a \approx -4.38 r_0$, which is not much larger than r_0, so this three-body bound state is different from an Efimov state. It is stable because there is no dimer state that it can decay into. In the region $v_s^{(0)} < v_0 < -2.1308$, where $v_s^{(0)} \approx -2.6840$, D should have an infinite number of simple poles with the accumulation point at $v = v_s^{(0)}$ due to the Efimov effect [32, 31].

We show two more three-body resonances at $v_0 \approx -16.163$ and $v_0 \approx -42.32$ in Fig-

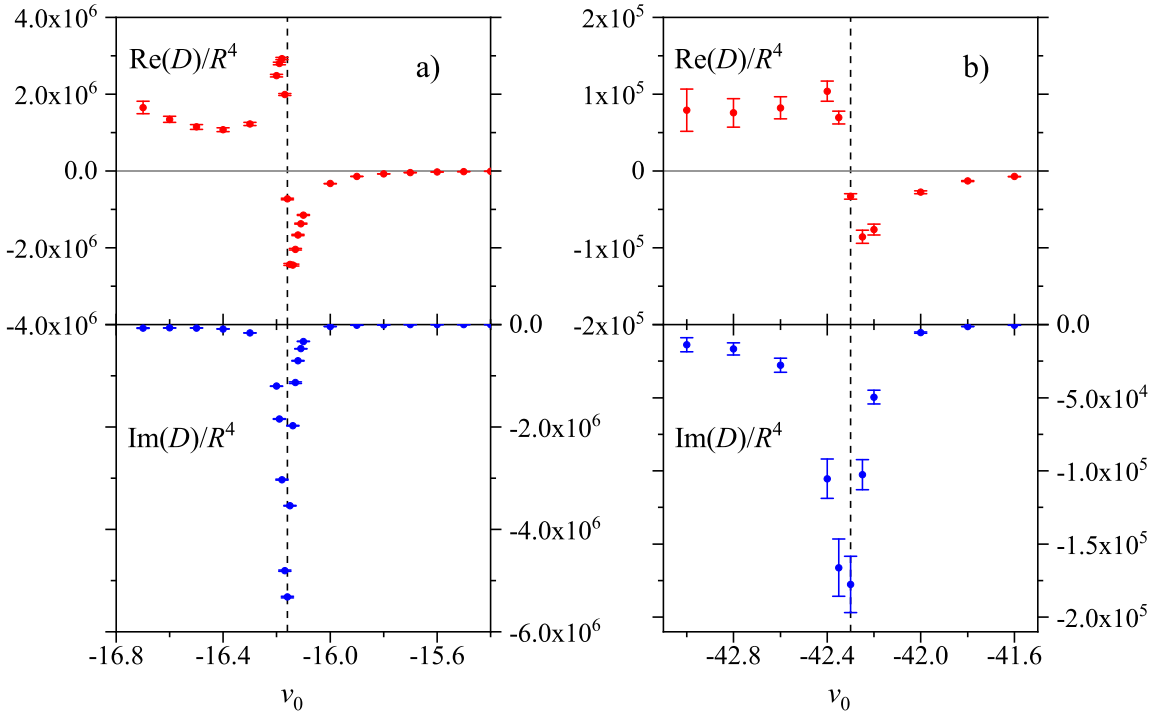

Figure 2.10: The three body scattering hypervolume D as a function of v_0 near the two three-body resonances at $v_0 \approx -16.163$ and -42.32 (indicated by the vertical black dashed lines). The red (blue) dots in the upper (lower) part of the figures represents the numerical results of the real (imaginary) part.

ure 2.10. We see that $\mathrm{Re}(D)$ experiences a sharp transition from a large negative peak to a large positive peak as we decrease v_0. Meanwhile, $\mathrm{Im}(D)$ has a sharp dip right at the resonance, indicating rapid three-body recombination. Near each of these resonances we expect a shallow metastable three-body state, which decays due to three-body recombination or three-body dissociation.

We find some other prominent features in Figure 2.7. Near the d-wave resonance at $v_0 = v_d^{(0)} \approx -26.901$, we find an upward peak for $\mathrm{Re}(D)$ as we approach $v_d^{(0)}$ from above (see Figure 2.11). We do not know whether $\mathrm{Re}(D)$ diverges or not at $v_0 = v_d^{(0)}$. We also find that $\mathrm{Im}(D)$ exhibits a possible discontinuity at $v_0 = v_d^{(0)}$. Close to the resonance, the d-wave scattering length a_d is large, and the size of the d-wave bound states is large if $a_d > 0$. This requires larger hyper radius ρ_c and larger number of basis functions on the

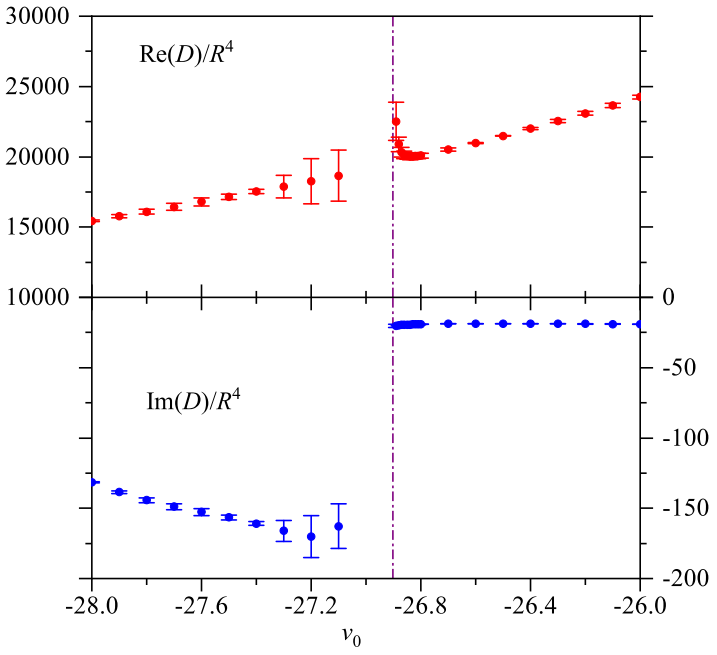

Figure 2.11: The three body scattering hypervolume D as a function of v_0 near the the two-body d-wave resonances at $v_0 \approx -26.901$ (indicated by the vertical purple dotdashed line). The red (blue) dots in the upper (lower) part of the figures represents the numerical results of the real (imaginary) part.

hyperspherical surface. As being limited by the computation power, this leads to relatively large error when the system is close to the d-wave resonance.

Right at the d-wave resonance, as $a_d \to \infty$, the three-body wave function at large interparticle distances, namely, the 21- and 111-expansions in Eq. (2.15) and (2.14), will be modified. In Appendix B, we derive the 21- and 111-expansions up to $1/\rho^4$ order when $a_d \to \infty$. We show that an extra $1/\rho^4$ order term appears and the definition of the three-body scattering hypervolume might be changed due to the d-wave resonance. Whether or not the three-body scattering hypervolume D undergoes discontinuity or divergence across the two-body d-wave resonance is still an open question.

At $v_0 \approx -23.9$ where $a \approx 2.24R$, $|\mathrm{Im}(D)|$ reaches a local minimum $\approx 0.194(10)$, indicating a local minimum of the three-body recombination rate. A similar pattern is seen when a is large and positive, due to the destructive interference of competing pathways [34].

2.5.4 Nonuniversal effect

From Figure 2.7, we have showed that D varies for a vast range of the interaction strength v_0 for the Gaussian interaction potential. Then, we have determined the nonuniversal effect for bosons with the nonzero-range strength-variable interactions for the first time.

In addition, we calculate D for the FD potentials with for several different large values of χ listed in Table 2.1. As $\chi \to \infty$, the FD-10 and FD-5 models respectively approach the SS-10 and SS-5 models, which are considered in Ref. [13]. From the formula of D for weak interactions in Eq. (2.53), we infer that at large χ

$$D_{\rm FD} \approx D_{\rm SS} + \frac{c^\chi}{\chi^2}, \tag{2.100}$$

where c^χ is a constant. Therefore, we can do a quadratic fitting about the parameter $1/\chi$ using the data for the FD potentials. In Figure 2.12, we show the plot of D for the models FD-5 and FD-10 with $\chi = 10, 12, 14$, and 16. From the fitting to Eq. (2.100), we find the three-body scattering hypervolume for SS-10 and SS-5:

$$\frac{D_{\rm SS-10}}{a^4} = 2502.4(6), \text{ and } \frac{D_{\rm SS-5}}{a^4} = 1609.9(2), \tag{2.101}$$

where $a = R/10$ for SS-10 and $a = R/5$ for SS-5. Moreover, we use the CW potential in Eq. (2.97) to approach for the HCSW potential considered in Ref. [13]. For CW potential with a large scattering length $a = 10R$, and the corresponding parameters $v_1 = 20$ and $v_2 \approx 3.0388$ (more listed in Table 2.2), we obtain a preliminary result

$$\frac{D_{\rm CW-10}}{a^4} = 1787(19) - 1.523(16) \times \mathrm{i}. \tag{2.102}$$

All the results showed above reveal the nonuniversal effect of a dilute BEC consisting with the corresponding bosons.

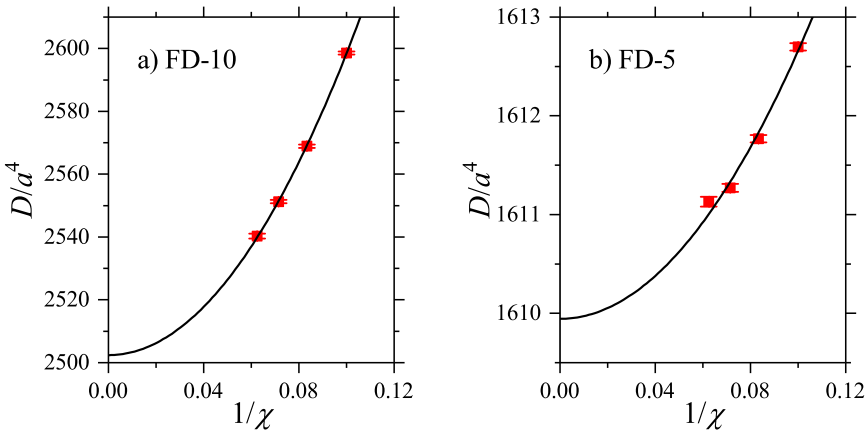

Figure 2.12: Three-body scattering hypervolume D in units of R^4 as a function of $1/\chi$ for FD-5 and FD-10. The solid lines represent the fitting of a constant plus a $1/\chi^2$ correction term. From the fitting, we find that at $\chi \to +\infty$, $D/a^4 = 2502.4(6)$ for FD-10, and $D/a^4 = 1609.9(2)$ for FD-5.

2.6 Experimental observables: collective mode frequencies

As the three-body scattering hypervolume D affects many important properties of systems with at least three particles, we can experimentally determine D by measuring some observables. Based on Eq. (2.64), the imaginary part of the three-body scattering hypervolume D can be obtained straightforwardly by measuring the three-body loss rate L_3 of a ultracold Bose gas. As for the real part, we can investigate the dynamic properties of a dilute BEC.

In order for the three-body effect to be prominent, we study systems with vanishing two-body scattering length a. Then, the leading order term of the ground state energy of a dilute BEC is only determined by D and the number density n (see Eq. (1.5)). As a result, the Gross-Pitaevskii equation [81] becomes

$$\mathrm{i}\frac{\partial}{\partial t}\Psi = -\frac{1}{2}\nabla^2\Psi + V_{\mathrm{ext}}(\mathbf{r})\Psi + \frac{1}{2}D|\Psi|^4\Psi, \tag{2.103}$$

where $V_{\mathrm{ext}}(\mathbf{r})$ is the external potential, and Ψ is the condensate wave function under normalization condition $\int \mathrm{d}^3r|\Psi|^2 = N$. Here the imaginary part of D corresponds to the three-body loss. For simplicity, we can assume that the time scale of investigation is much

smaller than the time scale of the three-body loss and the loss is negligible. Then, in the above equation, D is replaced by the real part of D, and we only study the dynamics of the BEC without atomic loss.

Also, in experiments, the two-body scattering length a cannot be tuned exactly to be zero and there is a minimum uncertainty of a [80, 82]. When the two-body scattering length is small, the effect of the magnetic dipole interaction becomes relatively prominent. Therefore, in addition to the three-body term, we include the two-body term and the magnetic dipole interaction term as necessary corrections. Then, the Gross-Pitaevskii equation becomes

$$\begin{aligned} \mathrm{i}\frac{\partial}{\partial t}\Psi &= -\frac{1}{2}\nabla^2\Psi + V_{\mathrm{ext}}(\mathbf{r})\Psi + 4\pi a|\Psi|^2\Psi + \frac{1}{2}\mathrm{Re}(D)|\Psi|^4\Psi \\ &\quad + \frac{\mu_0\mu_{\mathrm{m}}^2}{4\pi}\Big[\int \mathrm{d}^3r'\,\frac{1-3(\hat{\mathbf{r}}\cdot\hat{\mathbf{r}}')^2}{|\mathbf{r}-\mathbf{r}'|^3}|\Psi(\mathbf{r}',t)|^2\Big]\Psi, \end{aligned} \tag{2.104}$$

where μ_0 is the vacuum permeability, and μ_{m} is the magnetic dipole moment of the atom, aligned by a magnetic field along the z-direction. When a is nonzero, the three-body term gains another part dependent on a in addition to D [16]. As a is assumed to be small, we have neglected that part and only retained the term containing D. Note that previously Yi and You studied the above equation with two-body and dipole interactions [83]; while Al-Jibbouri et al. studied it with two-body and three-body interactions [38].

To solve the above equation, we use the time-dependent variational approach [84]. First, we get the corresponding Lagrangian density

$$\begin{aligned} \mathcal{L} &= \frac{\mathrm{i}}{2}\Big[\Psi\frac{\partial}{\partial t}\Psi^* - \Psi^*\frac{\partial}{\partial t}\Psi\Big] + \frac{1}{2}|\nabla\Psi|^2 + V_{\mathrm{ext}}(\mathbf{r})|\Psi|^2 + 2\pi a|\Psi|^4 + \frac{1}{6}\mathrm{Re}(D)|\Psi|^6 \\ &\quad + \frac{\mu_0\mu_{\mathrm{m}}^2}{8\pi}|\Psi|^2\int \mathrm{d}^3r'\,\frac{1-3(\hat{\mathbf{r}}\cdot\hat{\mathbf{r}}')^2}{|\mathbf{r}-\mathbf{r}'|^3}|\Psi(\mathbf{r}',t)|^2. \end{aligned} \tag{2.105}$$

The Gross-Pitaevskii equation Eq. (2.104) can be obtained from the minimization of the action $S = \int \mathrm{d}^3r\mathrm{d}t\,\mathcal{L}$. To simplify the variational calculation, we can use a Gaussain-like

trial wave function [84, 83]

$$\Psi(x,y,z,t) = A(t) \prod_{\xi=x,y,z} \exp\Big\{ -\frac{[\xi-\xi_0(t)]^2}{2w_\xi^2} + \mathrm{i}\xi\alpha_\xi(t) + \mathrm{i}\xi^2\beta_\xi(t)\Big\}, \tag{2.106}$$

where A (complex amplitude), w_ξ (width), ξ_0 (center of the condensate), α_ξ (slope), and β_ξ [$(\mathrm{curvature\ radious})^{1/2}$] are the variational parameters. The conservation of the atom number gives

$$N = \pi^{3/2}|A(t)|^2 w_x(t) w_y(t) w_z(t) = \mathrm{constant}. \tag{2.107}$$

We can find the Lagrangian $L = \int \mathrm{d}^3 r\ \mathcal{L}$ by integration over the space.

By treating the variational parameters as the generalized coordinates

$$q_j = \{x_0, y_0, z_0, w_x, w_y, w_z, A, A^*, \alpha_x, \alpha_y, \alpha_z, \beta_x, \beta_y, \beta_z\}, \tag{2.108}$$

we obtain the equations governing these parameters from the Euler-Lagrangian equation

$$\frac{\mathrm{d}}{\mathrm{d}t}\Big(\frac{\partial L}{\partial \dot{q}_j}\Big) - \frac{\partial L}{\partial q_j} = 0. \tag{2.109}$$

Let the external potential be a harmonic trap

$$V_{\mathrm{ext}}(\mathbf{r}) = \frac{1}{2l_{\mathrm{ho}}^4}(\lambda_x^2 x^2 + \lambda_y^2 y^2 + \lambda_z^2 z^2), \tag{2.110}$$

where $(\lambda_x, \lambda_y, \lambda_z)$ are dimensionless parameters controlling the shape of the harmonic trap, $l_{\mathrm{ho}} = \sqrt{1/\omega_{\mathrm{ho}}}$ is the oscillator length, and $(\lambda_x\omega_{\mathrm{ho}}, \lambda_y\omega_{\mathrm{ho}}, \lambda_z\omega_{\mathrm{ho}})$ are the angular trapping frequencies along each direction.

We find equations for the center of the condensate

$$\frac{\mathrm{d}^2}{\mathrm{d}t^2}\xi_0 + \lambda_\xi^2\omega_{\mathrm{ho}}^2\xi_0 = 0, \tag{2.111}$$

where $\xi = x, y, z$. This means that the center of the condensate moves like a classical harmonic oscillator with the frequencies of the trap. The parameters α_ξ and β_ξ can be obtained from the widths and the center

$$\alpha_\xi = \frac{\mathrm{d}\xi_0}{\mathrm{d}t} - \frac{\xi_0}{w_\xi}\frac{\mathrm{d}w_\xi}{\mathrm{d}t}, \quad \beta_\xi = \frac{1}{2w_\xi}\frac{\mathrm{d}w_\xi}{\mathrm{d}t}. \tag{2.112}$$

We define the dimensionless parameters

$$\tau = \omega_{\mathrm{ho}} t, \quad v_\xi = \frac{w_\xi}{l_{\mathrm{ho}}}, \tag{2.113}$$

and find the equation for the widths

$$\begin{aligned} \frac{\mathrm{d}^2}{\mathrm{d}\tau^2} v_\xi + \lambda_\xi^2 v_\xi &= \frac{1}{v_\xi^3} + \frac{P}{v_\xi (v_x v_y v_z)} + \frac{K}{v_\xi (v_x v_y v_z)^2} \\ &\quad - \mathcal{E}_{\mathrm{dd}} \frac{\partial}{\partial v_\xi} \Big\{ \frac{1}{v_x v_y v_z} \int \mathrm{d}^3 r \, \frac{1 - 3z^2/r^2}{r^3} \exp\Big[- \frac{x^2}{2v_x^2} - \frac{y^2}{2v_y^2} - \frac{z^2}{2v_z^2} \Big] \Big\}. \end{aligned} \tag{2.114}$$

Here P, K, and $\mathcal{E}_{\mathrm{dd}}$ are the dimensionless parameters corresponding to the two-body interaction, three-body interaction, and magnetic dipole interaction, respectively. They are defined as

$$P = \sqrt{\frac{2}{\pi}} \frac{Na}{l_{\mathrm{ho}}}, \quad K = \frac{2}{9\sqrt{3}\pi^3} \frac{N^2 \mathrm{Re}(D)}{l_{\mathrm{ho}}^4}, \quad \mathcal{E}_{\mathrm{dd}} = \frac{\mu_0 \mu_{\mathrm{m}}^2}{4\pi} \frac{N}{(2\pi)^{3/2} \hbar \omega_{\mathrm{ho}} l_{\mathrm{ho}}^3}, \tag{2.115}$$

where the SI units are restored. Equation (2.114) can be viewed as the equation of motion for a particle with coordinates (v_x, v_y, v_z) in an effective potential

$$\begin{aligned} U(v_x, v_y, v_z) &= \frac{1}{2}(\lambda_x^2 v_x^2 + \lambda_y^2 v_y^2 + \lambda_z^2 v_z^2) + \frac{1}{2}\Big(\frac{1}{v_x^2} + \frac{1}{v_y^2} + \frac{1}{v_z^2}\Big) + \frac{P}{v_x v_y v_z} + \frac{K}{2(v_x v_y v_z)^2} \\ &\quad + \frac{\mathcal{E}_{\mathrm{dd}}}{v_x v_y v_z} \int \mathrm{d}^3 r \, \frac{1 - 3z^2/r^2}{r^3} \exp\Big[- \frac{x^2}{2v_x^2} - \frac{y^2}{2v_y^2} - \frac{z^2}{2v_z^2} \Big]. \end{aligned} \tag{2.116}$$

The equilibrium widths (v_{x0}, v_{y0}, v_{z0}) are obtained by solving Eq. (2.114) with $\mathrm{d}^2 v_\xi/\mathrm{d}\tau^2$ replaced by zero, namely,

$$\begin{aligned}\lambda_\xi^2 v_{\xi 0} &= \frac{1}{v_{\xi 0}^3} + \frac{P}{v_{\xi 0}(v_{x0}v_{y0}v_{z0})} + \frac{K}{v_{\xi 0}(v_{x0}v_{y0}v_{z0})^2} \\ &\quad -\mathcal{E}_{\rm dd}\frac{\partial}{\partial v_{\xi 0}}\Big\{\frac{1}{v_{x0}v_{y0}v_{z0}}\int \mathrm{d}^3 r\, \frac{1-3z^2/r^2}{r^3}\exp\Big[-\frac{x^2}{2v_{x0}^2}-\frac{y^2}{2v_{y0}^2}-\frac{z^2}{2v_{z0}^2}\Big]\Big\}.\end{aligned} \tag{2.117}$$

Then, the collective mode frequencies are the oscillation frequencies around the equilibrium widths. They are given by the eigenvalues of the Hessian matrix of the effective potential $U(v_x, v_y, v_z)$ denoted by

$$\begin{pmatrix} U_{11} & U_{12} & U_{13} \\ U_{21} & U_{22} & U_{23} \\ U_{31} & U_{32} & U_{33} \end{pmatrix}, \tag{2.118}$$

where $U_{ij} = U_{ji}$ denoting the commuting second derivative of two coordinates.

For a cylindrically symmetric trap with $\lambda_x = \lambda_y = 1$, the integrals related to the magnetic dipole interaction can be calculated analytically [83]. With those analytic results, we derive the analytic formula for the collective mode frequencies. Let the equilibrium width $v_{x0} = v_{y0} = v_0$, and the ratio $\iota_0 = v_0/v_{z0}$. Due to the symmetry, we have $U_{11} = U_{22}$ and $U_{13} = U_{23}$. Then, we find the collective mode frequencies

$$\begin{aligned}\omega_1/\omega_{\rm ho} &= \sqrt{U_{11}-U_{12}} \\ \omega_2/\omega_{\rm ho} &= \frac{1}{\sqrt{2}}\Big(U_{11}+U_{12}+U_{33} \\ &\quad +\sqrt{U_{11}^2+2U_{11}U_{12}+U_{12}^2+8U_{13}^2-2U_{11}U_{33}-2U_{12}U_{33}+U_{33}^2}\,\Big)^{1/2} \\ \omega_3/\omega_{\rm ho} &= \frac{1}{\sqrt{2}}\Big(U_{11}+U_{12}+U_{33} \\ &\quad -\sqrt{U_{11}^2+2U_{11}U_{12}+U_{12}^2+8U_{13}^2-2U_{11}U_{33}-2U_{12}U_{33}+U_{33}^2}\,\Big)^{1/2},\end{aligned}$$

(2.119)

and

$$
\begin{aligned}
U_{11} &= 1+\frac{3}{v_0^4}+\frac{2P}{v_0^4 v_{z0}}+\frac{3K}{v_0^6 v_{z0}^2}-\frac{\mathcal{E}_{\rm dd}}{v_0^4 v_{z0}}\frac{\pi}{6(1-\iota_0^2)^3}\Big[32\iota_0^6 \\
&\quad +141\iota_0^4-54\iota_0^2+16-9(11\iota_0^2+4)\iota_0^4\frac{\operatorname{arctanh}(\sqrt{1-\iota_0^2})}{\sqrt{1-\iota_0^2}}\Big], \\
U_{33} &= \lambda_z^2+\frac{3}{v_{z0}^4}+\frac{2P}{v_0^2 v_{z0}^3}+\frac{3K}{v_0^4 v_{z0}^4}-\frac{\mathcal{E}_{\rm dd}}{v_0^2 v_{z0}^3}\frac{4\pi}{3(1-\iota_0^2)^3}\Big[4\iota_0^6 \\
&\quad -12\iota_0^4+51\iota_0^2+2-9(\iota_0^2+4)\iota_0^2\frac{\operatorname{arctanh}(\sqrt{1-\iota_0^2})}{\sqrt{1-\iota_0^2}}\Big], \\
U_{12} &= \frac{P}{v_0^4 v_{z0}}+\frac{2K}{v_0^6 v_{z0}^2}-\frac{\mathcal{E}_{\rm dd}}{v_0^4 v_{z0}}\frac{\pi}{6(1-\iota_0^2)^3}\Big[16\iota_0^6 \\
&\quad +51\iota_0^4-30\iota_0^2+8-45\iota_0^6\frac{\operatorname{arctanh}(\sqrt{1-\iota_0^2})}{\sqrt{1-\iota_0^2}}\Big], \\
U_{13} &= \frac{P}{v_0^3 v_{z0}^2}+\frac{2K}{v_0^5 v_{z0}^3}-\frac{\mathcal{E}_{\rm dd}}{v_0^3 v_{z0}^2}\frac{2\pi}{3(1-\iota_0^2)^3}\Big[4\iota_0^6 \\
&\quad -36\iota_0^4-15\iota_0^2+2+45\iota_0^4\frac{\operatorname{arctanh}(\sqrt{1-\iota_0^2})}{\sqrt{1-\iota_0^2}}\Big],
\end{aligned}
\tag{2.120}
$$

where $\operatorname{arctanh}(x)$ is the inverse hyperbolic tangent function. So, given the interaction parameters P, K, and $\mathcal{E}_{\rm dd}$, we can first obtain the equilibrium width from Eq. (2.117) and then determine the collective mode frequencies from Eq. (2.119). Here ω_1 corresponds to the radial quadrapole mode, characterizing by out-of-phase oscillations in the x and y directions and no oscillation in the (axial) z direction, while ω_2 (ω_3) corresponds to the breathing (quadrapole) mode, characterizing by in-phase (out-of-phase) oscillations in the radial and axial directions [83, 38]. In the above formulas, after setting the three-body interaction parameter $K=0$, we reproduce the analytic results of Ref. [83].

When the interactions are weak ($P, K, \mathcal{E}_{\rm dd} \ll 1$), we find the expressions for the col-

lective mode frequencies to the first order in the small parameters P, K, and $\mathcal{E}_{\rm dd}$,

$$\begin{aligned}
\omega_1/\omega_{\rm ho} &\approx 2-\frac{1}{2}\lambda_z^{1/2}P-\frac{1}{2}\lambda_z K+C_1^{(\rm dd)}(\lambda_z)\mathcal{E}_{\rm dd},\\
\omega_2/\omega_{\rm ho} &\approx \begin{cases} 2\lambda_z-\frac{1}{4}\lambda_z^{1/2}P+C_2^{(\rm dd)}(\lambda_z)\mathcal{E}_{\rm dd}, & \text{if } \lambda_z>1,\\ 2+\frac{1}{2}\lambda_z K+C_3^{(\rm dd)}(\lambda_z)\mathcal{E}_{\rm dd}, & \text{if } 0<\lambda_z<1,\end{cases}\\
\omega_3/\omega_{\rm ho} &\approx \begin{cases} 2+\frac{1}{2}\lambda_z K+C_3^{(\rm dd)}(\lambda_z)\mathcal{E}_{\rm dd}, & \text{if } \lambda_z>1,\\ 2\lambda_z-\frac{1}{4}\lambda_z^{1/2}P+C_2^{(\rm dd)}(\lambda_z)\mathcal{E}_{\rm dd}, & \text{if } 0<\lambda_z<1,\end{cases}
\end{aligned} \tag{2.121}$$

where we have defined the coefficients

$$\begin{aligned}
C_1^{(\rm dd)}(\lambda_z)&=\tfrac{\pi\lambda_z^{1/2}}{12(1-\lambda_z)^3}\Big[8-42\lambda_z-27\lambda_z^2+16\lambda_z^3+9(8-3\lambda_z)\lambda_z^2\tfrac{\operatorname{arctanh}(\sqrt{1-\lambda_z})}{\sqrt{1-\lambda_z}}\Big],\\
C_2^{(\rm dd)}(\lambda_z)&=\tfrac{\pi\lambda_z^{1/2}}{3(1-\lambda_z)^3}\Big[1-24\lambda_z-24\lambda_z^2+2\lambda_z^3+9(1+4\lambda_z)\lambda_z\tfrac{\operatorname{arctanh}(\sqrt{1-\lambda_z})}{\sqrt{1-\lambda_z}}\Big],\\
C_3^{(\rm dd)}(\lambda_z)&=\tfrac{\pi\lambda_z^{3/2}}{2(1-\lambda_z)^3}\Big[-2-13\lambda_z+3(4+\lambda_z)\lambda_z\tfrac{\operatorname{arctanh}(\sqrt{1-\lambda_z})}{\sqrt{1-\lambda_z}}\Big].
\end{aligned} \tag{2.122}$$

These coefficients $C_1^{(\rm dd)}(\lambda_z)$, $C_2^{(\rm dd)}(\lambda_z)$ and $C_3^{(\rm dd)}(\lambda_z)$ are plotted in Figure 2.13.

In the strong interaction limit, we consider two scenarios. First, we let the two-body interaction parameter $|P|\gg 1$ and keep K and $\mathcal{E}_{\rm dd}$ constant. This is known as the Thomas-Fermi limit [36, 84]. Then, we can neglect the effects of K and $\mathcal{E}_{\rm dd}$ and find the collective mode frequencies

$$\begin{aligned}
\omega_1/\omega_{\rm ho} &\approx \sqrt{2},\\
\omega_2/\omega_{\rm ho} &\approx \frac{1}{\sqrt{2}}\Big(4+3\lambda_z^2+\sqrt{16-16\lambda_z^2+9\lambda_z^4}\Big)^{1/2},\\
\omega_3/\omega_{\rm ho} &\approx \frac{1}{\sqrt{2}}\Big(4+3\lambda_z^2-\sqrt{16-16\lambda_z^2+9\lambda_z^4}\Big)^{1/2}.
\end{aligned} \tag{2.123}$$

This is consistent with the previous calculations [36, 84]. At small λ_z, $\omega_2/\omega_{\rm ho}\approx 2$, and $\omega_3/\omega_{\rm ho}\approx\sqrt{5/2}\lambda_z$; at large λ_z, $\omega_2/\omega_{\rm ho}\approx\sqrt{3}\lambda_z$, and $\omega_3/\omega_{\rm ho}\approx\sqrt{10/3}$. Second, we tune two-body scattering length a to a relatively small value by Feshbach resonances such that

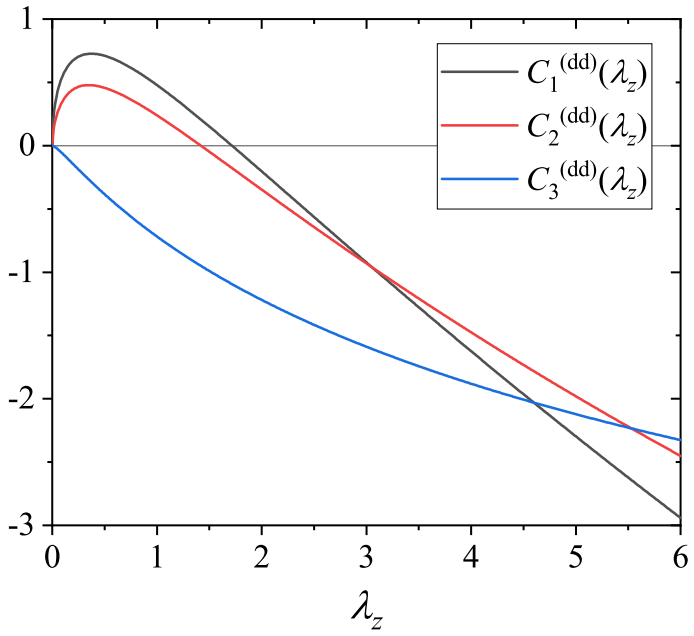

Figure 2.13: The coefficients $C_1^{(\mathrm{dd})}(\lambda_z)$, $C_2^{(\mathrm{dd})}(\lambda_z)$ and $C_3^{(\mathrm{dd})}(\lambda_z)$ as a function of λ_z.

$|P|$ is not large and assume $|K| \gg 1$. We call it the large-K limit. In this limit, we neglect the effects of P and $\mathcal{E}_{\mathrm{dd}}$, and find

$$\begin{aligned} \omega_1/\omega_{\mathrm{ho}} &\approx \sqrt{2}, \\ \omega_2/\omega_{\mathrm{ho}} &\approx \left(3+2\lambda_z^2+\sqrt{9-4\lambda_z^2+4\lambda_z^4}\right)^{1/2}, \\ \omega_3/\omega_{\mathrm{ho}} &\approx \left(3+2\lambda_z^2-\sqrt{9-4\lambda_z^2+4\lambda_z^4}\right)^{1/2}. \end{aligned} \tag{2.124}$$

At small λ_z, $\omega_2/\omega_{\mathrm{ho}} \approx \sqrt{6}$, and $\omega_3/\omega_{\mathrm{ho}} \approx \sqrt{8/3}\lambda_z$; at large λ_z, $\omega_2/\omega_{\mathrm{ho}} \approx 2\lambda_z$, and $\omega_3/\omega_{\mathrm{ho}} \approx 2$. We see that in the Thomas-Fermi limit and the large-K limit, $\omega_{2,3}$ has distinct asymptotic behaviors at either small or large λ_z.

To estimate the effect of D on the collective mode frequencies of a dilute BEC in a trap, we choose a typical set of parameters: the number of atoms $N = 10^5$, the radial trap frequency $\omega_{\mathrm{ho}} = 2\pi \times 150\mathrm{Hz}$. To maximize the effect of D, we tune the two-body scattering length a to zero. However, due to the limit of experimental magnetic field stability [82],

Table 2.4: The two-body, three-body, and magnetic dipole interaction parameters $(P, K, \mathcal{E}_{\rm dd})$ defined in Eq. (2.115) for some bosonic alkali atoms. We have choose a typical set of parameters: the number of atoms $N = 10^5$, the two-body scattering length $a = 1a_B$, the three-body scattering hypervolume $\mathrm{Re}(D) = 2000 l_{\rm vdw}^4$, the radial trap frequency $\omega_{\rm ho} = 2\pi \times 150\mathrm{Hz}$. The second column shows whether broad Feshbach resonances (BFR) have been found for the atom species [80].

Species	BFR[a]	$l_{\rm vdw}/a_B$	μ_m/μ_B	P	K	$\mathcal{E}_{\rm dd}$
^{7}Li	Yes	65.0[b]	0.94[c]	1.36	0.1255	0.0163
^{23}Na		89.9[b]	0.91[c]	2.47	4.942	0.0907
^{39}K	Yes	129[b]	0.95[c]	3.21	60.18	0.218
^{41}K		131[b]	0.07[c]	3.29	69.92	0.00128
^{85}Rb	Yes	164[b]	−0.57[c]	4.74	739.3	0.253
^{87}Rb		165[b]	0.73[c]	4.80	792.7	0.429
^{133}Cs	Yes	202[d]	−0.75[c]	5.93	4190	0.856

[a] Ref. [80]
[b] Ref. [85].
[c] Ref. [82].
[d] Ref. [86].

there is a minimum scattering length that can be achieved experimentally. Here we assume a small value of the scattering length $a = 1a_B$ with a_B the Bohr radius. Note that the hard-sphere bosons, $D_{\rm HS}/a^4 \approx 1761.5$, where a is both the scattering length and the range of interaction. Accordingly, we can roughly estimate $\mathrm{Re}(D) = 2000 l_{\rm vdw}^4$, where $l_{\rm vdw}$ is the van der Waals length defined as $l_{\rm vdw} = C_6^{1/4}$ and C_6 is the coefficient of the van der Waals interaction $V_{\rm vdw}(r) = -C_6/r^6$. Note that the real part of the effective three-body coupling strength g_3 for rubidium atoms is estimated to be $(10^{-27} \sim 10^{-26}) \times \hbar\,\mathrm{cm}^6 s^{-1}$ in the SI units [87]. This provides another estimation $\mathrm{Re}(D) = (470 \sim 4700) \times l_{\rm vdw}^4$, which is consistent with the estimation from the hard-sphere model. Then, we list some basic parameters including the interaction parameters K, P, and $\mathcal{E}_{\rm dd}$ for some bosonic alkali atoms in Table 2.4. We see that for atoms with larger sizes, the three-body interaction

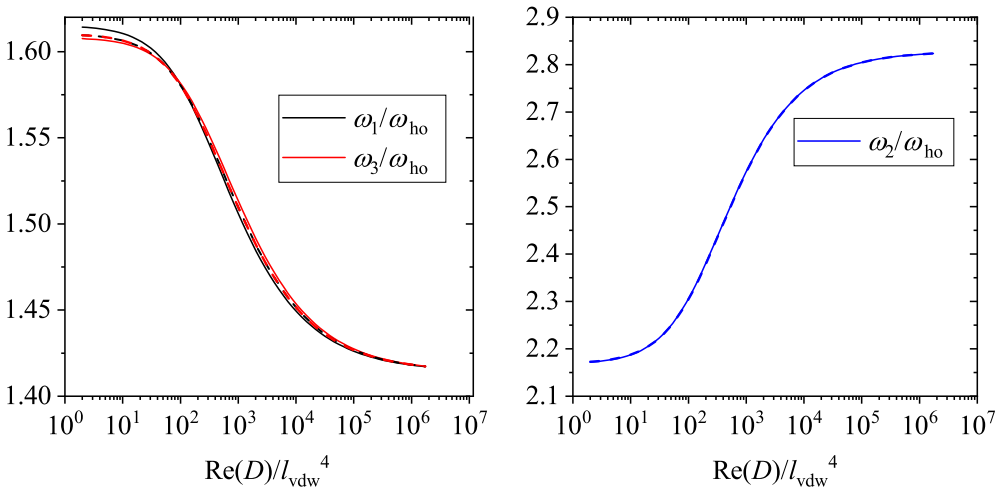

Figure 2.14: The collective mode frequencies as a function of the real part of the three-body scattering hypervolume D in units of $l_{\rm vdw}^4$ for a ultracold Bose gas of ^{39}K in an isotropic harmonic trap ($\lambda_z = 1$). The black, blue, and red solid line corresponds to the three frequencies ω_1, ω_2, and ω_3 in units of $\omega_{\rm ho}$, respectively. The black, blue, and red dashed lines corresponds to the ω_1, ω_2, and ω_3 values calculated without the magnetic dipole interaction, respectively. In the left graph, the dashed black and red lines nearly coincide. In the right graph, the blue dashed and solid line nearly coincide.

parameter K is larger. We have marked the atom species ^{7}Li, ^{39}K, ^{85}Rb, and ^{133}Cs, for which the broad Feshbach resonances have been found [80]. Broad Feshbach resonances have open-channel dominated characteristics and can be modeled by the single-channel scattering. They usually feature small two-body and three-body losses. Also, the scattering length can be tuned to the zero-crossing more accurately.

For a promising candidate ^{39}K, we numerically calculate the collective mode frequencies as a function of $\mathrm{Re}(D)$ given the above typical set of parameters. In Figure 2.14 and 2.15, we show the results for a ultracold Bose gas of ^{39}K in a isotropic harmonic trap ($\lambda_z = 1$) and a cigar-shape harmonic trap ($\lambda_z = 1/10$), respectively. We see that at large $\mathrm{Re}(D)$, the frequencies approach the large-K limit values $(\omega_1 = 1.414, \omega_2 = 2.828, \omega_3 = 1.414)$ for the isotropic trap, or $(\omega_1 = 1.414, \omega_2 = 2.452, \omega_3 = 0.1631)$ for the cigar-shape trap. The effect of the magnetic dipole interaction is more prominent in the cigar-shape trap than that in the isotropic trap. If we measure the collective mode frequencies of the axial direc-

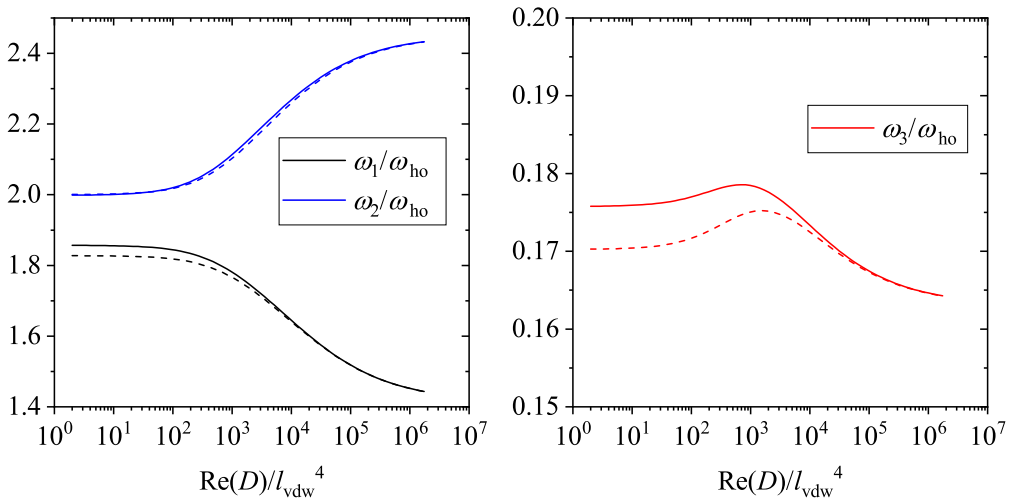

Figure 2.15: The collective mode frequencies as a function of the real part of the three-body scattering hypervolume D in units of $l_{\rm vdw}^4$ for a ultracold Bose gas of ^{39}K in a cigar-shape harmonic trap ($\lambda_z = 1/10$). The format is the same as Figure 2.14.

tion (ω_2 and ω_3) in a long-cigar-shape trap (small λ_z), the inclusion of the magnetic dipole interaction is necessary for good accuracy. Most importantly, we see that the corrections due to the three-body interaction term is quite prominent for some relatively large values of $\mathrm{Re}(D)$. Then, by measuring the collective mode frequencies at the zero-crossing of the scattering length and comparing to the theoretical calculation, we can obtain the real part of the three-body scattering hypervolume $\mathrm{Re}(D)$.

2.7 Conclusion and outlook

Through investigating the three-body scattering hypervolume D analytically and numerically, we identified the nonuniversal effect of a dilute BEC. For weak two-body interactions, we derived a approximate formula for D with the leading and subleading order terms. We extended the concept of D to the complex plane when the interaction supports two-body bound states, and established a relation between the imaginary part of D and the three-body recombination rate. We developed a numerical method for calculating D for nonzero-range interactions. We numerically calculated D for bosons with some model potentials, such as the Gaussian potential, the FD potentials and the CW potential. When the potential is

strongly repulsive or weak, it agrees well with the hard-sphere result or the weak interaction formula, respectively. When the potential is sufficiently attractive, we identified several three-body resonances. When the system is away from the two-body resonances and the zeros of the scattering length, D is approximately given by the value for the hard-sphere bosons $D_{\mathrm{HS}} \approx 1761.5a^4$. Also, we calculated the collective mode frequencies of ultracold Bose gases in a harmonic trap as a function of $\mathrm{Re}(D)$ when the two-body scattering length is tuned to be close to a zero-crossing.

The concept of the three-body scattering hypervolume can also be generalized to fermionic systems. This may help understand the three-body physics in nuclear systems. Other generalization can be made for distinguishable particles with unequal masses and particles in lower dimensions. Also, as mentioned in Section 2.5.3, across a two-body d-wave resonance, we saw that D may be discontinuous or divergent. However, we do not have a concrete conclusion because of the large numerical error due to the limit of computation power. Then, to resolve this problem, a proper definition of D near higher partial wave resonances is needed. Moreover, when the interaction contains a Van der Waals $1/r^6$ tail, the $1/\rho^4$ term of the three-body wave function at large ρ will be modified. Accordingly, the definition of D will be changed. One may find the right definition by analytically deriving the three-body wave function of three particles with Van der Waals interactions.

CHAPTER 3

LÜSCHER'S FORMULA IN D SPATIAL DIMENSIONS

3.1 Preliminaries

3.1.1 Pseudo wave function and effective range expansion in d dimensions

In this section, we introduce the two-body scattering theory at low energies in d dimensions. The three-dimensional case has been discussed in Section 2.1.1. Here we generalize the dicussion and consider the scattering of two particles with short-range interactions in d dimensions. Also, we use the units such that $M = \hbar = 1$, where M is the mass of the particle and $\hbar$ is the Planck constant divided by 2π. Similarly, We write the Schrödinger equation of the relative motion

$$\Big[-\nabla^2 + V(\mathbf{r}) \Big] \phi(\mathbf{r}) = E\phi(\mathbf{r}). \tag{3.1}$$

where E and $\mathbf{r}$ are the colliding energy and the relative position vector, respectively. Different from Eq. (2.1), here ∇^2 and $\mathbf{r}$ are the Laplace operator and the relative position vector in d dimensions, respectively.

Then, outside the range of interaction ($r > r_e$), the wave function takes the form

$$\phi(\mathbf{r}) = \sum_{l=0}^{\infty} \sum_{\mu} C_{l\mu} \Big[j_l^{(d)}(pr) \cot \delta_l^{(d)} - y_l^{(d)}(pr) \Big] Y_{l\mu}(\hat{\mathbf{r}}), \tag{3.2}$$

where $C_{l\mu}$ is a constant, the energy $E = p^2$, and $\delta_l^{(d)}$ is the phase shift in d dimensions. $Y_{l\mu}(\hat{\mathbf{r}})$ denotes the hyperspherical harmonics in d dimensions. l is the orbital angular momentum quantum number and μ represents a set of indices $(\mu_1, \mu_2, \ldots, \mu_{d-2})$ labeling different hyperspherical harmonics of the same l. The hyperspherical harmonics satisfy the

orthonormality condition

$$\int \mathrm{d}^{d-1}\Omega \; Y_{l\mu}(\hat{\mathbf{r}}) Y_{l'\mu'}(\hat{\mathbf{r}}) = \delta_{ll'}\delta_{\mu\mu'}, \tag{3.3}$$

where the integration is over the solid angle of the hypersphere and $\mathrm{d}^{d-1}\Omega$ denotes $d-1$-dimensional hyperspherical surface area element. $\hat{\mathbf{r}} \equiv \mathbf{r}/r$ denotes the direction of the position vector $\mathbf{r}$, and $\delta_{\mu\mu'} \equiv \delta_{\mu_1\mu_1'}\delta_{\mu_2\mu_2'}\cdots\delta_{\mu_{d-2}\mu_{d-2}'}$ is the shorthand of the product of the Kronecker deltas. Also, we have defined the "hyperspherical" Bessel function of the first and second kind in d dimensions, respectively,

$$j_l^{(d)}(x) = \sqrt{\frac{\pi}{2}}\frac{J_{l+d/2-1}(x)}{x^{d/2-1}}, \tag{3.4}$$

$$y_l^{(d)}(x) = \sqrt{\frac{\pi}{2}}\frac{Y_{l+d/2-1}(x)}{x^{d/2-1}}, \tag{3.5}$$

where $J_l(x)$ and $Y_l(x)$ are the Bessel function of the first and second kind, respectively. $j_l^{(d)}(x)$ is smooth at the origin, while $y_l^{(d)}(x) \sim 1/x^{d+2l-1}$ is singular at the origin. Using the "hyperspherical" Bessel function of the first kind and hyperspherical harmonics, we construct the plane wave expansion in d dimensions [88]

$$\mathrm{e}^{\mathrm{i}\mathbf{k}\cdot\mathbf{r}} = \sqrt{\frac{2}{\pi}}(2\pi)^{d/2}\sum_{l=0}^{\infty}\sum_{\mu}\mathrm{i}^l j_l^{(d)}(kr) Y_{l\mu}^*(\hat{\mathbf{k}}) Y_{l\mu}(\hat{\mathbf{r}}). \tag{3.6}$$

As mentioned in Section 2.4.1, we can view the wave function in Eq. (3.2) and its continuation inside the range of interaction as the *pseudo wave function*. The details of the interaction are encapsulated in the phase shift $\delta_l^{(d)}$. Then, the pseudo wave function can be viewed as a boundary condition at small r. At low energies, the phase shift obeys the effective range expansion [89],

$$p^{2l+d-2}\Big[\cot\delta_l^{(d)} - \tau_d\frac{2}{\pi}\ln(pR_{dl})\Big] = -\frac{1}{a_{dl}} + \frac{1}{2}r_{dl}p^2 + \frac{1}{4!}r'_{dl}p^4 + O(p^6), \tag{3.7}$$

where the parameter $\tau_d = 1$ or 0 when d is even or odd, respectively. Here a_{dl} is the l-wave scattering length with dimension $[\text{length}]^{2l+d-2}$, r_{dl} is the l-wave effective range with dimension $[\text{length}]^{-2l-d+4}$, and r'_{dl} is the higher order scattering parameter with dimension $[\text{length}]^{-2l-d+6}$, and R_{dl} is some length scale. We use symbols $s, p, d, f, \cdots$ for $l = 0, 1, 2, 3, \cdots$.

When $2l + d - 2 = 0$ (namely $d = 2$ and $l = 0$), a_{dl} is dimensionless. We can simplify the effective range expansion by defining

$$\widetilde{a}_{2,0} = 2\pi R_{2,0} \exp\Big(- \frac{\pi}{2a_{2,0}}\Big), \tag{3.8}$$

which can be viewed as the reduced s-wave scattering length in two dimensions. Then, when $d = 2$ and $l = 0$, the effective range expansion becomes,

$$\cot \delta_0^{(2)} = \frac{2}{\pi} \ln \Big(p\frac{\widetilde{a}_{2,0}}{2\pi}\Big) + \frac{1}{2} r_{2,0} p^2 + \frac{1}{4!} r'_{2,0} p^4 + O(p^6). \tag{3.9}$$

Similarly, when $2l + d - 2 = 2$ (namely $d = 2, l = 1$ or $d = 4, l = 0$), r_{dl} is dimensionless. We define

$$\widetilde{r}_{2,1} = 2\pi R_{2,1} \exp(\pi r_{2,1}/4), \tag{3.10}$$

$$\widetilde{r}_{4,0} = 2\pi R_{4,0} \exp(\pi r_{4,0}/4), \tag{3.11}$$

which can be viewed as the reduced p-wave effective range in two dimensions and the reduced s-wave effective range in four dimensions, respectively. Then, when $d = 2, l = 1$ or $d = 4, l = 0$, the effective range expansion becomes

$$p^2 \cot \delta_l^{(d)} = -\frac{1}{a_{dl}} + \frac{2}{\pi} p^2 \ln \Big(p\frac{\widetilde{r}_{dl}}{2\pi}\Big) + \frac{1}{4!} r'_{dl} p^4 + O(p^4). \tag{3.12}$$

3.1.2 Two-body s-wave resonance in d dimensions

In three dimensions, we say that the system is at a two-body s-wave resonance when the s-wave scattering length $a \to \infty$. In d dimensions, this definition does not work when $d = 2$. Instead, we can define the s-wave resonance through the wave function of the s-wave channel at zero energy.

From Eq. (3.2), the zero-energy wave function of the s-wave channel behaves

$$\phi_0(r) \propto \begin{cases} 1 - \frac{2^{d-2}\Gamma(d/2-1)\Gamma(d/2)}{\pi} \frac{a_{d,0}}{r^{d-2}}, & \text{when } d \neq 2, \\ \ln\left(r/\frac{\widetilde{a}_{2,0}}{\pi \mathrm{e}^{\gamma}}\right), & \text{when } d = 2, \end{cases} \tag{3.13}$$

where $\Gamma(x)$ is the Gamma function, and $\gamma \approx 0.5772156649$ is the Euler-Mascheroni constant.

When $d \geq 3$, we say that the system is at a s-wave resonance if $a_{d,0} \to \infty$, or equivalently the zero-energy wave function of the s-wave channel

$$\phi_0(r) \propto r^{2-d}. \tag{3.14}$$

When $d = 1$, we say that the interaction is strongly repulsive or attractive if $a_{1,0} \to \infty$, or equivalently the zero-energy s-wave function

$$\phi_0(r) \propto r. \tag{3.15}$$

3.1.3 Regularized Fourier transform and pseudo wave function in the momentum space

Notice that in the momentum space the d-dimensional Laplace operator ∇^2 corresponds to a very simple form $-k^2$ with $\mathbf{k}$ the wave vector. Then, we expect the wave function to have a simpler form in the momentum space. The wave function can be obtained through the

regularized Fourier transform:

$$\phi(\mathbf{r}) = \lim_{\epsilon\to 0^+} \int_{\mathbf{k}} \widetilde{\phi}(\mathbf{k}) \mathrm{e}^{\mathrm{i}\mathbf{k}\cdot\mathbf{r}-\epsilon k^2}, \tag{3.16}$$

where $\int_{\mathbf{k}}$ is the shorthand of $\int \frac{\mathrm{d}^d k}{(2\pi)^d}$. We have added a regularization factor $\mathrm{e}^{-\epsilon k^2}$ to make the integral convergent and well-defined.

When the energy is positive $p^2 > 0$, we can easily prove the following two identities,

$$\begin{aligned} j_0^{(d)}(pr) &= \frac{1}{\pi}(2\pi)^{\frac{d+1}{2}} p^{2-d} \int_{\mathbf{k}} \pi\delta(k^2-p^2)\mathrm{e}^{\mathrm{i}\mathbf{k}\cdot\mathbf{r}}, & (3.17)\\ y_0^{(d)}(pr) &= \lim_{\epsilon\to 0^+} \frac{1}{\pi}(2\pi)^{\frac{d+1}{2}} p^{2-d}\, \mathrm{P}\int_{\mathbf{k}} \frac{-1}{k^2-p^2}\mathrm{e}^{\mathrm{i}\mathbf{k}\cdot\mathbf{r}-\epsilon k^2}, & (3.18) \end{aligned}$$

where $\int_{\mathbf{k}}$ is the shorthand of $\int \frac{\mathrm{d}^d k}{(2\pi)^d}$, the symbol P denotes the principal value, and $\epsilon \to 0^+$ is a positive infinitesimal. We generalize the above to formula to higher partial waves:

$$\begin{aligned} j_l^{(d)}(pr) Y_{l\mu}(\hat{\mathbf{r}}) &= \frac{(-\mathrm{i})^l}{\pi}(2\pi)^{\frac{d+1}{2}} p^{2-d-l} \int_{\mathbf{k}} Q_{l\mu}(\mathbf{k})\pi\delta(k^2-p^2)\mathrm{e}^{\mathrm{i}\mathbf{k}\cdot\mathbf{r}}, & (3.19)\\ y_l^{(d)}(pr) Y_{l\mu}(\hat{\mathbf{r}}) &= \lim_{\epsilon\to 0^+} \frac{(-\mathrm{i})^l}{\pi}(2\pi)^{\frac{d+1}{2}} p^{2-d-l}\mathrm{P}\int_{\mathbf{k}} Q_{l\mu}(\mathbf{k})\frac{-1}{k^2-p^2}\mathrm{e}^{\mathrm{i}\mathbf{k}\cdot\mathbf{r}-\epsilon k^2}, & (3.20) \end{aligned}$$

where $Q_{l\mu}(\mathbf{r})$ is the l-degree harmonic polynomial defined as

$$Q_{l\mu}(\mathbf{r}) = r^l Y_{l\mu}(\hat{\mathbf{r}}), \tag{3.21}$$

We have used the following two identities

$$\begin{aligned} Q_{l\mu}(\nabla) j_0^{(d)}(pr) &= (-p)^l j_l^{(d)}(pr) Y_{l\mu}(\hat{\mathbf{r}}), & (3.22)\\ Q_{l\mu}(\nabla) y_0^{(d)}(pr) &= (-p)^l y_l^{(d)}(pr) Y_{l\mu}(\hat{\mathbf{r}}). & (3.23) \end{aligned}$$

When $p^2 > 0$, we can find the wave function in the momentum space

$$\widetilde{\phi}(\mathbf{k}) = \sum_{l=0}^{\infty} \sum_{\mu} \widetilde{C}_{l\mu} p^{2-d-l} Q_{l\mu}(\mathbf{k}) \Big[\pi \delta(k^2 - p^2) \cot \delta_{dl} + \frac{\mathrm{P}}{k^2 - p^2} \Big] Y_{l\mu}(\hat{\mathbf{r}}), \tag{3.24}$$

where $\delta(x)$ is the Dirac delta function, the coefficient $\widetilde{C}_{l\mu} = \frac{(-\mathrm{i})^l}{\pi} (2\pi)^{\frac{d+1}{2}} C_{l\mu}$. Here we have defined

$$\frac{\mathrm{P}}{k^2 - p^2} \equiv \frac{1}{2} \Big(\frac{1}{k^2 - p^2 - \mathrm{i}\epsilon} + \frac{1}{k^2 - p^2 + \mathrm{i}\epsilon} \Big), \tag{3.25}$$

where $\epsilon \to 0^+$ is a positive infinitesimal. The symbol P means that it is equivalent to taking the principal value in an integral.

When $p^2 < 0$ and $p = \mathrm{i}\kappa$ with $\kappa > 0$, the right hand side of Eq. (3.18) give a exponentially decaying function at large r. Because the Fourier transform of a exponentially growing function at large r does not exist, Eq. (3.24) fails for negative energies. Instead, we have the following identity

$$[y_l^{(d)}(pr) - \mathrm{i} j_l^{(d)}(pr)] Y_{l\mu}(\hat{\mathbf{r}}) = \lim_{\epsilon \to 0^+} \frac{(-\mathrm{i})^l}{\pi} (2\pi)^{\frac{d+1}{2}} p^{2-d-l} \mathrm{P} \int_{\mathbf{k}} Q_{l\mu}(\mathbf{k}) \frac{-1}{k^2 - p^2} \mathrm{e}^{\mathrm{i}\mathbf{k}\cdot\mathbf{r} - \epsilon k^2}. \tag{3.26}$$

3.1.4 Helmholtz equation

The pseudo wave function does not satisfies the Schrödinger equation in Eq. (3.1), but a Helmholtz equation

$$(\nabla^2 + p^2) \phi(\mathbf{r}) = \sum_{l=0}^{\infty} \sum_{\mu} \frac{\widetilde{C}_{l\mu}}{p^{d+l-2}} Q_{l\mu}(\nabla) \delta(\mathbf{r}). \tag{3.27}$$

We see that the source is a sum of the delta function and its derivatives, which gives the equation a simple form in the momentum spapce. This Helmholtz equation is equivalent to the Schrödinger equation in Eq. (3.1) with the two-body potential replaced with the zero-range pseudo potential [90, 91, 92, 93, 94, 95].

3.2 Periodic wave function in a d-dimensional finite volume

Now consider two particles colliding in a d-dimensional finite volume, namely, a d-dimensional box of size L with periodic boundary condition. We assume that the two particles have momenta $(-\mathbf{p}, \mathbf{p})$. As the total momentum is zero, we can only consider the relative motion. The wave function is periodic and satisfies

$$\psi(\mathbf{r}) = \psi(\mathbf{r} - \mathbf{n}L), \tag{3.28}$$

where $\mathbf{n} \in \mathbb{Z}^d$ is a d-dimensional integral vector and $\mathbb{Z}^d$ is the d-dimensional integer lattice. Compared to Eq. (3.27), the periodic pseudo wave function satisfies the Helmholtz equation with a periodic source:

$$(\nabla^2 + p^2)\psi(\mathbf{r}) = \sum_{l=0}^{\infty} \sum_{\mu} \frac{\widetilde{C}_{l\mu}}{p^{d+l-2}} Q_{l\mu}(\nabla) \sum_{\mathbf{n}\in\mathbb{Z}^d} \delta(\mathbf{r} - \mathbf{n}L). \tag{3.29}$$

One can conveniently find a trial solution to the above equation in the momentum space,

$$\widetilde{\psi}(\mathbf{k}) = \sum_{l=0}^{\infty} \sum_{\mu} B_{l\mu} Q_{l\mu}(\mathbf{k}) \frac{I(\mathbf{k})}{k^2 - p^2}, \tag{3.30}$$

where $B_{l\mu} = C_{l\mu} \frac{(-\mathrm{i})^l}{\pi} (2\pi)^{\frac{d+1}{2}} p^{2-d-l}$, and $\widetilde{\psi}(\mathbf{k})$ is defined such that

$$\psi(\mathbf{r}) = \lim_{\epsilon\to 0^+} \int_{\mathbf{k}} \widetilde{\psi}(\mathbf{k}) \mathrm{e}^{\mathrm{i}\mathbf{k}\cdot\mathbf{r} - \epsilon k^2}. \tag{3.31}$$

Here $I(\mathbf{k})$ is a lattice of delta functions defined as

$$I(\mathbf{k}) = \sum_{\mathbf{n}\in\mathbb{Z}^d} \Big(\frac{2\pi}{L}\Big)^d \delta\Big(\mathbf{k} - \frac{2\pi\mathbf{n}}{L}\Big), \tag{3.32}$$

and its Fourier transform gives a lattice of delta functions in the real space

$$\sum_{\mathbf{n}\in\mathbb{Z}^d} \delta(\mathbf{r}-\mathbf{n}L) = \int_{\mathbf{k}} I(\mathbf{k}) \mathrm{e}^{\mathrm{i}\mathbf{k}\cdot\mathbf{r}}. \tag{3.33}$$

Note that in Eq. (3.30), we have assume that the energy does not take the singular values, namely, $p \neq 2\pi n/L$ for any $\mathbf{n} \in \mathbb{Z}^d$. This condition will be satisfied consistently after the energy eigenvalues is obtained from the quantization condition. The cases of the energy taking the singular values can be addressed with similar techniques as in Ref. [41].

When the box size L is large, $\sum_{\mathbf{n}\in\mathbb{Z}^d} \delta(\mathbf{r}-\mathbf{n}L)$ approximately only contains one isolated delta function located at the origin in any fixed spacial region. Its Fourier transform is approximately 1. This suggests that $I(\mathbf{k}) \approx 1$ for fixed $\mathbf{k}$ when $L \to \infty$. We can appreciate this approximate equation intuitively from another prospective. At large L and fixed $\mathbf{k}$, the reciprocal lattice points $\delta(\mathbf{k} - 2\pi\mathbf{n}/L)$ become so dense that it almost "looks" like a uniform continuum. If we replace $I(\mathbf{k})$ by 1 in Eq. (3.30) and take the principal value of the integral in the Fourier transform, the pseudo wave function reduces to the singular solution of Eq. (3.27) in the free space.

3.3 Quantization condition

In order to obtain quantization condition, we need to match the trial wave function in Eq. (3.30) with the boundary condition Eq. (3.2) at $r < L$. A straightforward way is to project the pseudo wave function $\psi(\mathbf{r})$ into each partial wave channel and compare it to Eq. (3.2).

We first deduct a singular part from the wave function and obtain

$$g(\mathbf{r}) = \lim_{\epsilon\to 0^+} \sum_{l=0}^{\infty} \sum_{\mu} B_{l\mu} \mathrm{P} \int_{\mathbf{k}} Q_{l\mu}(\mathbf{k}) \frac{I(\mathbf{k})-1}{k^2-p^2} \mathrm{e}^{\mathrm{i}\mathbf{k}\cdot\mathbf{r}-\epsilon k^2}. \tag{3.34}$$

We see that $g(\mathbf{r})$ is a smooth function in the vicinity of the origin $r \to 0$ and a solution

to the homogeneous Helmholtz equation $(\nabla^2 + p^2)g(\mathbf{r}) = 0$. Then, we compare it to the smooth part of the pseudo wave function in Eq. (3.2). After projection to each partial wave channel, we find

$$\sum_{l'=0}^{\infty}\sum_{\mu'}\Big[\frac{2\mathrm{i}^{l-l'}}{\pi q^{l+l'+d-2}}m_{l\mu,l'\mu'} - \delta_{ll'}\delta_{\mu\mu'}\Big(\cot\delta_l^{(d)} - \mathrm{i}\theta_E\Big)\Big]C_{l'\mu'} = 0, \tag{3.35}$$

where

$$m_{l\mu,l'\mu'} = \lim_{\epsilon\to 0^+}\Big[\sum_{\mathbf{n}\in\mathbb{Z}^d}\frac{Q^*_{l\mu}(\mathbf{n})Q_{l'\mu'}(\mathbf{n})}{n^2-q^2}\mathrm{e}^{-\epsilon(n^2-q^2)} - \mathrm{P}\int \mathrm{d}^d n\ \frac{Q^*_{l\mu}(\mathbf{n})Q_{l'\mu'}(\mathbf{n})}{n^2-q^2}\mathrm{e}^{-\epsilon(n^2-q^2)}\Big]. \tag{3.36}$$

Here the dimensionless parameter $q = pL/2\pi$, and $\theta_E = 0$ or 1 if $p^2 > 0$ or < 0, respectively. When the energy is negative ($p^2 < 0$), we assume $p = \mathrm{i}\kappa$ with $\kappa > 0$. The term with θ_E appears due to the Fourier transform in Eq. (3.26) at $p^2 < 0$. Note that $m_{l\mu,l'\mu'}$ is a real function of q^2. In the expression of $m_{l\mu,l'\mu'}$, we have added a factor $\exp(\epsilon q^2)$ so that it converges exponentially fast with error $O[\exp(-\pi^2/\epsilon)]$.

For fixed p and L, Eq. (3.35) is a system of linear equations for the set of unknowns $C_{l'\mu'}$. Let $\ell = (l\mu)$ to be a collective index arranged in a proper order. Then, let the matrix element $\mathcal{M}_{\ell\ell'}$ denote the factor in the square bracket. In order for $C_{\ell'}$ to have nontrivial solutions, we reach the following quantization condition

$$\det\mathcal{M} = 0, \tag{3.37}$$

where the matrix elements

$$\mathcal{M}_{\ell\ell'} \equiv \frac{2\mathrm{i}^{l-l'}}{\pi q^{l+l'+d-2}}m_{\ell\ell'} - \delta_{\ell\ell'}\Big(\cot\delta_\ell^{(d)} - \mathrm{i}\theta_E\Big) \tag{3.38}$$

where $\ell = (l\mu)$ is the collective index, $\delta_{\ell\ell'} \equiv \delta_{ll'}\delta_{\mu\mu'}$, and $\delta_\ell^{(d)} \equiv \delta_l^{(d)}$. This quantization condition is the generalized Lüscher's formula in a d-dimensional finite volume. We see

that $m_{l\mu,l'\mu'}$ in Eq. (3.36) is well-defined for arbitrary d dimensions. The regularization factor $\mathrm{e}^{-\epsilon n^2}$ appears naturally from the regularized Fourier transform.

As the matrix $\mathcal{M}$ includes all the partial waves, the dimension of $\mathcal{M}$ is infinitely large. To solve Eq. (3.37) and obtain the energy eigenvalues, we need to assume a cutoff orbital angular momentum l_m, and neglect all the higher partial waves with $l > l_m$. In the following sections, we obtain the energy spectrum by assuming that the matrix $\mathcal{M}$ only contains the s-wave or p-wave part.

3.4 s-wave approximation

For two bosons scattering in the finite volume, the wave function is invariant under inversion of the relative position vector. The smallest possible angular momentum is $l = 0$ (s-wave), which belongs to the A_1^+ irreducible representation of the cubic group in d dimensions [41]. Here we only consider the s-wave channel, which is the most important channel for bosonic systems. Let $C_{l\mu} = 0$ for $l \geq 1$ in Eq. (3.35). Then, the matrix $\mathcal{M}$ reduces to a scalar, and the quantization condition to a simple relation

$$q^{d-2}\Big(\cot\delta_0^{(d)}(p) - \mathrm{i}\theta_{\mathrm{H}}(-p^2)\Big) = \frac{\Gamma(d/2)}{\pi^{d/2+1}} S_d(q^2), \tag{3.39}$$

where $\theta_{\mathrm{H}}(x)$ is the Heaviside step function. $\theta_{\mathrm{H}}(x) = 1$ if $x > 0$, or $\theta_{\mathrm{H}}(x) = 0$ if $x < 0$. The function $S_d(x)$ is defined as

$$S_d(x) = \lim_{\epsilon\to 0^+}\Big(\sum_{\mathbf{n}\in\mathbb{Z}^d}\frac{\mathrm{e}^{-\epsilon(n^2-x)}}{n^2-x} - \mathrm{P}\int \mathrm{d}^d n\,\frac{\mathrm{e}^{-\epsilon(n^2-x)}}{n^2-x}\Big). \tag{3.40}$$

Here we have used the fact that $Q_{0,1}(\mathbf{n}) = \sqrt{\frac{\Gamma(d/2)}{2\pi^{d/2}}}$. In 2010, Beane derived a similar formula of the s-wave approximation in d dimensions using a different method of regularization [71]. When $d \leq 3$, Eq. (3.39) agrees well with Beane's formula and the other previous works [39, 41, 70, 96]. However, when $d \geq 4$, Beane's formula becomes diver-

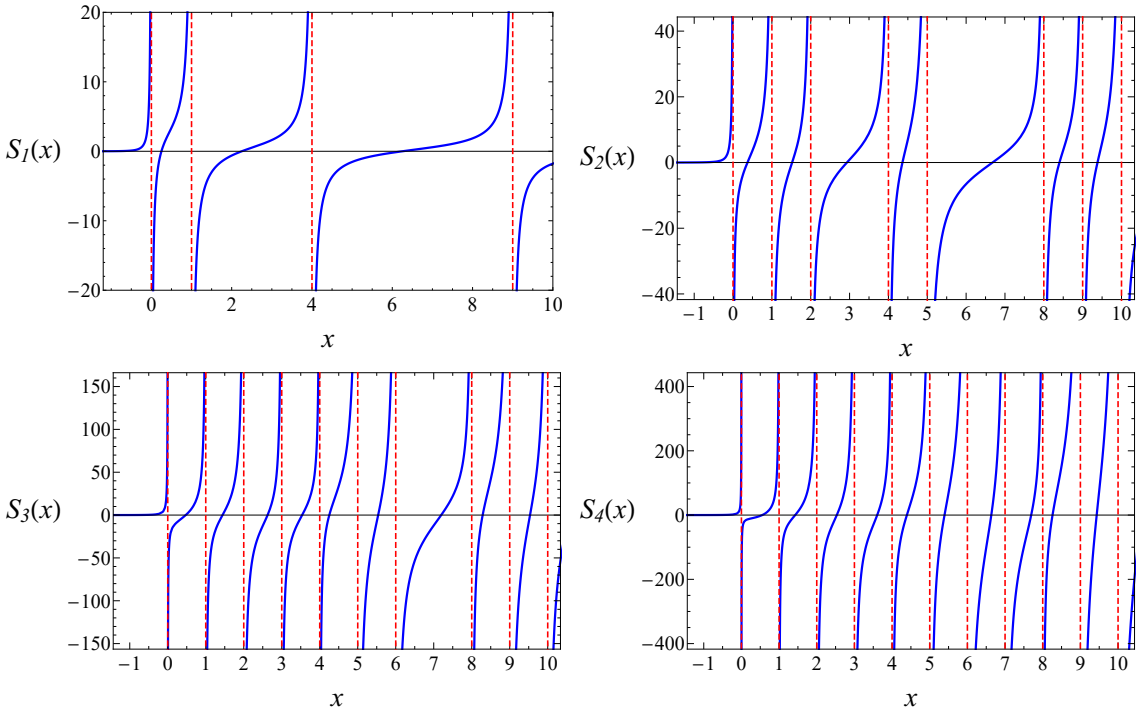

Figure 3.1: The function $S_d(x)$ when $d = 1, 2, 3, 4$. It exponentially decays when x is large and negative, and has a simple pole when x is equal to the norm square of a nonzero integral vector in $\mathbb{Z}^d$.

gent, while Eq. (3.39) remains valid.

The function $S_d(x)$ is a real-valued function. In Figure 3.1, we show the plot of the function $S_d(x)$ when $d = 1, 2, 3, 4$. When $d = 1$, we have an analytic expression at the real axis

$$S_1(x) = -\frac{\pi}{\sqrt{x}} \cot(\pi\sqrt{x}) - \frac{\pi}{\sqrt{-x}} \theta_{\mathrm{H}}(-x). \tag{3.41}$$

At large and negative argument, $S_d(x)$ is exponentially small and has the following asymptotic expansion at $x \to +\infty$,

$$S_d(-x^2) = 2d\pi x^{\frac{d-3}{2}} \mathrm{e}^{-2\pi x} + O(\mathrm{e}^{-2\sqrt{2}\pi x}). \tag{3.42}$$

If there is a bound state in the free space with a finite negative energy, then the argument q^2 is large and negative when $L \to \infty$. Therefore, the correction to the bound state energy due to a large periodic box is exponentially small. This has been previously addressed in

Ref. [39, 41, 96, 97, 98].

At small x, $S_d(x)$ have the following expansion:

1) when d is even,

$$S_d(x) = \sum_{s=0}^{\infty} \alpha_{ds} x^{s-1} + \frac{\pi^{d/2}}{2\Gamma(d/2)} x^{d/2-1} \ln(x^2), \tag{3.43}$$

2) when d is odd,

$$S_d(x) = \sum_{s=0}^{\infty} \alpha_{ds} x^{s-1} + (-1)^{\frac{d+1}{2}} \frac{\pi^{d/2+1}}{\Gamma(d/2)} (-x)^{d/2-1} \theta_{\mathrm{H}}(-x). \tag{3.44}$$

Here the coefficients α_{ds} is defined as the regularized lattice sums:

$$\alpha_{ds} = \lim_{\epsilon \to 0^+} \Big(\sum_{\mathbf{n} \neq \mathbf{0}} \frac{\mathrm{e}^{-\epsilon n^2}}{n^{2s}} - \int \mathrm{d}^d n \, \frac{\mathrm{e}^{-\epsilon n^2}}{n^{2s}} \Big), \quad \text{when} \;\; s < d/2, \tag{3.45a}$$

$$\alpha_{ds} = \lim_{N \to +\infty} \Big(\sum_{\mathbf{n} \neq \mathbf{0}, n < N} \frac{1}{n^{2s}} - \frac{2\pi^{d/2}}{\Gamma(d/2)} \ln N \Big), \quad \text{when} \;\; s = d/2, \tag{3.45b}$$

$$\alpha_{ds} = \sum_{\mathbf{n} \neq \mathbf{0}} \frac{1}{n^{2s}}, \quad \text{when} \;\; s > d/2. \tag{3.45c}$$

The summations are over the integral vector $\mathbf{n} \in \mathbb{Z}^d$. We can easily see that $\alpha_{d,0} = -1$. The numerical calculation of these parameters is discussed in Appendix C, and some numerical results of $\alpha_{d,1}$ and $\alpha_{d,2}$ are listed in Table C.1. So, using the small x expansions of $S_d(x)$, we can find the energies of the low-lying states (satisfying $q^2 \ll 1$) at large box size L.

3.4.1 Weak interactions

If there is no interaction between the two particles, they just move freely in the finite volume. Then, the wave function of the relative motion is proportional to $\exp(\mathrm{i}2\pi \mathbf{n} \cdot \mathbf{r}/L)$ with $\mathbf{n} \in \mathbb{Z}^d$. Then, the energy eigenvalues is simply

$$E_n = \frac{4\pi^2 n^2}{L^2}, \tag{3.46}$$

where $n = |\mathbf{n}|$ is the length of the integral vector $\mathbf{n}$. When $n \neq 0$, each energy eigenvalue is $2d$-fold degenerate. When the interaction is weak, we expect that the energy eigenvalues are modified by small corrections. We see that in the limit of large L, the length scale set by a fixed scattering length $a_{d,0}$ is small compared to L. Then, those corrections are higher order terms in $1/L$.

The extreme case of weak interaction is reached when the scattering length $a_{d,0} = 0$. In this limit, the zero-energy wave function in the free space is a constant outside the range of interaction. Then, the zero-energy state is naturally an energy eigenstate in the finite volume. For nonzero energy eigenvalues, the interaction introduces small corrections. When $a_{d,0} = 0$, the effective range expansion in Eq. (2.3) becomes

$$\cot \delta_0^{(d)} = \frac{1}{p^d}\Big(v_{d,0} + v_{d,1}p^2 + O(p^4)\Big) + \tau_d \frac{2}{\pi} \ln(pR_{dl}), \tag{3.47}$$

where the parameters $v_{d,0}$ and $v_{d,1}$ are defined as

$$v_{d,0} = -\frac{2}{a_{d,0}^2 r_{d,0}}, \tag{3.48}$$

$$v_{d,1} = \frac{1}{a_{d,0}} + \frac{r'_{d,0}}{6a_{d,0}^2 r_{d,0}^2}, \tag{3.49}$$

which remain finite when $a_{d,0} \to 0$. The above formula has been previously obtained in three dimensions [27, 99]. As a result, the left hand side of Eq. (3.39) is proportional to L^d/q^2. Then, the solutions to the Eq. (3.39) are found near the singular points of the function $S_d(x)$ (see Figure 3.1). We obtain a general formula for the energy eigenvalues with a subleading correction term in arbitraray d dimensions ($d > 0$) ,

$$p^2 = \frac{4\pi^2 n^2}{L^2}\Big[1 - \frac{u_d \omega_d(n^2)}{2v_{d,0}} \frac{1}{L^d} + o\Big(\frac{1}{L^d}\Big)\Big], \tag{3.50}$$

where $u_d = 2^{d+1}\pi^{d/2-1}\Gamma(d/2)$, and $\omega_d(s)$ is the number of integral vectors $\mathbf{n} \in \mathbb{Z}^d$ satisfying $s = |\mathbf{n}|^2$.

$d=2$	$p^2 = \frac{2\pi}{L^2\widetilde{L}_{2,0}} - \frac{\alpha_{2,1}}{L^2\widetilde{L}_{2,0}^2} + \frac{\alpha_{2,1}^2-\alpha_{2,2}}{2\pi L^2\widetilde{L}_{2,0}^3} + O\Big(\frac{1}{L^2\widetilde{L}_{2,0}^4}\Big)$
$d=3$	$p^2 = \frac{u_3}{2}\frac{a_{3,0}}{L^3} - \frac{u_3^2\alpha_{3,1}}{16\pi^2}\frac{a_{3,0}^2}{L^4} + \frac{4(\alpha_{3,1}^2-\alpha_{3,2})}{\pi}\frac{a_{3,0}^3}{L^5} + O\Big(\frac{1}{L^6}\Big)$
$d=4$	$p^2 = \frac{u_4}{2}\frac{a_{4,0}}{L^4} - \frac{u_4^2\alpha_{4,1}}{16\pi^2}\frac{a_{4,0}^2}{L^6} + O\Big(\frac{\ln L}{L^8}\Big)$
$d\geq 5$	$p^2 = \frac{u_d}{2}\frac{a_{d,0}}{L^d} - \frac{u_d^2\alpha_{d,1}}{16\pi^2}\frac{a_{d,0}^2}{L^{2d-2}} + \frac{1}{8}u_d^2\frac{a_{d,0}^3 r_{d,0}}{L^{2d}} + O\Big(\frac{1}{L^{3d-4}}\Big)$

Table 3.1: Large L expansion of the low-lying state energy when $a_{d,0}$ ($d \neq 2$) or $\widetilde{a}_{2,0}$ is finite. When $d=2$, we have defined $\widetilde{L}_{2,0} = \ln(L/\widetilde{a}_{2,0})$.

When $a_{d,0}$ ($d \neq 2$) or $\widetilde{a}_{2,0}$ of the weak interaction is nonzero and finite, the effective range expansion Eq. (2.3) remains valid. The solutions to the Eq. (3.39) are found near the singular points of $S_d(x)$ when $d \geq 2$ or the zeros of $S_d(x)$ when $d=1$. We obtain the the energy eigenvalues with a subleading order correction,

$$p^2 = \frac{4\pi^2 n^2}{L^2} + \frac{u_d\omega_d(n^2)}{2}\frac{a_{d,0}}{L^d} + o\Big(\frac{1}{L^d}\Big), \text{ when d} \geq 3, \tag{3.51}$$

$$p^2 = \frac{4\pi^2 n^2}{L^2} + \frac{2\pi\omega_2(n^2)}{L^2\ln(L/\widetilde{a}_{2,0})} + O\Big(\frac{1}{L^2\ln^2 L}\Big), \text{ when d} = 2, \tag{3.52}$$

$$p^2 = \frac{(i\pi)^2}{L^2}\Big[1 - \frac{4}{a_{1,0}L} + \frac{12}{a_{1,0}^2L^2} + O\Big(\frac{1}{L^3}\Big)\Big], \text{ when d} = 1, \tag{3.53}$$

where $\mathbf{n} \in \mathbb{Z}^d$ ($d \geq 2$) and $i = 1, 3, 5, 7, \cdots$ ($d=1$). We see that when $n=0$, the energy of the low-lying state $E \sim 1/L^d$ when $d \neq 2$ or $E \sim 1/L^2\ln L$ when $d=2$. The formula agrees with the previous calculations in three dimensions [40, 96] and two dimensions [71]. We lists the formulas with more correction terms for the low-lying state ($n=0$) in Table 3.1.

3.4.2 Resonant s-wave interactions

First let us focus on $d \geq 4$ dimensions. When $a_{d,0} \to \infty$, we say the system is at a s-wave resonance. In the free space, there exists a bound state right at the threshold. In the finite volume, the energy of this bound states is modified.

Then, it is particularly interesting to investigate the low-lying states close to the threshold with energies much smaller than $1/L^2$. From Eq. (3.39), we discover two low-lying states with nearly opposite energies. We obtain the leading order formula

$$p^2 = \pm\frac{2\sqrt{2}\pi}{L^2\ln^{1/2}(L/\widetilde{r}_{4,0})}, \text{ when } d=4, \tag{3.54}$$

$$p^2 = \pm\frac{u_d^{1/2}}{(-r_{d,0})^{1/2}}\frac{1}{L^{d/2}}, \text{ when } d\geq 5, \tag{3.55}$$

where $r_{d,0}$ and $\widetilde{r}_{4,0}$ are the s-wave effective range, and the reduced s-wave effective range, previously defined in Sec. 3.1.1. Note that $r_{d,0}<0$ [89].

As discussed in Sect. 3.1.1, at the s-wave resonance in the free space, the zero-energy wave function behaves like r^{2-d} ($d\geq 3$). Naively, we expect that the correction due to the periodic box is proportional to $1/L^{d-2}$, which proves to be wrong according to the formulas above.

Notice that there is only one bound state at the threshold when $a_{d,0}\to\infty$ in the free space. However, here we find two low-lying states near the threshold in the finite volume. How does the extra state come from? We can appreciate this by considering a model separable potential with a tunable interaction strength in the periodic box. Initially, the interaction strength is zero, and there are one zero-energy ground state and $2d$ degenerate first excited states with energy $(2\pi/L)^2$. Then, we gradually increase the interaction strength to a point such that the s-wave resonance occurs. We shall see that the negative energy state evolves from the zero-energy ground state, and the positive energy state evolves from an equal superposition of the $2d$ first excited states. As a results, two low-lying states appears with energies given by Eq. (3.54) and (3.55).

For three bosons colliding in a three-dimensional finite volume, the system can be directly mapped to the two-body scattering problem in a six-dimensional finite volume if the interaction between the three bosons only contains the finite-range three-body interaction. Then, Eq. (3.55) suggests that when three bosons is at a three-body resonance in a

$d=4$	$p^2=\pm\frac{2\sqrt{2}\pi}{L^2\ln^{1/2}(L/\widetilde{r}_{4,0})}-\frac{\alpha_{4,1}}{L^2\ln(L/\widetilde{r}_{4,0})}+\pm\frac{\alpha_{4,1}^2-4\alpha_{4,2}}{4\sqrt{2}\pi L^2\ln^{3/2}(L/\widetilde{r}_{4,0})}+O\Big(\frac{1}{L^2\ln^2(L/\widetilde{r}_{4,0})}\Big)$
$d=5$	$p^2=\pm\frac{u_d^{1/2}}{(-r_{d,0})^{1/2}}\frac{1}{L^{d/2}}+\frac{u_d\alpha_{d,1}}{8\pi^2 r_{d,0}}\frac{1}{L^{d-2}}+\pm\frac{u_d^{3/2}(\alpha_{d,1}^2-4\alpha_{d,2})}{128\pi^4(-r_{d,0})^{3/2}}\frac{1}{L^{3d/2-4}}+O\Big(\frac{1}{L^4}\Big)$
$d=6$	$p^2=\pm\frac{u_d^{1/2}}{(-r_{d,0})^{1/2}}\frac{1}{L^{d/2}}+\frac{u_d\alpha_{d,1}}{8\pi^2 r_{d,0}}\frac{1}{L^{d-2}}+\pm\frac{u_d^{3/2}(\alpha_{d,1}^2-4\alpha_{d,2})}{128\pi^4(-r_{d,0})^{3/2}}\frac{1}{L^{3d/2-4}}+O\Big(\frac{\ln L}{L^6}\Big)$
$d\geq 7$	$p^2=\pm\frac{u_d^{1/2}}{(-r_{d,0})^{1/2}}\frac{1}{L^{d/2}}+\frac{u_d\alpha_{d,1}}{8\pi^2 r_{d,0}}\frac{1}{L^{d-2}}+\pm\frac{u_d^{3/2}(\alpha_{d,1}^2-4\alpha_{d,2})}{128\pi^4(-r_{d,0})^{3/2}}\frac{1}{L^{3d/2-4}}+\frac{u_d r'_{d,0}}{24 r_{d,0}^2}\frac{1}{L^d}+\cdots$

Table 3.2: Large L expansion of the energies of the two low-lying states at s-wave resonance when $d\geq 4$. Note that the $1/L^{3d/2-4}$ term becomes more important than the $1/L^d$ term when $d>8$.

three-dimensional finite volume, two low-lying states exist near the threshold with energies behaves like $\pm 1/L^3$. Simlarly, from Eq. (3.54), when three bosons is at a three-body resonance in a two-dimensional finite volume, two low-lying states exist near the threshold with energies behaves like $\pm 1/L^2\sqrt{\ln L}$.

In Table 3.2, we list the energies of the two low-lying state with more correction terms at large L. The higher order terms contain the coefficients α_{ds}, defined as the regularized lattice sums in Eq. (3.45) and numerically calculated in Appendix C. We also discuss the energy eigenvalues at a s-wave resonance in one or three dimensions in Appendix D

3.5 p-wave approximation

For two bosons scattering in the finite volume, the wave function is invariant under inversion of the relative position vector. The smallest possible angular momentum is $l=0$ (s-wave). However, for two fermions scattering in the finite volume, the wave function changes sign under inversion of the relative position vector, and then the smallest possible angular momentum is $l=1$ (p-wave). We can neglect the higher partial waves and set $C_{l\mu}=0$ for $l\geq 2$ in Eq. (3.35). As the s-wave channel and p-wave channel belongs to different irreducible representations [41], the s-wave and p-wave channel decouple in Eq. (3.35). Here we obtain the p-wave approximation by just considering the p-wave channel, which is most important for fermionic systems.

The p-wave harmonic polynomials in d dimensions can be defined as

$$Q_{1,\mu}(\mathbf{r}) = \Big(\pi^{-d/2}\Gamma(d/2+1)\Big)^{1/2} r_\mu, \tag{3.56}$$

where $\mu = 1, 2, \cdots, d$ and r_μ is the μ-th component of vector $\mathbf{r}$. These harmonic polynomials are orthonormalized in the sense that their corresponding hyperspherical harmonics are orthonormalized. Then, the quantization condition Eq. (3.37) reduces to a simple relation

$$q^{d-2}\Big(\cot\delta_1^{(d)} - \mathrm{i}\theta_{\mathrm{H}}(-p^2)\Big) = \frac{2\Gamma(d/2)}{d\pi^{d/2+1}} S_d(q^2). \tag{3.57}$$

We see that the above formula is similar to Eq. (3.39). The difference is that $\cot\delta_1^{(d)}$ has a different effective range expansion according to Eq. (3.7).

When the p-wave scattering length $a_{d,1}$ is finite, the solutions to the Eq. (3.57) are found near the singular points of $S_d(x)$. We obtain the energy eigenvalues with a subleading order correction at large L,

$$p^2 = \frac{4\pi^2 n^2}{L^2}\Big[1 + \frac{u_d\omega_d(n^2)}{d}\frac{a_{d,1}}{L^d} + o\Big(\frac{1}{L^d}\Big)\Big], \tag{3.58}$$

with $\mathbf{n} \in \mathbb{Z}^d$ and $n \neq 0$. Different from the s-wave case, there is no low-lying state with energy $p^2 \ll 1/L^2$.

At a p-wave resonance ($a_{d,1} \to \infty$), the solutions to Eq. (3.57) are found near the singular points ($d \geq 2$) or the zeros ($d = 1$) of the function $S_d(x)$. We list the energy eigenvalues at large L:

$$p^2 = \frac{4\pi^2 n^2}{L^2} + \frac{2u_d\omega_d(n^2)}{d}\frac{1}{(-r_{d,1})L^d} + o\Big(\frac{1}{L^d}\Big), \ \text{ when } \ d \geq 3, \tag{3.59}$$

$$p^2 = \frac{4\pi^2 n^2}{L^2} + \frac{2\pi\omega_d(n^2)}{L^2\ln(L/\widetilde{r}_{2,1})} + O\Big(\frac{1}{L^2\ln^2 L}\Big), \ \text{ when } \ d = 2, \tag{3.60}$$

$$p^2 = \frac{(i\pi)^2}{L^2}\Big[1 + \frac{r_{1,1}}{L} + \frac{3r_{1,1}^2}{4L^2} + O\Big(\frac{1}{L^3}\Big)\Big], \ \text{ when } \ d = 1, \tag{3.61}$$

$d \geq 5$	$p^2 = \frac{2u_d}{d}\frac{1}{(-r_{d,1})L^d} - \frac{u_d^2\alpha_{d,1}}{d^2\pi^2}\frac{1}{(-r_{d,1})^2L^{2d-2}} + \frac{u_d^2 r'_{d,1}}{3d^2}\frac{1}{(-r_{d,1})^3L^{2d}} + O\Big(\frac{1}{L^{3d-4}}\Big)$
$d = 4$	$p^2 = \frac{2u_d}{d}\frac{1}{(-r_{d,1})L^d} - \frac{u_d^2\alpha_{d,1}}{d^2\pi^2}\frac{1}{(-r_{d,1})^2L^{2d-2}} + O\Big(\frac{\ln L}{L^8}\Big)$
$d = 3$	$p^2 = \frac{2u_d}{d}\frac{1}{(-r_{d,1})L^d} - \frac{u_d^2\alpha_{d,1}}{d^2\pi^2}\frac{1}{(-r_{d,1})^2L^{2d-2}} + \frac{4u_d^2(\alpha_{d,1}^2-\alpha_{d,2})}{d^3\pi^3}\frac{1}{(-r_{d,1})^3L^5} + O\Big(\frac{1}{L^6}\Big)$
$d = 2$	$p^2 = \frac{2\pi}{L^2\ln(L/\widetilde{r}_{2,1})} - \frac{\alpha_{2,1}}{L^2\ln^2(L/\widetilde{r}_{2,1})} + \frac{\alpha_{2,1}^2-\alpha_{2,2}}{2\pi L^2\ln^3(L/\widetilde{r}_{2,1})} + O\Big(\frac{1}{L^2\ln^4(L/\widetilde{r}_{2,1})}\Big)$

Table 3.3: Large L expansion of the energies of the low-lying state at p-wave resonance ($a_{d,1} \to \infty$) when $d \geq 2$.

where $\mathbf{n} \in \mathbb{Z}^d$ ($d \geq 2$) and $i = 1, 3, 5, 7, \cdots$ ($d = 1$). Here we find that there is only one low-lying state with energy $p^2 \ll 1/L^2$. The energy of the low-lying state behaves like $p^2 \propto 1/L^d$ when $d \geq 3$, and $p^2 \propto 1/L^2 \ln L$ when $d = 2$. In Table 3.3, we list the energies of the low-lying state ($n = 0$) with more correction terms at large L.

3.6 Conclusion

We have studied the scattering of two particles with short-range interactions in a d-dimensional finite volume (a periodic box with a large size L). We have generalized Lüscher's formula to arbitrary d dimensions.

By only considering the s-wave channel, we obtained the s-wave approximation of Lüscher's formula. In $d \geq 4$ dimensions, at a s-wave resonance, there exist two low-lying states with nearly opposite energies, $E \sim \pm 1/L^{d/2}$ when $d \geq 5$, or $E \sim \pm 1/L^2\sqrt{\ln L}$ when $d = 4$. This suggests that when three bosons is at a three-body resonance in a three-dimensional finite volume, two low-lying states exist near the threshold with energies behaves like $\pm 1/L^3$. Simlarly, when three bosons is at a three-body resonance in a two-dimensional finite volume, two low-lying states exist near the threshold with energies behaves like $\pm 1/L^2\sqrt{\ln L}$.

Moreover, by only considering the p-wave channel, we obtained the p-wave approximation of Lüscher's formula. At a p-wave resonance, there exist one low-lying state with

energy $E \sim 1/L^d$ when $d \geq 3$, or $E \sim 1/L^2 \ln L$ when $d = 2$.

Appendices

APPENDIX A

THE EXTRA TERMS IN THE IMPROVED 111-EXPANSION

A.1 Solution of the Poisson equation with a point-like source in six-dimensional space

Here we introduce the method to solve the following Poisson equation

$$(\nabla^2_{\mathbf{x}} + \nabla^2_{\mathbf{y}})\psi(\mathbf{x},\mathbf{y}) = S(\mathbf{x},\mathbf{y}). \tag{A.1}$$

For simplicity, here we only consider one part of the source in Eq. (2.73). The solutions due to the other two parts of the source can be obtained by rotations $(\mathbf{x} \to \mathbf{x}_+, \mathbf{y} \to \mathbf{y}_+)$ and $(\mathbf{x} \to \mathbf{x}_-, \mathbf{y} \to \mathbf{y}_-)$. The whole solution is the sum of the three.

The source $S(\mathbf{x},\mathbf{y})$ can be obtained by applying the Laplace operator $(\nabla^2_{\mathbf{x}} + \nabla^2_{\mathbf{y}})$ on the 21-expansion in Eq. (2.15). Due to additivity, we consider a general term in the 21-expansion,

$$S(\mathbf{x},\mathbf{y}) = W(y)\nabla^2_x \phi^{(l)}_{\hat{\mathbf{y}}}(\mathbf{x}), \tag{A.2}$$

Here $\phi^{(l)}_{\hat{\mathbf{y}}}(\mathbf{x})$ are the two-body pseudo wave function at zero energy with orbital angular momentum l, with expression given by Eq. (2.5) and the continuation inside the range of interaction. Then, $\nabla^2_x \phi^{(l)}_{\hat{\mathbf{y}}}(\mathbf{x}) \propto Q^{(l)}_{\hat{\mathbf{y}}}(\nabla_{\mathbf{x}})\delta(\mathbf{x})$ vanishes at $x > 0$. $W(y)$ are usually the Z functions [16], such as $1/y$, $1/y^2$, $Z_b(y)/y^3$, $1/y^4$, $Z_b(y)/y^5$, $1/y^6$, etc.

It is convenient to work in the momentum space. First we define the Fourier transforms

$$\psi(\mathbf{x},\mathbf{y}) = \int_{\mathbf{k}}\int_{\mathbf{q}} \widetilde{\psi}(\mathbf{k},\mathbf{q}) \mathrm{e}^{\mathrm{i}\mathbf{k}\cdot\mathbf{x}} \mathrm{e}^{\mathrm{i}\mathbf{q}\cdot\mathbf{y}}, \qquad S(\mathbf{x},\mathbf{y}) = \int_{\mathbf{k}}\int_{\mathbf{q}} \widetilde{S}(\mathbf{k},\mathbf{q}) \mathrm{e}^{\mathrm{i}\mathbf{k}\cdot\mathbf{x}} \mathrm{e}^{\mathrm{i}\mathbf{q}\cdot\mathbf{y}}, \tag{A.3}$$

where $\int_{\mathbf{q}}$ is the shorthand of $\int \frac{\mathrm{d}^3q}{(2\pi)^3}$. Then, we easily find

$$\widetilde{S}(\mathbf{k},\mathbf{q}) = \mathrm{i}^{-l} 4\pi a_l W_q^{(l)} Q_{\hat{\mathbf{q}}}^{(l)}(\mathbf{k}), \qquad \widetilde{\psi}(\mathbf{k},\mathbf{q}) = \frac{-1}{k^2+q^2}\widetilde{S}(\mathbf{k},\mathbf{q}), \tag{A.4}$$

where a_l is the l-wave scattering length, $Q_{\hat{\mathbf{q}}}^{(l)}(\mathbf{k}) = k^l P_l(\hat{\mathbf{q}}\cdot\hat{\mathbf{k}})$ is the harmonic polynomials, and $W_q^{(l)}$ is a Hankel transform of $W(y)$ defined as

$$W_q^{(l)} = \int \mathrm{d}^3y\, W(y) P_l(\hat{\mathbf{q}}\cdot\hat{\mathbf{y}}) \mathrm{e}^{-\mathrm{i}\mathbf{q}\cdot\mathbf{y}}, \quad W(y) = \int_{\mathbf{q}} W_q^{(l)} P_l(\hat{\mathbf{q}}\cdot\hat{\mathbf{y}}) \mathrm{e}^{\mathrm{i}\mathbf{q}\cdot\mathbf{y}}. \tag{A.5}$$

Now we can obtain the wave function by Fourier transforming back from the momentum space,

$$\psi(\mathbf{x},\mathbf{y}) = -\sqrt{\frac{\pi}{2x}} \frac{\mathrm{i}^l a_l}{\pi^3} P_l(\hat{\mathbf{x}}\cdot\hat{\mathbf{y}}) \int_0^\infty \mathrm{d}q\, q^{l+5/2} W_q^{(l)} K_{l+1/2}(qx) j_l(qy), \tag{A.6}$$

where j_l is the spherical Bessel function of the first kind, and K_l is the modified Bessel function of the second kind. Here we have used an identity

$$\int \mathrm{d}\Omega_y \int \mathrm{d}\Omega_x\, P_l(\hat{\mathbf{x}}\cdot\hat{\mathbf{y}}) \mathrm{e}^{\mathrm{i}\mathbf{k}\cdot\mathbf{x}} \mathrm{e}^{\mathrm{i}\mathbf{q}\cdot\mathbf{y}} = (-1)^l 16\pi^2 j_l(kx) j_l(qy) P_l(\hat{\mathbf{q}}\cdot\hat{\mathbf{k}}). \tag{A.7}$$

Therefore, given the form of $W(y)$, we can obtain $W_q^{(l)}$ through Eq. (A.5) and further the wave function through the above equation. This is how we calculate all the extra terms in the modified 111-expansion in Eq. (2.77) from their corresponding terms in th 21-expansion.

A.2 Calculation of $W_q^{(l)}$

In many cases, we have to deal with the Fourier transform of functions like $1/x^\alpha$, that is, $\int \mathrm{d}^3x\, \mathrm{e}^{\mathrm{i}\mathbf{k}\cdot\mathbf{x}} x^\alpha$. When $\alpha \geq 3$, there is divergence near the origin and therefore the integral is not well-defined. Then, to eliminate the divergence, we define some general functions,

namely Z functions [16]. When $n = 4, 6, 8, 10, \cdots$, we define Z/x^n and $Z \ln x/x^n$,

$$\frac{Z}{x^n} = \frac{1}{x^n}\ (x > 0), \qquad \int \mathrm{d}^3x\ \frac{Z}{x^n} p_s(\mathbf{x}) = 0\ \ (s \leq n-4), \tag{A.8}$$

$$\frac{Z\ln x}{x^n} = \frac{\ln x}{x^n}\ (x > 0), \qquad \int \mathrm{d}^3x\ \frac{Z\ln x}{x^n} p_s(\mathbf{x}) = 0\ \ (s \leq n-4). \tag{A.9}$$

When $n = 3, 5, 7, 9, \cdots$, we define $Z_b(x)/x^n$, and $Z_b(x)\ln x/x^n$,

$$\frac{Z_b(x)}{x^n} = \frac{1}{x^n}\ (x > 0), \qquad \int_{|\mathbf{x}|<b} \mathrm{d}^3x\ \frac{Z_b(x)}{x^n} p_s(\mathbf{x}) = 0\ (s \leq n-3), \tag{A.10}$$

$$\frac{Z_b(x)\ln x}{x^n} = \frac{\ln x}{x^n}\ (x > 0), \qquad \int_{|\mathbf{x}|<b} \mathrm{d}^3x\ \frac{Z_b(x)\ln x}{x^n} p_s(\mathbf{x}) = 0\ (s \leq n-3). \tag{A.11}$$

Here $p_s(\mathbf{x})$ is the homogeneous polynomial of $\mathbf{x}$ with degree s and $p_s(\mathbf{x}) = 1$ when $s \leq 0$.

Using these definitions, we can calculate the corresponding Hankel transform $W_q^{(l)}$ in Eq. (A.5). Now we present some examples of how to do the calculations. By integrating out the angular part, we write Eq. (A.5) in the following form

$$W_q^{(l)} = 4\pi \mathrm{i}^{-l} \int_0^\infty \mathrm{d}y\ y^2 j_l(qy) W(y), \tag{A.12}$$

$$W(y) = \frac{\mathrm{i}^l}{2\pi^2} \int_0^\infty \mathrm{d}y\ y^2 j_l(qy) W_q^{(l)}. \tag{A.13}$$

Example 1. Assume $W(y) = Z/y^n$ with $n = 4, 6, 8, \cdots$. Note that the integral

$$I_\nu(l,q) = 4\pi \mathrm{i}^{-l} \int_0^\infty \mathrm{d}y\ y^2 j_l(qy) \frac{1}{y^\nu} = \mathrm{i}^{-l}\pi^{3/2} \Big(\frac{q}{2}\Big)^{\nu-3} \frac{\Gamma(\frac{l+3-\nu}{2})}{\Gamma(\frac{l+\nu}{2})},\ 1 < \nu < l+3, \tag{A.14}$$

where $\Gamma(x)$ is the Gamma function. The right hand side is regular at $\nu = 4, 6, 8, \cdots$ and may have simple poles when ν is an odd positive integer. Then, we can directly do an analytical continuation and get for $n = 4, 6, 8, \cdots$,

$$W_q^{(l)} = \mathrm{i}^{-l}\pi^{3/2} \Big(\frac{q}{2}\Big)^{n-3} \frac{\Gamma(\frac{l+3-n}{2})}{\Gamma(\frac{l+n}{2})}. \tag{A.15}$$

Example 2. Assume $W(y) = Z_b(y)/y^n$ when $n = 3, 5, 7, \cdots$. Notice that $I_\nu(l, q)$ may have a simple pole when ν approaches an odd positive integer. Also, the definition requires that the integral inside a ball of radius b vanishes for $n = 3$. Then we can represent $Z_b(y)/y^3$ in the following form

$$\frac{Z_b(y)}{y^3} = \lim_{\epsilon\to 0^+} \frac{1}{2}\Big(b^\epsilon \frac{Z}{y^{3+\epsilon}} + b^{-\epsilon}\frac{Z}{y^{3-\epsilon}}\Big). \tag{A.16}$$

Therefore,

$$W_q^{(l)} = \lim_{\epsilon\to 0^+} \frac{1}{2}\Big[b^\epsilon I_{n+\epsilon}(l, q) + b^{-\epsilon} I_{n-\epsilon}(l, q)\Big]. \tag{A.17}$$

For example, when $n = 3$ and $l = 0$, $W_q^{(l)} = 4\pi[1 - \gamma - \ln(qb)]$, where $\gamma \approx 0.5772$ is the Euler-Mascheroni constant.

Example 3. Assume $W(y) = Z\ln(\kappa y)/y^n$ with $n = 4, 6, 8, \cdots$. Here κ is some constant. Note that at $1 < \nu < l + 3$, the integral

$$\begin{aligned} J_\nu(l, q) &= 4\pi \mathrm{i}^{-l} \int_0^\infty \mathrm{d}y\, y^2 j_l(qy) \frac{\ln(\kappa y)}{y^\nu} \\ &= \mathrm{i}^{-l}\pi^{3/2}\Big(\frac{q}{2}\Big)^{\nu-3} \frac{\Gamma(\frac{l+3-\nu}{2})}{\Gamma(\frac{l+\nu}{2})}\Big[\ln(\frac{2\kappa}{q}) + \frac{\Gamma'(\frac{l+3-\nu}{2})}{2\Gamma(\frac{l+3-\nu}{2})} + \frac{\Gamma'(\frac{l+\nu}{2})}{2\Gamma(\frac{l+\nu}{2})}\Big]. \end{aligned} \tag{A.18}$$

It is regular at $n = 4, 6, 8, \cdots$. Then, after an analytical continuation, we get for $n = 4, 6, 8, \cdots$, $W_q^{(l)} = J_n(l, q)$.

Example 4. Assume $W(y) = Z_b(y)\ln(\kappa y)/y^n$ with $n = 3, 5, 7, \cdots$. Notice that $J_\nu(l, q)$ may diverge when ν approaches an odd positive integer. Also, the definition requires that the integral inside a ball of radius b vanishes for $n = 3$. Then we can represent $Z_b(y)\ln(\kappa y)/y^3$ in the following form

$$\frac{Z_b(y)\ln(\kappa y)}{y^3} = \lim_{\epsilon\to 0^+} \frac{1}{6}\Big[4b^{2\epsilon}\frac{Z\ln(\kappa y)}{y^{3+2\epsilon}} + 4b^{-2\epsilon}\frac{Z\ln(\kappa y)}{y^{3-2\epsilon}} - b^\epsilon\frac{Z\ln(\kappa y)}{y^{3+\epsilon}} - b^{-\epsilon}\frac{Z\ln(\kappa y)}{y^{3-\epsilon}}\Big]. \tag{A.19}$$

Therefore, we obtain

$$W_q^{(l)} = \lim_{\epsilon \to 0^+} \frac{1}{6}\Big[4b^{2\epsilon}J_{n+2\epsilon}(l,q) + 4b^{-2\epsilon}J_{n-2\epsilon}(l,q) - b^{\epsilon}J_{n+\epsilon}(l,q) - b^{-\epsilon}J_{n-\epsilon}(l,q)\Big]. \quad \text{(A.20)}$$

For example, when $n = 5$ and $l = 0$,

$$W_q^{(l)} = \frac{\pi q^2}{108}[3\pi^2 - 170 + 132\gamma - 36\gamma^2 + 36\ln^2(b\kappa) - 36\ln^2(q/\kappa) + (132 - 72\gamma)\ln(q/\kappa)]. \quad \text{(A.21)}$$

APPENDIX B

THREE-BODY WAVE FUNCTION AT A D-WAVE RESONANCE

Here we calculate the three-boson wave function at d-wave resonance where $a_d \to \infty$. Outside the range of interaction, the d-wave two-body special functions are defined as

$$\phi^{(d)}_{\hat{\mathbf{n}}}(\mathbf{x}) = -\frac{3}{x^3}P_2(\hat{\mathbf{n}}\cdot\hat{\mathbf{x}}), \tag{B.1}$$

$$f^{(d)}_{\hat{\mathbf{n}}}(\mathbf{x}) = \Big[-\frac{r_d}{30}x^2 - \frac{1}{x}\Big]P_2(\hat{\mathbf{n}}\cdot\hat{\mathbf{x}}), \tag{B.2}$$

where r_d is the d-wave effective range. We can do the "zigzag" approach, by considering two expansions of wave function at two regions: 1) the 21-expansion

$$\psi = \sum_{s=0}^{\infty} S^{(s)}_{\mathbf{y}}(\mathbf{x}), \ \text{ when } \ y \to \infty, \tag{B.3}$$

where $S^{(s)}_{\mathbf{y}}(\mathbf{x})$ scales like $1/y^s$, and 2) the 111-expansion

$$\psi = \sum_{s=0}^{\infty} T^{(s)}(\mathbf{x}_1, \mathbf{x}_2, \mathbf{x}_3), \ \text{ when } \ x_1, x_2, x_3 \to \infty, \tag{B.4}$$

where $T^{(s)}(\mathbf{x}_1, \mathbf{x}_2, \mathbf{x}_3)$ scales like $1/x_i^s$.Both expansions satisfy the Schrödinger equation at zero energy. Meanwhile, they shall match in the intermediate region where $1 \ll x \ll y$, in such way

$$T^{(s)}(\mathbf{x}_1, \mathbf{x}_2, \mathbf{x}_3) = \sum_{n=0}^{\infty} t^{(s-n,n)}_{\mathbf{x},\mathbf{y}}, \tag{B.5}$$

$$S^{(s)}_{\mathbf{y}}(\mathbf{x}) = \sum_{m=0}^{\infty} t^{(m,s)}_{\mathbf{x},\mathbf{y}}, \tag{B.6}$$

where $t_{\mathbf{x},\mathbf{y}}^{(m,n)}$ scales like $\frac{1}{x^m y^n}$. Then, by doing the matching, we can systematically determine the higher order terms of each expansion in a zigzag way.

Step 1. We assume that the wave function approaches 1 at large distances. Then, we have the zeroth order term

$$T^{(0)} = 1. \tag{B.7}$$

Also, $[-\nabla_x^2 + V(x)]S_{\mathbf{y}}^{(0)}(\mathbf{x}) = 0$. Then, we get

$$S_{\mathbf{y}}^{(0)}(\mathbf{x}) = \phi(x). \tag{B.8}$$

Step 2. Apply the kinetic operator on $S_{\mathbf{y}}^{(0)}(\mathbf{x})$ to get the source, and we seek the solution to the equation $(-\nabla_x^2 - \nabla_y^2)\psi = -4\pi a \sum_{i=1}^{3} \delta(\mathbf{x}_i)$. Then, we find

$$T^{(1)} = \sum_{i=1}^{3} -\frac{a}{x_i}. \tag{B.9}$$

We can find its large y expansion and obtain

$$t_{\mathbf{x},\mathbf{y}}^{(0,1)} = -\frac{a}{x},\ \ t_{\mathbf{x},\mathbf{y}}^{(1,0)} = -\frac{4a}{\sqrt{3}y},\ \ t_{\mathbf{x},\mathbf{y}}^{(3,-2)} = -\frac{4ax^2}{3\sqrt{3}y^3}P_2(\hat{\mathbf{x}}\cdot\hat{\mathbf{y}}),\ \ t_{\mathbf{x},\mathbf{y}}^{(5,-4)} = \cdots. \tag{B.10}$$

Step 3. Considering the equation $[-\nabla_x^2 + V(x)]S_{\mathbf{y}}^{(1)}(\mathbf{x}) = 0$ and the term $t_{\mathbf{x},\mathbf{y}}^{(1,0)} = -\frac{4a}{\sqrt{3}y}$, we find

$$S_{\mathbf{y}}^{(1)}(\mathbf{x}) = -\frac{4a}{\sqrt{3}y}\phi(x) + \frac{c_d^{(1)}}{y}\phi_{\hat{\mathbf{y}}}^{(d)}(\mathbf{x}), \tag{B.11}$$

where $c_d^{(1)}$ is an unknown parameter to be determined by higher order terms. Notice that, away from d-wave resonance, we do not have this second term. It is allowed here because the x^3 terms disappears in $\phi_{\hat{\mathbf{y}}}^{(d)}(\mathbf{x})$ when $a_d \to \infty$. Apply the kinetic operator on the first term to get the source, and we find

$$T^{(2)} = \sum_{i=1}^{3} \frac{8a^2\theta_i}{\sqrt{3}\pi x_i y_i}, \tag{B.12}$$

where $\theta_i = \arctan(y_i/x_i)$. Therefore the large y expansion gives

$$t^{(1,1)}_{\mathbf{x},\mathbf{y}} = \frac{4a^2}{\sqrt{3}xy},\ \ t^{(2,0)}_{\mathbf{x},\mathbf{y}} = \frac{8wa^2}{3\pi y^2},\ \ t^{(4,-2)}_{\mathbf{x},\mathbf{y}} = \cdots, \tag{B.13}$$

where $w = 4\pi/3 - \sqrt{3}$.

Step 4. Considering the equation $[-\nabla_x^2 + V(x)]S^{(2)}_{\mathbf{y}}(\mathbf{x}) = 0$ and the term $t^{(2,0)}_{\mathbf{x},\mathbf{y}} = -\frac{8wa^2}{3\pi y^2}$, we find

$$S^{(2)}_{\mathbf{y}}(\mathbf{x}) = \frac{8wa^2}{3\pi y^2}\phi(x) + \frac{c_d^{(2)}}{y^2}\phi^{(d)}_{\hat{\mathbf{y}}}(\mathbf{x}). \tag{B.14}$$

Apply the kinetic operator on the first term to get the source, and we find

$$T^{(3)} = \sum_{i=1}^{3} -\frac{2wa^3}{\pi\rho^2 x_i}, \tag{B.15}$$

where $\rho = \sqrt{\frac{x_1^2+x_2^2+x_3^2}{2}}$ is the hyper radius. Therefore the large y expansion gives

$$t^{(2,1)}_{\mathbf{x},\mathbf{y}} = -\frac{8a^3 w}{3\pi x y^2},\ \ t^{(3,0)}_{\mathbf{x},\mathbf{y}} = -\frac{32a^3 w}{3\sqrt{3}\pi y^3},\ \ t^{(4,-1)}_{\mathbf{x},\mathbf{y}} = -\frac{8a^3 wx}{3\pi y^4},\ \ \cdots, \tag{B.16}$$

Step 5. Considering the equation $[-\nabla_x^2 + V(x)]S^{(3)}_{\mathbf{y}}(\mathbf{x}) - \nabla_y^2 S^{(1)}_{\mathbf{y}}(\mathbf{x}) = 0$ and the terms $t^{(3,0)}_{\mathbf{x},\mathbf{y}} = -\frac{32a^3 w}{3\sqrt{3}\pi y^3}$ and $t^{(3,-2)}_{\mathbf{x},\mathbf{y}} = -\frac{4ax^2}{3\sqrt{3}y^3}P_2(\hat{\mathbf{x}}\cdot\hat{\mathbf{y}})$, we find

$$S^{(3)}_{\mathbf{y}}(\mathbf{x}) = -\frac{32a^3 w}{3\sqrt{3}\pi y^3}\phi(x) + \frac{40a}{\sqrt{3}r_d y^3}f^{(d)}_{\hat{\mathbf{y}}}(\mathbf{x}) + \frac{c_d^{(3)}}{y^3}\phi^{(d)}_{\hat{\mathbf{y}}}(\mathbf{x}). \tag{B.17}$$

This is the crucial step that the d-wave part makes a difference. From the second term, we can determine $c_d^{(1)} = -\frac{20a}{3\sqrt{3}r_d}$. Apply the kinetic operator on the first term of $S^{(3)}_{\mathbf{y}}(\mathbf{x})$ and the second term of $S^{(1)}_{\mathbf{y}}(\mathbf{x})$ to get the source, and we find

$$\begin{aligned} T^{(4)} \ &= \ -\frac{\sqrt{3}\widetilde{D}}{8\pi^3\rho^4} + \sum_{i=1}^{3}\Big[\frac{8\sqrt{3}wa^4[t-1-\theta_i\cot(2\theta_i)]}{\pi^2\rho^4} + \\ &\quad \frac{5\sqrt{3}a(-24\theta_i\cos 2\theta_i + 9\sin 2\theta_i + \sin 6\theta_i)}{2\pi r_d\rho^4\sin^3 2\theta_i}P_2(\hat{\mathbf{x}}\cdot\hat{\mathbf{y}})\Big], \end{aligned} \tag{B.18}$$

where $t = \ln \frac{e^{\gamma}\rho}{|a|}$ and $\gamma \approx 0.5772$ is the Euler-Mascheroni constant. Here the first comes from a source term like $\delta(\mathbf{x})\delta(\mathbf{y})$ and the definition of $\widetilde{D}$ is fixed by choosing a specific length scale in the log term t. Here $\widetilde{D}$ is the three-body scattering hypervolume, which might be different from the definition in Ref. [16] due to the d-wave resonance.

APPENDIX C

LATTICE SUMS

Here we discuss the calculation of the lattice sums defined in Eq. (3.45). In the light of the similar method in Ref. [16], based on the Poisson summation formula, we find an exponentially accurate formula for the function $S_d(x)$

$$S_d(x) = \sum_{\mathbf{n}\in\mathbb{Z}^d} \frac{\mathrm{e}^{-\epsilon(n^2-x)}}{n^2-x} - \mathrm{P}\int \mathrm{d}^d n\, \frac{\mathrm{e}^{-\epsilon(n^2-x)}}{n^2-x} + O(\mathrm{e}^{-\pi^2/\epsilon}). \tag{C.1}$$

The second term on the right hand side has an analytic expression

$$\mathrm{P}\int \mathrm{d}^d n\, \frac{\mathrm{e}^{-\epsilon(n^2-x)}}{n^2-x} = \mathrm{Re}\Big[\pi^{d/2}\epsilon^{1-d/2}E_{d/2}(-\epsilon x)\Big], \tag{C.2}$$

where $E_n(x)$ is the exponential integral function and the symbol Re takes the real part. Note that $\pi^{d/2}\epsilon^{1-d/2}E_{d/2}(-\epsilon x)$ is real when $x < 0$. So we only need to take the real part when $x > 0$.

Compared to the definition in Eq. (3.43) and (3.44), the small x expansion of Eq. (C.1) gives the exponentially accurate formula for the parameter $\alpha_{d,s}$. We obtain

$$\alpha_{d,1} = \sum_{\mathbf{n}\neq\mathbf{0}} \frac{\mathrm{e}^{-\epsilon n^2}}{n^2} - \epsilon + \begin{cases} \frac{-2\pi^{d/2}}{d-2}\epsilon^{1-d/2} + O(\mathrm{e}^{-\pi^2/\epsilon}), & \text{when } d \neq 2, \\ \pi(\ln\epsilon + \gamma) + O(\mathrm{e}^{-\pi^2/\epsilon}), & \text{when } d = 2, \end{cases} \tag{C.3}$$

$$\alpha_{d,2} = \sum_{\mathbf{n}\neq\mathbf{0}} (1+\epsilon n^2)\frac{\mathrm{e}^{-\epsilon n^2}}{n^4} - \frac{1}{2}\epsilon^2 + \begin{cases} \frac{-2\pi^{d/2}}{d-4}\epsilon^{2-d/2} + O(\mathrm{e}^{-\pi^2/\epsilon}), & \text{when } d \neq 4, \\ \pi^2(\ln\epsilon + \gamma - 1) + O(\mathrm{e}^{-\pi^2/\epsilon}), & \text{when } d = 4, \end{cases} \tag{C.4}$$

where the integral vector $\mathbf{n} \in \mathbb{Z}^d$, and $\gamma \approx 0.5772156649$ is the Euler-Mascheroni constant.

When $s = d/2$, we have used an equivalent definition to Eq. (3.45b),

$$\alpha_{ds} = \lim_{\epsilon \to 0^+} \Big(\sum_{\mathbf{n} \neq \mathbf{0}} \frac{\mathrm{e}^{-\epsilon n^2}}{n^{2s}} + \frac{\pi^{d/2}}{\Gamma(d/2)} (\gamma + \ln \epsilon) \Big), \tag{C.5}$$

where $\Gamma(x)$ is the Gamma function. Note that when $d = 1$,

$$\alpha_{1,s} = 2\zeta(2s), \tag{C.6}$$

where $\zeta(x)$ is the Riemann zeta function.

As the error is $O(\mathrm{e}^{-\pi^2/\epsilon})$, we can choose a small positive ϵ to have high accuracy. Then, we need a large cutoff to numerically evaluate the lattice sum of the function with a factor $\exp(-\epsilon n^2)$. The cutoff n_c satisfies the condition $\epsilon n_c^2 \gg 1$. The numerical evaluation of the lattice sum of the form $\sum_{\mathbf{n} \neq \mathbf{0}} f(n^2)$ may be time-consuming in high dimensions, as its computation cost scales like $O(n_c^d)$. To reduce the computation cost, we convert the lattice sum to the form

$$\sum_{\mathbf{n} \neq \mathbf{0}} f(n^2) = \sum_{s=1}^{\infty} \omega_d(s) f(s), \tag{C.7}$$

where $\omega_d(s)$ is defined as the number of integral vectors in $\mathbb{Z}^d$ satisfying $s = |\mathbf{n}|^2$. The function $\omega_d(s)$ can be easily evaluated using the following recurrence relation

$$\omega_d(s) = \omega_{d-1}(s) + \sum_{j=1}^{\lfloor \sqrt{s} \rfloor} 2\omega_{d-1}(s - j^2), \tag{C.8}$$

where s is a nonnegative integer, $\lfloor x \rfloor$ is the floor function defined as the largest integer less than or equal to x. Here d starts form 1, and we define $\omega_0(s) \equiv \delta_{s,0}$. Then, using Eq. (C.7), we reduce the computation cost to $O(n_c^2)$.

In Table C.1, we list some numerical results of $\alpha_{d,1}$ and $\alpha_{d,2}$.

d	$\alpha_{d,1}$	$\alpha_{d,2}$
1	3.289 868 133 696 452 872 944	2.164 646 467 422 276 383 032
2	2.584 981 759 579 253 217 065	6.026 812 039 691 940 123 546
3	−8.913 632 917 585 151 272 687	16.532 315 959 761 669 643 892
4	−5.545 177 444 479 562 475 337	4.632 326 383 366 237 654 956
5	−4.228 709 895 683 319 615 146	−21.421 171 696 960 725 548 702
6	−3.379 684 783 443 147 987 261	−10.617 592 887 114 204 993 381
7	−2.664 213 558 009 533 686 447	−6.235 317 876 719 048 885 979
8	−1.948 701 251 737 169 329 936	−3.289 868 133 696 452 872 944
9	−1.145 140 664 314 177 595 925	−0.723 391 161 980 715 859 958
10	−0.165 329 744 623 330 494 224	1.896 302 612 990 100 956 960

Table C.1: The numerical results of $\alpha_{d,1}$ and $\alpha_{d,2}$ when $d = 1, 2, 3, \cdots, 10$. We show 21 digits to the right of the decimal point.

APPENDIX D

S-WAVE RESONANCE IN ONE- OR THREE-DIMENSIONAL FINITE VOLUME

Here we discuss the energy eigenvalues at a s-wave resonance in one- or three- dimensional finite volume.

In one dimension, Eq. (3.39) reduces the formula obtained by Lüscher and Wolff [69]. At the s-wave resonance ($a_{1,0} \to \infty$), the interaction is infinitely repulsive or attractive. The solutions can be found near the zeros of the function $S_1(z)$. The energies of the states have the following large L expansion

$$p^2 = \frac{(i\pi)^2}{L^2} + 2(i\pi)^4 \frac{r_{1,0}}{L^5} + \frac{(i\pi)^6}{6} \frac{r'_{1,0}}{L^7} + O\Big(\frac{1}{L^8}\Big), \tag{D.1}$$

where $i = 1, 3, 5, 7, \cdots$. The above formula can be obtained by simply set $a_{1,0} \to \infty$ in Eq. (3.53).

In three dimensions at a s-wave reonance ($a_{3,0} \to \infty$), the solutions to the Eq. (3.39) can be found near the zeros of the function $S_3(x)$. Then, we obtain the energy eigenvalues

$$p^2 = \frac{4\pi^2 z_j}{L^2} + \frac{8\pi^5 z_j}{T'(z_j)} \frac{r_{3,0}}{L^3} + \frac{8\pi^8 z_j [2T'(z_j) - z_j T''(z_j)]}{[T'(z_j)]^3} \frac{r_{3,0}^2}{L^4} + O\Big(\frac{1}{L^5}\Big), \tag{D.2}$$

where $j = 0, 1, 2, 3, \ldots$. The coefficient z_j is the zeros of the function

$$T(x) = S_3(x) - 2\pi^2 (-x)^{1/2} \theta_{\mathrm{H}}(-x). \tag{D.3}$$

$z_0 < 0$ is the zero of $T(x)$ on the negative real axis, and $z_j > 0$ is the j-th zero on the positive real axis. The first two of the above formulas ($j = 0$ and 1) were obtained by Beane, et al. in the study of the two-nucleon system with large s-wave scattering length [96].

Here we list some numerical results of z_j, $T'(z_j)$, and $T''(z_j)$ with 30 digits to the right

of the decimal point:

$$z_0 = -0.095\,900\,719\,461\,176\,511\,014\,630\,087\,070, \tag{D.4a}$$

$$z_1 = 0.472\,894\,247\,259\,651\,468\,922\,730\,973\,625, \tag{D.4b}$$

$$z_2 = 1.441\,591\,312\,955\,972\,495\,696\,286\,930\,666, \tag{D.4c}$$

$$z_3 = 2.627\,007\,611\,756\,450\,957\,352\,064\,867\,924, \tag{D.4d}$$

$$z_4 = 3.536\,619\,946\,961\,690\,847\,649\,851\,448\,688, \tag{D.4e}$$

$$z_5 = 4.251\,705\,973\,256\,342\,483\,716\,352\,992\,425, \tag{D.4f}$$

$$T'(z_0) = 123.823\,863\,084\,183\,424\,152\,475\,695\,444\,931, \tag{D.5a}$$

$$T'(z_1) = 39.755\,259\,069\,374\,557\,631\,734\,429\,264\,651, \tag{D.5b}$$

$$T'(z_2) = 82.365\,536\,602\,007\,013\,846\,376\,963\,967\,049, \tag{D.5c}$$

$$T'(z_3) = 106.247\,745\,183\,288\,934\,788\,715\,983\,536\,519, \tag{D.5d}$$

$$T'(z_4) = 84.232\,177\,940\,640\,405\,063\,325\,468\,040\,818, \tag{D.5e}$$

$$T'(z_5) = 161.888\,638\,951\,656\,361\,019\,774\,535\,657\,948, \tag{D.5f}$$

$$T''(z_0) = 2167.737\,594\,235\,974\,375\,155\,549\,175\,987\,579, \tag{D.6a}$$

$$T''(z_1) = 72.301\,574\,314\,683\,065\,605\,729\,439\,419\,339, \tag{D.6b}$$

$$T''(z_2) = 4.941\,363\,010\,338\,470\,738\,104\,547\,929\,723, \tag{D.6c}$$

$$T''(z_3) = 218.462\,000\,085\,057\,495\,045\,097\,402\,632\,746, \tag{D.6d}$$

$$T''(z_4) = 29.514\,588\,853\,752\,717\,125\,883\,607\,788\,221, \tag{D.6e}$$

$$T''(z_5) = -637.704\,036\,778\,442\,467\,773\,149\,148\,969\,504. \tag{D.6f}$$

Note that z_0 and z_1 correspond to d_1 and d_1' defined in Ref. [96]. For comparison, we also obtain the numerical values of d_2 and d_2' defined in Ref. [96],

$$\begin{aligned} d_2 &= 0.025\,371\,463\,749\,713\,062\,531\,827\,061\,333, \\ d_2' &= 0.079\,023\,322\,376\,231\,662\,986\,314\,111\,909. \end{aligned}$$

REFERENCES

[1] J. Dalibard, in *Bose-Einstein Condensation in Atomic Gases*, edited by M. Inguscio, S. Stringari, and C. E. Wieman, (IOS Press, Amsterdam, 1999), pp. 321-349; D. J. Heinzen, *ibid.*, pp. 351-390.

[2] J. O. Andersen, "Theory of the weakly interacting bose gas," *Rev. Mod. Phys.*, vol. 76, pp. 599–639, 2 2004.

[3] E. Braaten and H.-W. Hammer, "Universality in few-body systems with large scattering length," *Phys. Rep.*, vol. 428, p. 259, 2006.

[4] N. N. Bogoliubov, "On the Theory of Superfluidity," *J. Phys. (USSR)*, vol. 11, p. 23, 1947.

[5] T. D. Lee and C. N. Yang, "Many-body problem in quantum mechanics and quantum statistical mechanics," *Phys. Rev.*, vol. 105, p. 1119, 3 1957.

[6] T. D. Lee, K. Huang, and C. N. Yang, "Eigenvalues and eigenfunctions of a bose system of hard spheres and its low-temperature properties," *Phys. Rev.*, vol. 106, pp. 1135–1145, 6 1957.

[7] K. A. Brueckner and K. Sawada, "Bose-einstein gas with repulsive interactions: General theory," *Phys. Rev.*, vol. 106, pp. 1117–1127, 6 1957.

[8] W. B. Riesenfeld and K. M. Watson, "Equation of state of gases and liquids at low temperatures," *Phys. Rev.*, vol. 108, p. 518, 3 1957.

[9] T. T. Wu, "Ground state of a bose system of hard spheres," *Phys. Rev.*, vol. 115, pp. 1390–1404, 6 1959.

[10] K. Sawada, "Ground-state energy of bose-einstein gas with repulsive interaction," *Phys. Rev.*, vol. 116, pp. 1344–1358, 6 1959.

[11] N. M. Hugenholtz and D. Pines, "Ground-state energy and excitation spectrum of a system of interacting bosons," *Phys. Rev.*, vol. 116, p. 489, 3 1959.

[12] E. Braaten and A. Nieto, "Quantum corrections to the energy density of a homogeneous bose gas," *Eur. Phys. J. B*, vol. 11, no. 1, p. 143, 1999.

[13] E. Braaten, H.-W. Hammer, and S. Hermans, "Nonuniversal effects in the homogeneous bose gas," *Phys. Rev. A*, vol. 63, p. 063 609, 6 2001.

[14] E. Braaten, H.-W. Hammer, and T. Mehen, "Dilute bose-einstein condensate with large scattering length," *Phys. Rev. Lett.*, vol. 88, p. 040 401, 4 2002.

[15] S. Giorgini, J. Boronat, and J. Casulleras, "Ground state of a homogeneous bose gas: A diffusion monte carlo calculation," *Phys. Rev. A*, vol. 60, pp. 5129–5132, 6 1999.

[16] S. Tan, *Phys. Rev. A*, vol. 78, p. 013 636, 2008.

[17] S. R. Beane, W. Detmold, and M. J. Savage, *Phys. Rev. D*, vol. 76, p. 074 507, 2007.

[18] S. R. Beane, W. Detmold, K. Orginos, and M. J. Savage, "Nuclear physics from lattice qcd," *Prog. Part. Nucl. Phys.*, vol. 66, p. 1, 2011.

[19] T. Frederico, A. Delfino, L. Tomio, and M. Yamashita, "Universal aspects of light halo nuclei," *Prog. Part. Nucl. Phys.*, vol. 67, p. 939, 2012.

[20] S. L. Cornish, N. R. Claussen, J. L. Roberts, E. A. Cornell, and C. E. Wieman, *Phys. Rev. Lett.*, vol. 85, pp. 1795–1798, 9 2000.

[21] L Khaykovich, F Schreck, G Ferrari, T Bourdel, J Cubizolles, L. D. Carr, Y Castin, and C Salomon, "Formation of a matter-wave bright soliton.," *Science (New York, N.Y.)*, vol. 296, no. 5571, pp. 1290–3, 2002.

[22] K. E. Strecker, G. B. Partridge, A. G. Truscott, and R. G. Hulet, *Nature*, vol. 417, no. 6885, pp. 150–153, 2002.

[23] G. Roati, M. Zaccanti, C. D'Errico, J. Catani, M. Modugno, A. Simoni, M. Inguscio, and G. Modugno, *Phys. Rev. Lett.*, vol. 99, p. 010 403, 1 2007.

[24] T. Lahaye, T. Koch, B. Fröhlich, M. Fattori, J. Metz, A. Griesmaier, S. Giovanazzi, and T. Pfau, "Strong dipolar effects in a quantum ferrofluid," *Nature*, vol. 448, no. 7154, pp. 672–675, 2007.

[25] M. Fattori, C. D'Errico, G. Roati, M. Zaccanti, M. Jona-Lasinio, M. Modugno, M. Inguscio, and G. Modugno, "Atom interferometry with a weakly interacting bose-einstein condensate," *Phys. Rev. Lett.*, vol. 100, p. 080 405, 8 2008.

[26] S. E. Pollack, D. Dries, M. Junker, Y. P. Chen, T. A. Corcovilos, and R. G. Hulet, *Phys. Rev. Lett.*, vol. 102, p. 090 402, 9 2009.

[27] Z. Shotan, O. Machtey, S. Kokkelmans, and L. Khaykovich, "Three-body recombination at vanishing scattering lengths in an ultracold bose gas," *Phys. Rev. Lett.*, vol. 113, p. 053 202, 5 2014.

[28] J. Söding, D. Guéry-Odelin, P. Desbiolles, F. Chevy, H. Inamori, and J. Dalibard, "Three-body decay of a rubidium bose–einstein condensate," *Appl. Phys. B*, vol. 69, p. 257, 1999.

[29] J. Stenger, S. Inouye, M. R. Andrews, H.-J. Miesner, D. M. Stamper-Kurn, and W. Ketterle, "Strongly enhanced inelastic collisions in a bose-einstein condensate near feshbach resonances," *Phys. Rev. Lett.*, vol. 82, p. 2422, 12 1999.

[30] J. L. Roberts, N. R. Claussen, S. L. Cornish, and C. E. Wieman, "Magnetic field dependence of ultracold inelastic collisions near a feshbach resonance," *Phys. Rev. Lett.*, vol. 85, p. 728, 4 2000.

[31] V. Efimov, "Energy levels arising from resonant two-body forces in a three-body system," *Phys. Lett. B*, vol. 33, no. 8, p. 563, 1970.

[32] V. N. Efimov, "Weakly-bound states of three resonantly-interacting particles," *Yad. Fiz.*, vol. 12, p. 1080, 1970.

[33] T Kraemer, M Mark, P Waldburger, J. G. Danzl, C Chin, B Engeser, A. D. Lange, K Pilch, A Jaakkola, H.-C. Nägerl, and R Grimm, "Evidence for Efimov quantum states in an ultracold gas of caesium atoms," *Nature*, vol. 440, no. 7082, p. 315, 2006.

[34] B. D. Esry, C. H. Greene, and J. P. Burke, "Recombination of three atoms in the ultracold limit," *Phys. Rev. Lett.*, vol. 83, p. 1751, 9 1999.

[35] P. F. Bedaque, E. Braaten, and H.-W. Hammer, "Three-body recombination in bose gases with large scattering length," *Phys. Rev. Lett.*, vol. 85, pp. 908–911, 5 2000.

[36] S. Stringari, "Collective excitations of a trapped bose-condensed gas," *Phys. Rev. Lett.*, vol. 77, pp. 2360–2363, 12 1996.

[37] D. S. Jin, J. R. Ensher, M. R. Matthews, C. E. Wieman, and E. A. Cornell, "Collective excitations of a bose-einstein condensate in a dilute gas," *Phys. Rev. Lett.*, vol. 77, pp. 420–423, 3 1996.

[38] H. Al-Jibbouri, I. Vidanović, A. Balaž, and A. Pelster, *Journal of Physics B: Atomic, Molecular and Optical Physics*, vol. 46, no. 6, p. 065 303, 2013.

[39] M. Lüscher, *Commun. Math. Phys.*, vol. 104, p. 177, 1986.

[40] ——, *Commun. Math. Phys.*, vol. 105, p. 153, 1986.

[41] M. Lüscher, *Nucl. Phys. B*, vol. 354, p. 531, 1991.

[42] E. Epelbaum, H.-W. Hammer, and U.-G. Meißner, *Rev. Mod. Phys.*, vol. 81, p. 1773, 4 2009.

[43] M. G. Endres, D. B. Kaplan, J.-W. Lee, and A. N. Nicholson, "Lattice monte carlo calculations for unitary fermions in a harmonic trap," *Phys. Rev. A*, vol. 84, p. 043 644, 4 2011.

[44] ——, "Lattice monte carlo calculations for unitary fermions in a finite box," *Phys. Rev. A*, vol. 87, p. 023 615, 2 2013.

[45] J. E. Drut, "Improved lattice operators for nonrelativistic fermions," *Phys. Rev. A*, vol. 86, p. 013 604, 1 2012.

[46] J. E. Drut and A. N. Nicholson, "Lattice methods for strongly interacting many-body systems," *J. Phys. G*, vol. 40, no. 4, p. 043 101, 2013.

[47] D. Lee, "Ground state energy at unitarity," *Phys. Rev. C*, vol. 78, p. 024 001, 2 2008.

[48] D. Lee, *Eur. Phys. J. A*, vol. 35, p. 171, 2008.

[49] S. Bour, X. Li, D. Lee, U.-G. Meißner, and L. Mitas, "Precision benchmark calculations for four particles at unitarity," *Phys. Rev. A*, vol. 83, p. 063 619, 6 2011.

[50] D. Lee and T. Schäfer, "Cold dilute neutron matter on the lattice. i. lattice virial coefficients and large scattering lengths," *Phys. Rev. C*, vol. 73, p. 015 201, 1 2006.

[51] ——, "Cold dilute neutron matter on the lattice. ii. results in the unitary limit," *Phys. Rev. C*, vol. 73, p. 015 202, 1 2006.

[52] X. Li and C. Liu, *Phys. Lett. B*, vol. 587, no. 1-2, p. 100, 2004.

[53] X. Feng, X. Li, and C. Liu, "Two particle states in an asymmetric box and the elastic scattering phases," *Phys. Rev. D*, vol. 70, p. 014 505, 1 2004.

[54] K. Rummukainen and S. Gottlieb, *Nucl. Phys. B*, vol. 450, no. 1-2, p. 397, 1995.

[55] C. Kim, C. Sachrajda, and S. R. Sharpe, *Nucl. Phys. B*, vol. 727, no. 1-2, p. 218, 2005.

[56] R. A. Briceño and Z. Davoudi, "Moving multichannel systems in a finite volume with application to proton-proton fusion," *Phys. Rev. D*, vol. 88, p. 094 507, 9 2013.

[57] M. T. Hansen and S. R. Sharpe, "Multiple-channel generalization of lellouch-lüscher formula," *Phys. Rev. D*, vol. 86, p. 016 007, 1 2012.

[58] K. Polejaeva and A. Rusetsky, *Eur. Phys. J. A*, vol. 48, no. 5, p. 67, 2012.

[59] M. T. Hansen and S. R. Sharpe, *Phys. Rev. D*, vol. 90, p. 116 003, 11 2014.

[60] ——, *Phys. Rev. D*, vol. 92, p. 114 509, 11 2015.

[61] P. Guo. eprint: arXiv:1303.3349v1.

[62] R. A. Briceño and Z. Davoudi, "Three-particle scattering amplitudes from a finite volume formalism," *Phys. Rev. D*, vol. 87, p. 094 507, 9 2013.

[63] S. Kreuzer and H.-W. Hammer, *Phys. Lett. B*, vol. 673, no. 4-5, p. 260, 2009.

[64] S. Kreuzer and H. W. Hammer, *Eur. Phys. J. A*, vol. 43, no. 2, p. 229, 2010.

[65] S. Kreuzer and H.-W. Hammer, *Phys. Lett. B*, vol. 694, no. 4-5, p. 424, 2011.

[66] U.-G. Meißner, G. Ríos, and A. Rusetsky, "Spectrum of three-body bound states in a finite volume," *Phys. Rev. Lett.*, vol. 114, p. 091 602, 9 2015.

[67] P. Guo and V. Gasparian, "A solvable three-body model in finite volume," *Phys. Lett. B*, vol. 774, pp. 441–445, 2017.

[68] J. Polchinski, *String Theory, Vol. 1&2*. Cambridge University Press, 2005.

[69] M. Lüscher and U. Wolff, *Nucl. Phys. B*, vol. 339, p. 222, 1990.

[70] H. Fiebig, R. Woloshyn, and A. Dominguez, *Nucl. Phys. B*, vol. 418, p. 649, 1994.

[71] S. R. Beane, *Phys. Rev. A*, vol. 82, p. 063 610, 6 2010.

[72] H. Bethe, "Theory of the effective range in nuclear scattering," *Phys. Rev.*, vol. 76, no. 1, p. 38, 1949.

[73] L. B. Madsen, "Effective range theory," *Am. J. Phys.*, vol. 70, no. 8, p. 811, 2002.

[74] Y. Simonov, "The Three body problem. a complete system of angular functions," *Sov. J. Nucl. Phys.*, vol. 3, p. 461, 1966.

[75] J. Macek, "Properties of autoionizing states of He," *Journal of Physics B: Atomic and Molecular Physics*, vol. 1, no. 5, p. 309, 1968.

[76] S. Balay, S. Abhyankar, M. F. Adams, J. Brown, P. Brune, K. Buschelman, L. Dalcin, V. Eijkhout, W. D. Gropp, D. Kaushik, M. G. Knepley, D. A. May, L. C. McInnes,

R. T. Mills, T. Munson, K. Rupp, P. Sanan, B. F. Smith, S. Zampini, H. Zhang, and H. Zhang, *PETSc Web page*, `http://www.mcs.anl.gov/petsc`, 2018.

[77] ——, *PETSc users manual*, 2018.

[78] S. Balay, W. D. Gropp, L. C. McInnes, and B. F. Smith, *Efficient management of parallelism in object oriented numerical software libraries*, E. Arge, A. M. Bruaset, and H. P. Langtangen, Eds., 1997.

[79] Y. Saad and M. H. Schultz, "Gmres: A generalized minimal residual algorithm for solving nonsymmetric linear systems," *SIAM J. Sci. Stat. Comput.*, vol. 7, no. 3, pp. 856–869, 1986.

[80] C. Chin, R. Grimm, P. Julienne, and E. Tiesinga, "Feshbach resonances in ultracold gases," *Rev. Mod. Phys.*, vol. 82, p. 1225, 2 2010.

[81] E. P. Gross, Nuovo Cimento **20**, 454 (1961); L. Pitaevskii, Sov. Phys. JETP **13**, 451 (1961).

[82] A. J. Olson, D. L. Whitenack, and Y. P. Chen, "Effects of magnetic dipole-dipole interactions in atomic bose-einstein condensates with tunable s-wave interactions," *Phys. Rev. A*, vol. 88, p. 043 609, 4 2013.

[83] S. Yi and L. You, "Trapped condensates of atoms with dipole interactions," *Phys. Rev. A*, vol. 63, p. 053 607, 5 2001.

[84] V. M. Pérez-García, H. Michinel, J. I. Cirac, M. Lewenstein, and P. Zoller, "Low energy excitations of a bose-einstein condensate: A time-dependent variational analysis," *Phys. Rev. Lett.*, vol. 77, pp. 5320–5323, 27 1996.

[85] J. Mitroy and M. W. J. Bromley, "Semiempirical calculation of van der waals coefficients for alkali-metal and alkaline-earth-metal atoms," *Phys. Rev. A*, vol. 68, p. 052 714, 5 2003.

[86] A. Derevianko, W. R. Johnson, M. S. Safronova, and J. F. Babb, "High-precision calculations of dispersion coefficients, static dipole polarizabilities, and atom-wall interaction constants for alkali-metal atoms," *Phys. Rev. Lett.*, vol. 82, pp. 3589–3592, 18 1999.

[87] A.-X. Zhang and J.-K. Xue, "Band structure and stability of bose-einstein condensates in optical lattices with two- and three-atom interactions," *Phys. Rev. A*, vol. 75, p. 013 624, 1 2007.

[88] J. S. Avery, *J. Comput. Appl. Math.*, vol. 233, p. 1366, 2010.

[89] H.-W. Hammer and D. Lee, *Ann. Phys. (N. Y.)*, vol. 325, p. 2212, 2010.

[90] E. Fermi, Ric. Sci. **7-II**, 13 (1936).

[91] K. Huang and C. N. Yang, *Phys. Rev.*, vol. 105, p. 767, 3 1957.

[92] A. Derevianko, "Revised huang-yang multipolar pseudopotential," *Phys. Rev. A*, vol. 72, p. 044 701, 4 2005.

[93] R. Stock, A. Silberfarb, E. L. Bolda, and I. H. Deutsch, "Generalized pseudopotentials for higher partial wave scattering," *Phys. Rev. Lett.*, vol. 94, p. 023 202, 2 2005.

[94] Z. Idziaszek and T. Calarco, "Pseudopotential method for higher partial wave scattering," *Phys. Rev. Lett.*, vol. 96, p. 013 201, 1 2006.

[95] L. Pricoupenko, "Pseudopotential in resonant regimes," *Phys. Rev. A*, vol. 73, p. 012 701, 1 2006.

[96] S. R. Beane, P. Bedaque, A. Parreño, and M. J. Savage, *Phys. Lett. B*, vol. 585, p. 106, 2004.

[97] S. König, D. Lee, and H.-W. Hammer, "Volume dependence of bound states with angular momentum," *Phys. Rev. Lett.*, vol. 107, p. 112 001, 11 2011.

[98] S. König, D. Lee, and H.-W. Hammer, *Ann. Phys.*, vol. 327, no. 6, p. 1450, 2012.

[99] C. L. Blackley, P. S. Julienne, and J. M. Hutson, *Phys. Rev. A*, vol. 89, p. 042 701, 4 2014.